IDENTIFICATION OF ARGONAUTES INVOLVED IN ANTIVIRAL RNA SILENCING IN *NICOTIANA BENTHAMIANA*

A Thesis

by

DENIS ODOKONYERO

Submitted to the Office of Graduate Studies of
Texas A&M University
in partial fulfillment of the requirements for the degree of

MASTER OF SCIENCE

Approved by:

Chair of Committee,	Herman B. Scholthof
Committee Members,	Erik T. Mirkov
	Cecilia Tamborindeguy
Head of Department,	Leland S. Pierson III

December 2012

Major Subject: Plant Pathology

ABSTRACT

ARGONAUTE proteins (AGOs) are generally accepted as key components of the post transcriptional gene silencing mechanism, also involved in plant antiviral defense. Except for reports on the antiviral roles of AGO1, AGO2 and AGO7 in *Arabidopsis*, the exact roles played by the individual AGOs in other plant species are largely unknown. This research focused on the identification and characterization of *AGOs* involved in antiviral RNAi response to various viruses in *N. benthamiana*. Based on the temporal and spatial distribution of *AGO* transcripts in 3 and 8-week old plant root, stem and leaf tissues, expressions of *NbAGO* mRNAs were found to vary with age and tissue specificity. Plant endogenous *AGO* mRNAs were knocked down through virus induced gene silencing techniques using the *Tobacco rattle virus* vector system and posteriorly challenged with a GFP-chimeric virus construct deficient of a silencing suppressor. Unlike in control non-silenced plants, the *Tomato bushy stunt virus* construct deficient of its P19 silencing suppressor was consistently seen to exhibit a strong fluorescence on *N. benthamiana* plants silenced for *NbAGOs 2* and *X*. Similar results were also obtained upon silencing of *NbAGO2* using hairpin vector techniques. Comparable observations were also made when *Tobacco mosaic virus* GFP constructs were agroinfiltrated on *NbAGO2* silenced plants further hinting the antiviral defense roles played by these AGOs. Agroinfiltration of *Foxtailmosaic virus*, *Sunnhemp mosaic virus*, and *Turnip crinkle virus* GFP chimeric constructs on *NbAGO2* silenced *N. benthamiana* plants, however did not result in accumulation of GFP indicating the AGO antiviral defense specificity to TBSV and TMV. The results also hinted at a role for AGO7. Collectively my findings suggest that the expression of *AGOs* in *N. benthamiana* is tissue and age dependent, and that unlike in the model plant *Arabidopsis* where the main antiviral AGO is thought to be AtAGO1; in *N. benthamiana*, NbAGOs 2 and X seem to be involved in an antiviral defense role against TBSV and TMV with other AGOs perhaps contributing.

ACKNOWLEDGMENTS

It is not every day that one says that the graduate school was a pleasure! I however, have been fortunate enough to be surrounded by several people who in various ways have helped me make the most of this experience and to whom I am deeply indebted and would hereby like to acknowledge.

Many, many thanks to Dr. Herman Scholthof, my advisor, for allowing me to work in his laboratory, as well as for his encouragement, advice, patience and overall friendliness. I could not have asked for a better mentor. My appreciation also goes to Dr. Karen-Beth Scholthof for her support, discussions, as well as her overall motherliness attitude throughout the course of graduate school. A special thank you to Drs. Veria Alvarado and Kranthi Mandadi for help with experimental design advice, expertise in troubleshooting, manuscript comments and for simply being the best friends both in and out of the lab.

To my committee members Drs. Cecilia Tamborindeguy and Erik Mirkov: thank you for all the advice on the thesis manuscript, suggestions and the general advice and encouragement! I can never thank Dr. Mirkov enough for all the help he offered me during the process of joining graduate school.

I would like to convey my gratitude to my past and present members of the Scholthof laboratories. Thank you to Olivia Duncan, Chantal Brosseau, Juanita Mclachlan, Christopher Lyons, Andrea Roque, Guili Salazar, Andrew Baker and Jesse Pyle for their support and lively conversations.

I would also like to express my appreciation to the faculty, staff, and students of Plant Pathology for their encouragement. I would however, especially like to thank Dr. Leland Pierson for his personal attention and concern pertaining graduate student's general welfare; the office staff Karen Hodges and Tracy Vann for always being so friendly and helpful; fellow graduate students especially David Laughlin, Eli Borrego, Brandon Hasset and Frankie Crutcher for all the awesome time we spent hanging out.

Additionally, I thank all my family and friends in Uganda; especially Aunts Sunday, Estelle, Jane and Stella, friends; Tony and Emmanuel, my brothers and sisters; Patrick, Joan, Geoffrey and Flavia, cousins; Nightingale, Eunice and Sandra and of course grandma Penina. Special thanks to Marco Guilcapi and my Ecuadorian and Costa Rican family for 'adopting' me and constantly looking out for me even from such great distances.

Finally, I would like to thank my wife Maria Regina Mendoza for sticking by my side throughout the rough patches of graduate school and helping me straighten priorities in life.

TABLE OF CONTENTS

LIST OF FIGURES

LIST OF TABLES

CHAPTER I

INTRODUCTION, SYSTEMS, HYPOTHESES AND OBJECTIVES

Introduction: RNA silencing

DNA, the hereditary unit that encodes for proteins, the main regulators of the cellular machinery, has always been considered the key component of biological systems. RNA on the other hand was considered a mere intermediate molecule, bridging the gap between DNA and protein simply serving basic functional roles during splicing and translation. Nonetheless, fairly recent discoveries of non-protein-coding RNAs with specific regulatory roles have changed our perceptions of gene regulation and expression (Vaucheret, 2006).

RNA-based regulation was first unknowingly reported in the late 1920s in a *Tobacco ringspot virus* infection of tobacco when following infection with the virus, a gradual decline in the development of ring spot symptoms on the progressively newer leaves until finally the top newest emerging leaves appeared perfectly symptomless and completely free of viral material (Wingard, 1928). The phenomenon was then again reported in much more detail in the now infamous experiment in an attempt to increase the intensity of the purple pigment in transgenic petunia by overexpression of the chalcone synthase gene; white patches instead resulted on the flower petals (Napoli, 1990).

Further research in genetics and biochemistry of other members of the *Plantae, Animalia, Protista* and *Fungi* kingdoms revealed the conservation of what is now known as the RNA silencing pathway across many species (Baulcombe, 2004, Vance, 2001). A surprising exception however was found in the model budding yeast *Saccharomyces cerevisiae* which seems to have lost certain critical components of the mechanism. Additional independent research later revealed the presence of the mechanism in *Saccharomyces castellii* and *Candida albicans* budding yeast species (Drinnenberg et al., 2009).

Non-protein coding RNAs regulate gene expression using a diverse array of mechanisms. In protists, they guide DNA elimination during the formation of the macronucleus, are involved in heterochromatin assembly in fungi and plants, target endogenous mRNA for cleavage and translational repression in plants and animals, control the movement of transposable elements, and protect both animal and plant cells against viruses through a post transcriptional gene silencing mechanism (Vaucheret, 2006). In general, non-protein coding RNA are involved in a variety of regulatory mechanism essential for genome stability, development, biotic and abiotic stress responses among others.

Since its discovery, various terms such as 'RNA interference' (RNAi) in *Caennorhabditis elegans*, *Drosophila melanogaster,* human as well as other mammalian cells (Romano & Macino, 1992, Bernstein et al., 2001, Liu et al., 2004a, Fire et al., 1998), 'quelling' in the *Neurospora crassa* (Romano & Macino, 1992), 'co-suppression of homologous genes' in petunia plants, and 'post transcriptional gene silencing' (PTGS) (Vance & Vaucheret, 2001) have been coined to describe RNA silencing which basically refers to a gene regulation strategy based on sequence-specific targeting and degradation of RNA.

A 2004 review by Baulcombe (Baulcombe, 2004) states that gene silencing pathways can be classified into three fairly distinct categories; cytoplasmic short-interfering RNA (siRNA) silencing, micro-RNA (miRNA) silencing, and DNA methylation/suppression of transcription. An intriguing aspect of these pathways is that the silencing signals can be triggered locally, amplified, transmitted between cells, and may even be self-regulated by feedback mechanism.

Cytoplasmic siRNA silencing is characterized by the abundance of 21 to 25-nucleotide antisense RNA synthesized from a complementary RNA template in the cytoplasm. These siRNAs initiate the PTGS based on nucleotide sequence–specific mechanism targeting endogenous, viral as well as other transgene-based RNA (Hamilton & Baulcombe, 1999).

Micro-RNAs (miRNAs), ~22-nucleotide non-coding RNAs regulate protein-coding RNAs and are processed from longer hairpin transcripts. Just like siRNA, miRNA also show a high degree of sequence complementarity to their potential targets, hence capable of directing the cleavage of their target RNAs. (Tang et al., 2003, Xie et al., 2003). Other miRNAs regulate tissue differentiation and development by acting as translational repressors, an example of which is the *Arabidopsis* miRNA172 which controls floral organ identity and floral stem cell proliferation (Chen, 2003).

DNA methylation/ transcription repression is achieved when transcriptional repressor proteins either directly associate with their target genes through a DNA-binding domain or indirectly by interacting with other DNA-bound proteins. Generally transcription is selectively inhibited by masking or blocking of a specific activation domain, displacement of an activator, and also through exertion of allosteric effects on transcription regulators (Maldonado et al., 1999). Evidence of silencing based on DNA methylation and suppression of transcription include the discovery that transgenes and viral RNA guide DNA methylation (Wassenegger et al., 1994). The siRNA directed DNA methylation has also been linked to histone modifications in plants (Zilberman et al., 2003) and heterochromatin formation in fission yeast centromere boundaries (Volpe et al., 2002). RNA silencing at the chromatin level is also thought to be associated with protecting the genome against damage caused by transposons (Lippman & Martienssen, 2004). Bioinformatics analyses of ARGONAUTE proteins (AGOs) believed to be involved in translational repression have also shown functional allosterity between sites involved in binding both the miRNA:target duplex and the 5' cap of mRNAs (Djuranovic et al., 2010).

A principal feature in the silencing pathway (described in Figure 1.1), is the importance of double stranded RNA (dsRNA) which serves both as a pathway trigger or intermediate. Virus-derived or host endogenous dsRNA are specifically cleaved into siRNAs of 21-24 nucleotides by DICER-LIKE (DCL) proteins assisted by dsRNA binding proteins (DRB). Dicers are members of the RNase III family of nucleases characterized by the distinct helicase domain, dual RNase III motifs, and also containing

a region of homology to the ARGONAUTE (AGO) family of proteins (Tang et al., 2001, Bernstein et al., 2001, Hammond, 2005). HEN1 protein, a methyl transferase recognizes the resulting siRNA duplexes and deposits a methyl group onto the 2′ OH of the 3′ terminal nucleotide (Zhiyong Yang, 2006). Non methylated siRNAs are polyuridylated and degraded in the exosome meanwhile methylated siRNA are recognized by and incorporated into the RNA induced silencing complex (RISC) whose catalytic component is thought to primarily consists of an AGO. RISC then targets and specifically cleaves cognate mRNA. The resulting products are either degraded by an exonuclease or used as templates for siRNA amplification requiring RNA dependent RNA polymerases (RDR), SDE3/SGS3, DCL-DRB and AGO (Alvarado, 2009). The amplified siRNA is then thought to serve as a silencing signal which may move from cell to cell through the plasmodesmata or systemically through the vasculature (Baulcombe et al., 1998, Palauqui et al., 1997).

Of the three aforementioned categories, cytoplasmic siRNA silencing, a type of PTGS is the most relevant in plant antiviral defense. The AGO family of proteins have been implicated as key components in all known RNA silencing pathways in both animals and plant species (Song & Joshua-Tor, 2006, Faehnle & Joshua-Tor, 2010, Hock & Meister, 2008) hence highlighting the relevance of our study on AGO recruitment for antiviral silencing in plants.

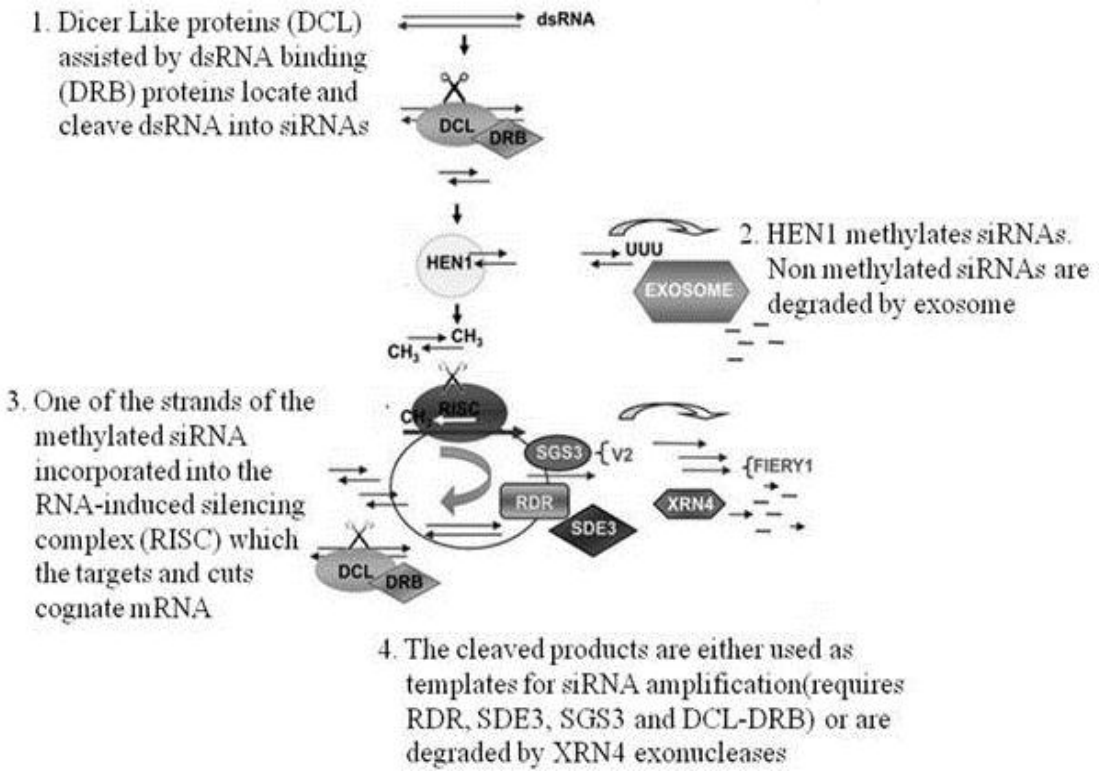

Figure 1.1. A proposed model of the PTGS pathway. The central role of AGO proteins as the catalytic engine of the programmed RISC is clearly evident (Alvarado, 2009).

The ARGONAUTE family of proteins (AGOs)

AGOs represent a highly conserved, ubiquitously expressed gene family present in almost all eukaryotes, bacteria and archaea (Hock & Meister, 2008, Hutvagner & Simard, 2008). AGOs are extremely diversified in abundance and function within different species; *C. elegans* for example has as many as 27 known AGO proteins (Kim et al., 2005), *Schizosaccharomyces pombe* on the other hand has only one AGO involved in both RNAi and transcriptional silencing (Sigova et al., 2004).

AGOs can be classified into three groups: the original Argonaute-like proteins discovered in *Arabidopsis thaliana* AGO1 (Benning, 1998), Piwi-like proteins closely related to *Drosophila melanogaster* PIWI, and *C. elegans*-specific group 3 Argonautes (Yigit, 2006). AGOs are principally characterized by the presence of the N-terminal, PAZ, MID and PIWI domains. The PAZ domains are responsible for siRNA binding, while the MID and PIWI domains for catalytic activities (Song & Joshua-Tor, 2006). With their functional domains, AGOs can bind small non-coding RNAs, affect messenger RNA stability thereby controlling protein synthesis and even participate in the production of a new class of small RNAs (Hutvagner & Simard, 2008). The phosphorylated 5′-end of the guide strand RNA is localized in the MID–PIWI domain interface with the 3′-end anchored to the PAZ domain. On binding to mRNA the catalytic RNase H-like active site located in the PIWI domain is in position to cleave the targeted mRNA (Faehnle & Joshua-Tor, 2010). And because of their siRNA binding as well as catalytic activities, AGO proteins are believed to form the core components of the RISC-mediated RNA silencing mechanism that, among other roles, have an antiviral function (Hock & Meister, 2008, Carmell et al., 2002).

Not all AGOs are capable of slicing mRNAs (Song & Joshua-Tor, 2006). A prerequisite for AGO catalytic activity was initially thought to be the presence of the crucial histidine residues on the DDH motif active sites, however, of the four human AGOs (hAGO), only hAGO2 possesses a slicing activity and hAGO3 has the correct DDH motif but is still inactive for slicing (Liu et al., 2004a, Rivas et al., 2005). In flies, AGO1 mutants are defective in miRNA-mediated silencing, but not in siRNA-directed

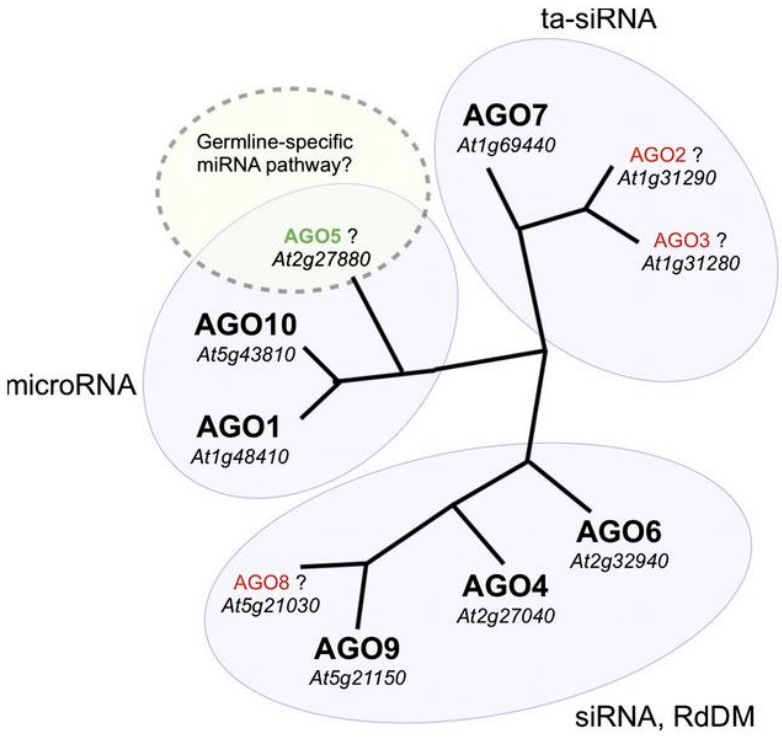

Figure 1.2. ARGONAUTE protein family in *Arabidopsis* (AtAGOs). Phylogenetic tree illustrating the 10 Argonaute family proteins in *Arabidopsis*, subdivided into the three main functional classes based on sequence homology: miRNA-guided slicing and translational repression of target transcripts, trans-acting siRNA (ta-siRNA) activity, and chromatin remodeling by siRNA-directed DNA methylation (RdDM). Although sequence analysis places AGO2 and AGO3 in the ta-siRNA class and AGO8 in the RdDM class, their functions have not been experimentally proven as yet and could fall in any of the other classes mentioned. AGO5, a close relative of AGO1 and AGO10, is thought to be involved in a novel miRNA pathway in the *Arabidopsis* male germline (Borges, 2011).

cleavage, whereas AGO2 mutants are defective in siRNA-directed cleavage but not in miRNA silencing (Okamura et al., 2004). Of the ten *Arabidopsis* AGOs (AtAGOs), eight have an intact DDH motif predicted for slicing activity; the other two, AtAGO2 and AtAGO3, have an aspartate in place of the histidine, which in analogy to RNase H should be able to functionally substitute for the histidine. However, only AtAGO1 has been empirically shown to be an RNA Slicer (Baumberger & Baulcombe, 2005b), and it is not clear whether the others are RNA slicers or even whether this activity is required for their function. AtAGO4, for example, appears to be involved in chromatin silencing; however, it is not known if it uses slicing activity in this role.

In the commonly used plant model *A. thaliana*, at least 10 AGOs have been identified with varying roles ranging from the regulation of developmental processes to defense responses (Hutvagner & Simard, 2008, Zhang, 2011, Benning, 1998, Manavella, 2011). AGO1, AGO7 and more recently AGO2 have been reported to play an antiviral defense role (Morel et al., 2002, Zhang et al., 2006, Baumberger et al., 2007, Bortolamiol et al., 2007, 2008., Qu et al., 2008, Wang et al., 2011, Harvey, 2011). Figure 1.2 shows a phylogenetic tree illustrating the 10 ARGONAUTE proteins in *Arabidopsis*, subdivided into the three main functional classes based on sequence homology (Borges, 2011).

In the plant-virus model host *Nicotiana benthamiana* however, as well as many other higher plants, the antiviral defense roles of specific AGOs have not been extensively investigated. As evidenced by the recent release of its draft genome by the Boyce Thompson Institute for Plant Research (News, 2012), genomic information for *N. benthamiana*, a well established host for plant-virus research (Goodin et al., 2008) is rapidly accumulating. It is also susceptible to many more viruses than the plant model *Arabidopsis* and mounts a biochemically tractable RNAi response to viral infections (Omarov et al., 2006, Pantaleo et al., 2007). *Arabidopsis*, for example is not susceptible to the *Tomato busy stunt virus* (TBSV) with a wide host range spanning approximately 120 plant species and an excellent virus for studying the RNA silencing pathway (Silhavy & Burgyan, 2004, Ding & Voinnet, 2007, Scholthof, 2006).

System: Virus induced gene silencing and the *Tobacco rattle virus* system

Viruses vary in shapes, size and nucleic composition; DNA-single (ss) or double stranded (ds), RNA positive or negative, single or double stranded and retro-transcribing (rt) which can be ssRNA or dsDNA. However, irrespective of their nature, all viruses while replicating produce transcripts which momentarily exists as dsRNA structures ideal to trigger the PTGS mechanism.

In molecular biology, transgenics is not always a viable option due to the costs and time required to obtain stable transformants. Furthermore, plant knockout lines are currently only available for *Arabidopsis*.

However, by using virus vectors carrying a fragment of a gene of interest, the PTGS mechanism is triggered against both the virus and the host mRNA sequence carried in the virus vector causing the gene of interest to be significantly down-regulated or knocked down (Baulcombe et al., 2001). Virus induced gene silencing (VIGS) offers the advantage of being a rapid experimental procedure with phenotypes being observed in as little as 3 weeks and does not require full-length cDNA sequences to function, therefore experiments can be initiated even in the absence of complete gene sequence information. Furthermore, since VIGS is transient, the phenotype affects only a portion of the plant unlike what occurs in stable RNAi or mutant plants where the loss-of-function phenotype occurs throughout the plant, increasing the occurrence of lethal phenotypes, hence limiting gene function evaluations (Scofield, 2009).

In *N. benthamiana*, our model plant system, *Tobacco rattle virus* (TRV) is a suitable candidate for use as a virus vector because it replicates abundantly and moves systemically yet does not cause symptoms that significantly deter normal plant growth and development (Baulcombe et al., 2001, Ratcliff et al., 2001, Burch-Smith et al., 2004) as seen in Figure 1.3. Because of these characteristics, TRV is suitable choice of a vector used to stimulate VIGS and induce an RNAi response with detectable characteristics. TRV is a bipartite virus of the *Tobravirus* genus and *Virgaviridae* family. It is a non-enveloped, helical, rod shaped positive ssRNA virus composed of two segments about 200 and 100 nm in length and 22 nm in diameter. Figure 1.4 illustrates the genome

structure of TRV while Figure 1.5 shows the schematic representation of the en empty TRV vector used to initiate silencing.

TBSV and the PTGS mechanism

Tomato bushy stunt virus (TBSV), a model virus for study in our laboratory is the type member of the *Tombusvirus* genus in the *Tombusviridae* family (Yamamura & Scholthof, 2005). It is a positive-sense single-stranded RNA plant virus whose entire genome (Figure 1.6) is approximately 4.8 kb, is encapsidated by a T=3 icosahedral particle composed of 180 subunits of a 41 kDa capsid protein (CP) and has a diameter of about 33 nm (Hearne et al., 1990, Yamamura & Scholthof, 2005). TBSV is a soil-borne pathogen with no known biological vector (Yamamura & Scholthof, 2005). It has a wide experimental host range, with more than 120 species from over 20 families showing varying degrees of susceptibility.

In *N. benthamiana*, our model host plant, TBSV abundantly accumulates and causes severe symptoms characterized by stunted growth, severe leaf necrosis and eventual plant demise (Figure 1.7). When RNA transcripts of full-length TBSV cDNA are rub-inoculated onto susceptible host plants, infection results with similar symptoms (Scholthof, 1999).

The PTGS mechanism is used by plant species to eradicate viral intruders. However many viruses encode proteins that interfere in various ways with the silencing process. *Tombusviruses* like TBSV are well suited to study antiviral RNA silencing because they generate abundant substrates for DCL to yield high levels of siRNA but also encode a 19-kDa protein that is a potent suppressor of RNA silencing (Vargason et al., 2003, Ye et al., 2003). The proposed mode of action of P19 shown in Figure 1.8 is the appropriation of virus-derived siRNAs thereby preventing their subsequent incorporation into an antiviral RISC (Scholthof, 2006b, Silhavy & Burgyan, 2004a).

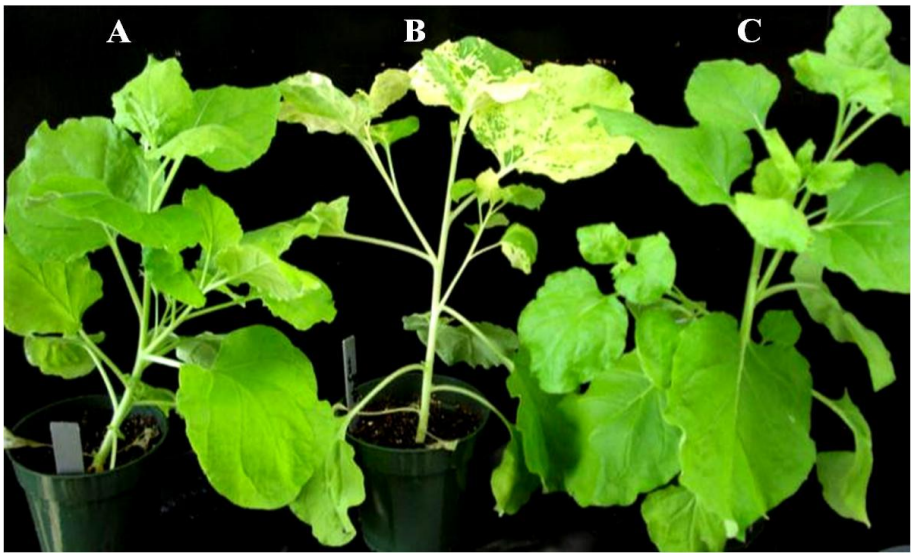

Figure 1.3. *N. benthamiana* plants approximately 4 weeks after inoculation with *Tobacco rattle virus* vectors. The healthy control plant **A** was not agro-inoculated; Plant **B** was inoculated with the TRV vector carrying a fragment of the *Magnesium Chelatase* gene (*TRV-MgCh*) exhibiting the photobleaching phenotype characteristic of successful silencing of this gene, while plant **C** was agroinfiltrated with an empty vector (*TRV-OO*).

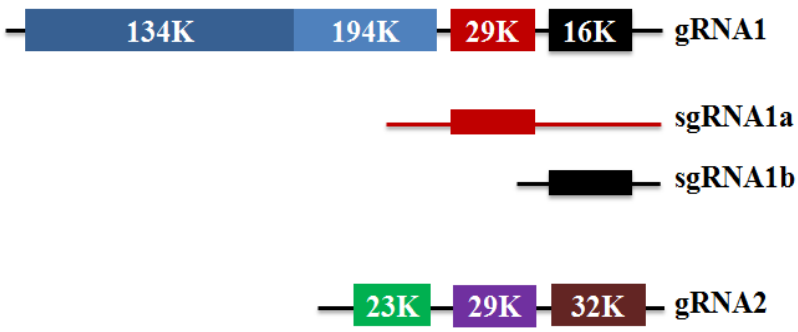

Figure 1.4. Genomic organization of TRV. Genomic RNA1 encodes four open reading frames (ORF); ORF1 translates directly into a 134 kDa protein with methyltransferase and helicase domains, and via ribosomal read-through into ORF 2, a 194 kDa product with RNA-dependent RNA polymerase function. ORF3, product of a subgenomic RNA produces a 29 kDa movement protein and the fourth ORF results in a cysteine-rich 16 kDa protein that is possibly involved in viral gene expression. Genomic RNA2 is encodes 3 ORFs; a 23kDa capsid protein, a 29 and 32 kDa proteins both involved in nematode transmission.

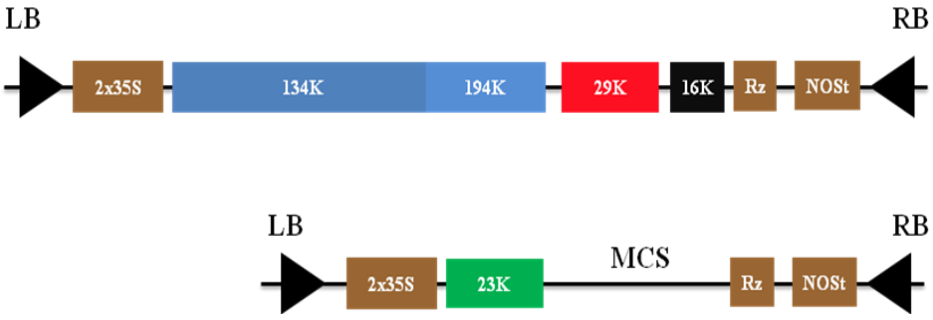

Figure 1.5. A schematic representation of the *TRV-00* vector used to initiate VIGS. A TRV-gRNA1 cDNA is inserted between duplicated *Cauliflower mosaic virus* (CaMV) 35S promotors (2x35S) and a nopaline synthase terminator (NOSt). LB and RB refer to the left and right borders of the T-DNA and Rz is a self-cleaving ribozyme that facilitates the release of 5' elements after Agroinfiltration (Liu et al., 2002a). In genomic RNA2 (also flanked by the 2X35S and NOst), the 29 and 32 kDa nematode transmission factors are removed to create a multiple cloning site (MCS) wherein the fragments of the gene of interest is to be inserted. Upon agro-inoculation, the cassette launches infective viral RNA.

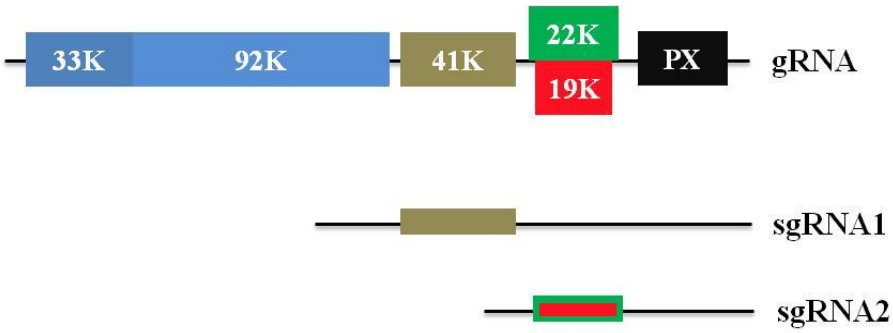

Figure 1.6. Organization of the TBSV genome. TBSV encodes five major ORFs, (computer translations however stipulate a sixth ORF of about 30–70 kDa at the 3' end (Boyko, 1992)) from the genomic RNA and two subgenomic RNAs (Fig. 7). ORF 1 and 2 constitute the replicase components of the virus; P33 is directly translated from the 5' end of the major sgRNA, and P92 by read-through from partial UAG stop codon (Scholthof et al., 1995b). sgRNA1 directly translates into a 41 kDa capsid protein, while sgRNA2 encodes two nested genes to yield P22 and P19. P22 the 22 kDa movement protein is directly translated and P19, a silencing suppressor is expressed as a result of leaky scanning P22 (Scholthof et al., 1999, Scholthof et al., 1995a). The enigmatic PX possesses its own start codon and is therefore possibly translated from another sgRNA (Boyko, 1992). It is seen to variably affect viral RNA accumulation in a host-dependent manner (Scholthof, 1997).

In *N. benthamiana* the 22 kDa P22 movement protein has been shown to be involved in cell-to-cell movement by binding viral RNA for transport to the plasmodesmata (Desvoyes, 2002) , meanwhile the 41 kDa capsid protein and the 19 kDa silencing suppressor are essential to facilitate and maintain systemic spread (Qu, 2002).

Our laboratory is in possession of agroinfiltrable TBSV-GFP chimeric constructs incapable of systemic spread since the CP has been replaced by GFP; one of which has a functional (TG) and another a defective (TGdP19) P19 silencing suppressor (Figure 1.9). Agroinfiltration of TG chimeric constructs leads to a rapid (visible in as little as 2 days) and high accumulation of GFP in wild type *N. benthamiana* plants. The leaf later exhibits necrosis and dies. However, P19 defective TBSV (TGdP19) mutants fail to accumulate visible amounts of GFP in plants due to the success of the PTGS pathway (Scholthof, 2011). And, because it universally blocks the programming of RISC by sequestering 21-bp duplex siRNAs, P19 is used in various RNA silencing research even with other non-tombusviruses as in our experiments.

Previous experiments in our laboratory show that in *N. benthamiana,* mutants of the *Tomato bushy stunt virus* (TBSV) lacking the P19 silencing suppressors are very susceptible to RNA silencing as expected and as shown in Figure 1.8. However, we also consistently found that in the absence of a newly identified AGO2-like protein (NbAGO2), silenced using the TRV-VIGS system, wt-TBSV as well as TBSV-P19 mutants accumulated high viral titers suggesting that the silencing mechanism may have been compromised as seen in Figures 1.10 and 1.11.

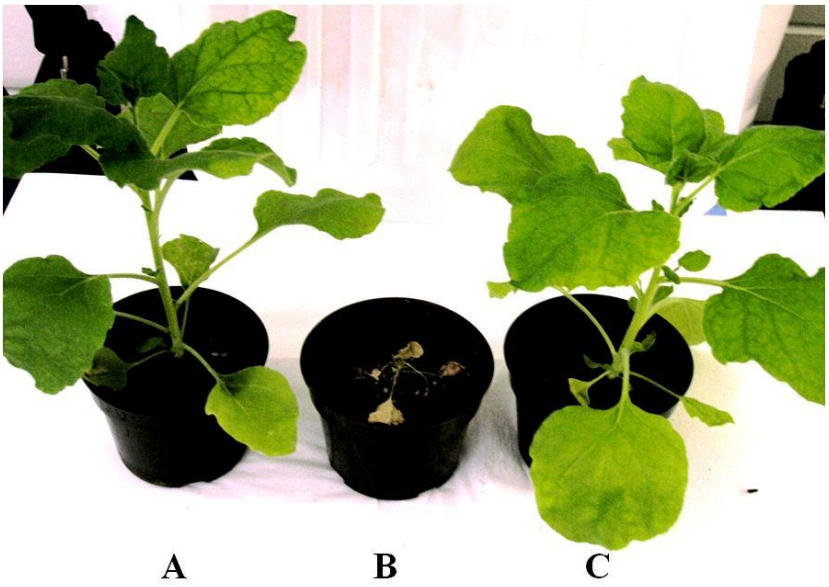

Figure 1.7. TBSV infection in *N. benthamiana* plants. Plant **A** is a healthy control not infected with TBSV. Plant **B** infected with wild type TBSV succumbs to the infection, while plant **C** infected with the mutant deficient for the silencing suppressor protein P19 recovers and eventually clears the infection (Ciomperlik, 2008).

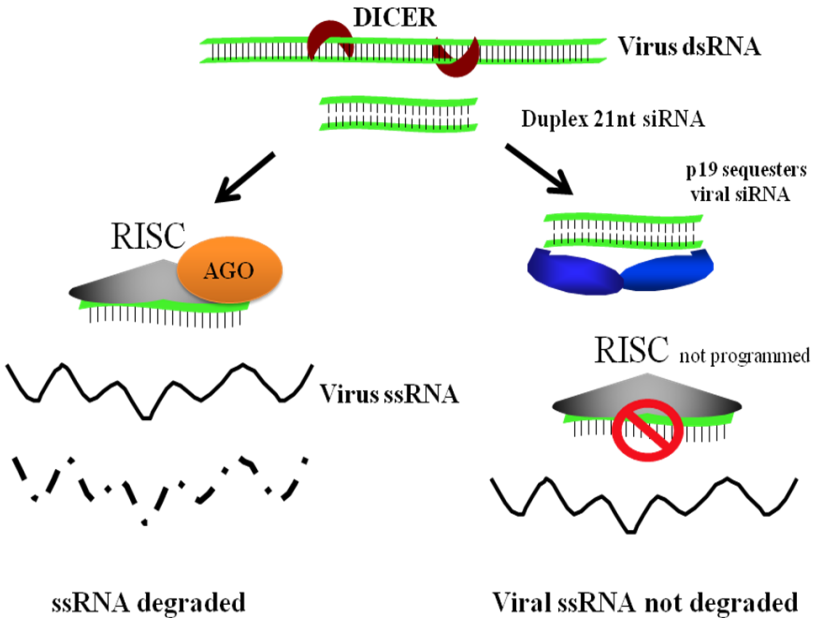

Figure 1.8. A simplified proposed model of the interaction between TBSV P19 and the PTGS pathway.

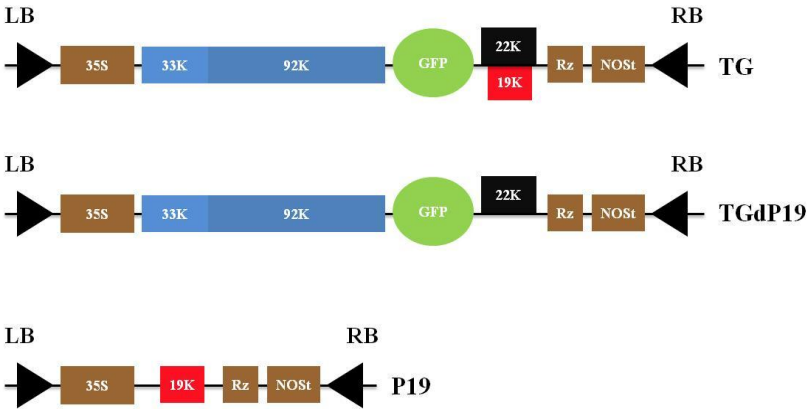

Figure 1.9. Agroinfiltrable versions of GFP-chimeric TBSV and P19 constructs. **TG**: TBSV construct whose CP has been replaced with GFP and encodes a functional *P19* silencing suppressor. **TGd19:** Same as TG only with a defective p19. **P19:** Agroinfiltrable *P19* construct that can be co-infiltrated with any other construct and universally suppresses silencing.

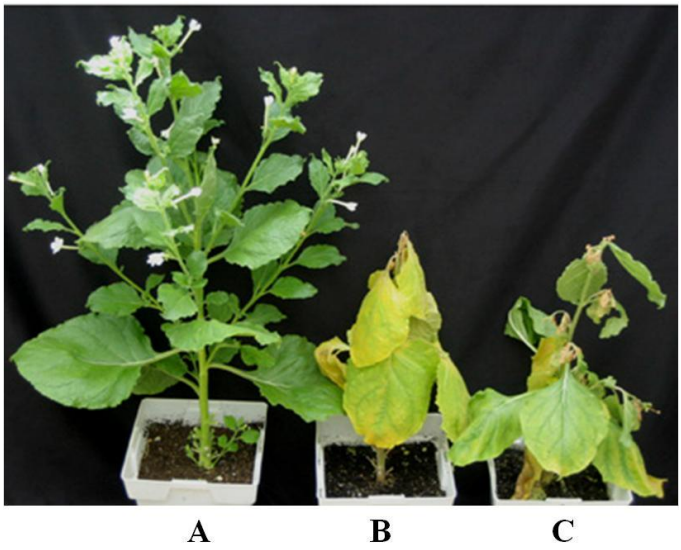

Figure 1.10. Effect of *NbAGO2* silencing on TBSV infection in *N. benthamiana*. **A:** Non-inoculated, **B:** inoculated with a WT TBSV and **C:** with the P19 defective mutant TBSV (Scholthof, 2011). In comparison to Figure 1.8, in a normal non-AGO2 silenced plant, the P19 defective mutant TBSV is subjected to silencing and the plant recovered.

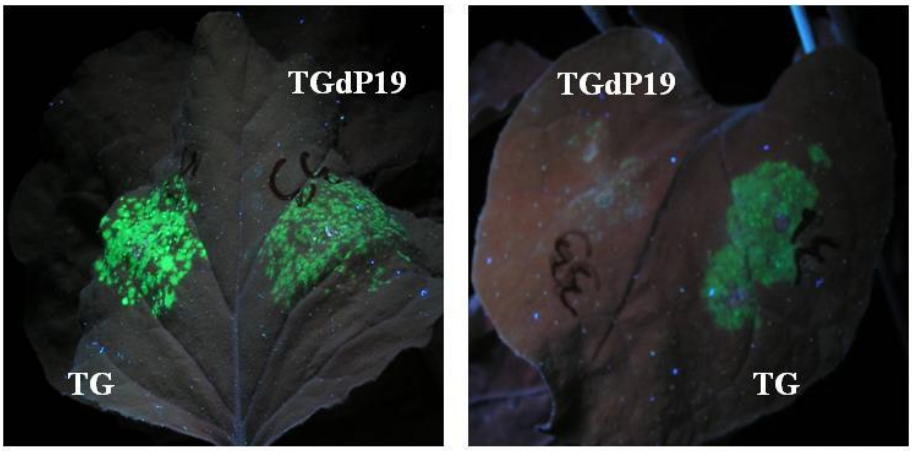

Figure 1.11. Half-leaf assays showing the effect of *NbAGO2* silencing on infection with TBSV-GFP chimeric constructs. Leaf **A**: from a *TRV-NbAGO2* silenced plant and **B**: from an empty TRV vector infiltrated plant. TGd19 is seen to accumulate visible GFP levels only in the absence of NbAGO2 (Odokonyero, D; unpublished data).

Similarly, half leaf assays using agroinfiltrable TBSV-GFP chimeric constructs defective for its P19 silencing suppressor TGdP19 showed the accumulation of GFP in *N. benthamiana* leaves exclusively silenced for NbAGO2 as shown in Figure 1.11.

Furthermore, the activity of this NbAGO2 was shown to be directly associated with anti-TBSV RNA silencing, and did not influence silencing of transiently expressed transgenes such as GFP; indicative of a primarily antiviral defense role (Scholthof et al, 2011). This is the first such discovery for any virus-host system not involving the commonly used plant model *Arabidopsis.* My principal intent therefore was to investigate whether additional antiviral activities could be identified for other NbAGO proteins against other plant viruses.

Hypotheses and Research objectives

Hypothesis 1

Specific AGOs may possess antiviral silencing roles that occur in a precise plant-virus type dependent manner. Evidence to support this hypothesis is our observation that NbAGO2 is involved in anti-TBSV silencing and not against other transgenes or some other viruses (Scholthof, 2011). The temporal abundance and distribution of the *AGO* genes hence their silencing roles may also be tissue dependent. To test this hypothesis, I therefore formulated the following objectives:

- Determine the distribution of the different *NbAGO* mRNA transcript levels in various plant tissues at different plant developmental stages through semi-quantitative PCR and real time quantitative PCR. Discussed in Chapter II.
- Test whether virus-induced gene silencing of *NbAGO2* as well as other known *AGOs* in *N. benthamiana* also renders the plants more susceptible to viruses other than TBSV. Discussed in Chapter III.

Hypothesis 2

Plant AGOs may have redundant functions, therefore silencing of only one of the AGOs may not result in any observable effects against a given virus. This hypothesis is

supported by a recent paper that reports the redundancy of NbAGO1 and NbAGO2 in miR408-mediated plantacyanin regulations (Maunoury, 2011) as well as observations that the *Arabidopsis* AGOs 4 and 6 may have redundant and or additive functions (Zheng et al., 2007). My objective therefore was to:

- Silence all the possible combinations of the different AGOs and test silenced plants against a wide array of viruses. Discussed in Chapter IV.

Hypothesis 3

Synergisms and or antagonisms may exist in mixed infections and mar experimental observations. The mechanisms by which multiple infections usually create unpredictable biological and epidemiological consequences are largely unknown (Syller, 2011). In our VIGS systems, we use TRV to induce systemic silencing and later infiltrate with test virus incapable of systemic spread. Prior TRV infection has been seen to exacerbate TBSV infection, meanwhile not much is known about the interaction between TRV and other test viruses. My objective therefore was to:

- To induce RNA silencing using hairpin vectors instead of TRV VIGS in both transient and transgenic assays and validate the observations made when using VIGS to silence *NbAGO2*. Discussed in Chapter V.

CHAPTER II

DETERMINATION OF THE TEMPORAL ABUNDANCE AND DISTRIBUTION OF ARGONAUTES IN *N. BENTHAMIANA* TISSUES

Introduction

The biogenesis of most small non-coding RNA classes, including micro-RNAs (miRNAs) and many short-interfering RNAs (siRNAs), requires the action of the RNase III family of proteins. In order to perform their effector functions, these short RNAs must be incorporated into ARGONAUTE-protein-containing complexes which vary in their degrees of specialization and expression patterns (Ender & Meister, 2010). Plant AGOs show preferences for distinct classes of siRNAs produced by result of specific pathways: AtAGO1 for example principally prefers miRNAs arising as a product of DCL1 processing, AtAGO4 prefers heterochromatin associated RNAs (hcRNAs) processed by DCL3 (Baulcombe et al., 2010), and AtAGO7 preferentially binds to ta-siRNAs. Furthermore, different Dicers produce distinct small RNAs: DCL1 and 4 produce 21-nt RNAs, DCL2 a 22 nt-RNA and DCL3 24 nt-RNAs. These Dicers have also been proposed to reside in different subcellular compartments (Mi et al., 2008a).

Results of deep sequencing of siRNA associated with AGO family members clearly indicated distinct preferences in siRNA terminal nucleotides. AGO1 preferentially recruited siRNA with a 5' terminal 'U', AGO2 and AGO4 were selectively associated with siRNA sequences beginning with 'A' while AGO5 mainly bound RNAs starting with a 5' 'C' (Takeda et al., 2008). A simple alteration of the terminal nucleotides redirected the observed siRNAs into different AGO complexes in a fairly predictable manner. An exception to the rule however, miR390 with an 'A' predicted to be recruited by AGO2 was instead, exclusively loaded by AGO7 and altering its terminal base nucleotides did not cause any redirection to another AGO complex (Montgomery et al., 2008) suggesting although critical, the nature of the terminal base is not the only factor involved in AGO recruitment. Table 2.1 outlines a

Table 2.1. A summary of the 5' terminal nucleotide and size preferences of *Arabidopsis* AGOs determined through immunoprecipitation experiments. Also included are the clade member assignations of the different AGOs (Ki Wook Kim, 2011).

Family member	Clade	5' terminal nucleotide preference	sRNA length preference (nt)
AGO1	1/5/10	U	21
AGO2	2/3/7	A	21
AGO3	2/3/7	Unknown	Unknown
AGO4	4/6/8/9	A	24
AGO5	1/5/10	C	24
AGO6	4/6/8/9	A	24
AGO7	2/3/7	Unknown	Unknown
AGO8	4/6/8/9	Unknown	Unknown
AGO9	4/6/8/9	A	24
AGO10	1/5/10	Unknown	Unknown

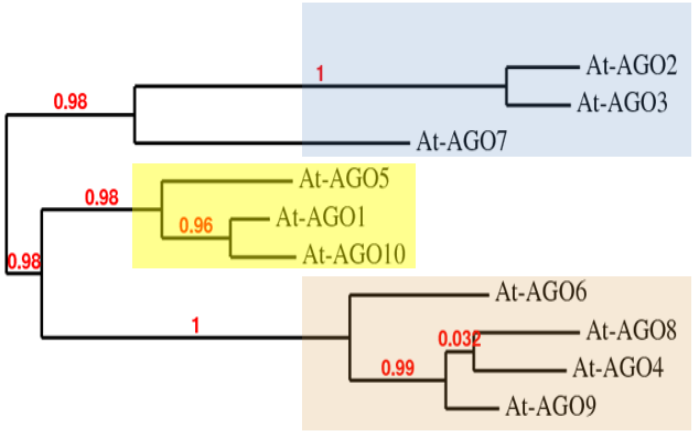

Figure 2.1. A non- rooted phylogenetic tree constructed from available full-length amino acid sequences of the ten *Arabidopsis* AGO family members. The three distinct clades are shaded in different colors. Using the online 'Méthodes et Algorithmes pour la Bio-informatique' software (Dereeper et al., 2008) at *phylogeny.fr*, bootstrapping was performed with 1,000 bootstrap replicates, and percentage of bootstrap support is shown by values at the branch nodes of the tree.

summary of the 5' terminal nucleotide and size preferences of *Arabidopsis* AGOs determined through immunoprecipitation experiments.

In the model plant *Arabidopsis*, different AGOs have been known to play critical roles in multiple developmental processes, such as the maintenance of undifferentiated stem cells in the stem apical meristems (Lynn & Barton, 1999, Moussian, 1998), establishment of leaf polarity (Liu, 2009), proper leaf, cotyledon, stem and inflorescence development as well as a general plant fertility (Mallory et al., 2009, Fagard et al., 2000, Benning, 1998, Adenot et al., 2006). In *Drosophila*, AGOs have also been known to be involved in tissue-specific antiviral response (Eleftherianos et al., 2011).

Phylogenetic analysis of amino acids (Figure 2.1) of the AGO protein family identified three distinct clades, namely the AGO1/AGO5/AGO10, AGO2/AGO3/AGO7, and AGO4/AGO6/AGO8/AGO9 clades (Vaucheret, 2008). Although the distribution of the 10 AGOs into the three clades was based purely on amino acid sequence homology and does not infer similarities in activity or redundancy in function, several examples of functional redundancy were identified between AGO clade members, namely between AGO1 and AGO10 of the AGO1/5/10 clade (Mallory et al., 2009, Manavella, 2011), and AGO4, AGO6 and AGO9 of the AGO4/6/8/9 clade (Havecker et al., 2010).

The AGO1/AGO5/AGO10 clade

AGO1 regulates sRNA-mediated gene expression for all known Arabidopsis miRNAs, hence most *ago1* mutants exhibit pleiotropic developmental defects that normally led to the eventual demise of the plant characterizing a defect in miRNA function (Baumberger & Baulcombe, 2005a, Vaucheret, 2005). As previously mentioned, AGO1 preferentially loads miRNA with a 5' terminal uracil residue. The majority of plant miRNAs also posses the 5' terminal uracil (Mi et al., 2008b) and are favored to be loaded onto AGO1 which is known to represses target gene expression via miRNA-mediated target transcript cleavage. Although Brodersen *et al* propose that AGO1 can also repress target gene expression via translational repression (Brodersen et

al., 2008), it has not been empirically determined that this is a widespread silencing mechanism in plants. *AGO1* transcript levels are regulated by a miRNA miR168 ensuring constant levels of the crucial *AGO1* gene (Mallory and Vaucheret, 2010).

AGO1 is also known to be involved in the biogenesis of trans-acting siRNAs (tasiRNA) by loading miRNAs miR173 and miR828 (Allen et al., 2005, Rajagopalan et al., 2006, Yoshikawa et al., 2005) to target the non-protein coding transcripts *Tas1*, *Tas2* and *Tas4* for miRNA-directed cleavage. This cleavage marks the products for dsRNA synthesis by the RNA-directed RNA polymerase RDR6 (Peragine et al., 2004) which processes the molecules and is loaded by AGO1-catalyzed RISC for sRNA-mediated transcript cleavage (Yoshikawa et al., 2005). AGO1 has also recently been shown to be involved in the generation of transitory siRNA from sRNA cleaved transcripts (Chen et al., 2010, Cuperus et al., 2010). It is also known to mediate siRNA-directed RNA silencing with siRNA sources being from an infecting virus or an introduced transgene. The involvement of AtAGO1 in antiviral defense is further discussed in the introductory section of Chapter III.

The importance of AGO1 is reflected in its ubiquitous expression at high levels as shown by transcriptome data in Figure 2.2. Furthermore, in an experiment using an AGO1 promoter fused to a GUS reporter gene, the reporter gene was found to be active in all tissues although activities were highest in meristematic cells and vascular tissue (Vaucheret et al., 2006). And, although AGO1 also seems to function in both the cytoplasm and nucleus of the plant cell, it appears to be process viral RNA only in the cytoplasm. While in the nuclei, AGO1 is most concentrated around small nuclear bodies termed ‘nuclear dicing bodies or D-bodies (Fang & Spector, 2007, Song et al., 2007).

The expression profile for *Arabidopsis AGO5* transcripts is highly specific to reproductive tissues (Figure 2.2) accumulating in the sperm cell cytoplasm in mature pollen and growing pollen tubes (Borges, 2011, Schmid et al., 2005). Unlike AGO1 however, AGO5 is able to bind a highly conserved miRNA miR169 (which does not have a 5’ U) (Mi et al., 2008, Takeda et al., 2008). Although its function in *Arabidopsis* has not been confirmed, miR169 is critical in petunia leaf development and anthirinum

(Cartolano et al., 2007, Combier et al., 2006) suggesting that the AGO5/miR169 may be involved in regulation of gene expression in *Arabidopsis*. Furthermore, *ago5* mutants do not appear to be susceptible to any other viruses tested (Harvey et al., 2011b, Wang et al., 2011b) and T-DNA knockout lines are wild-type in appearance.

The AGO10 mutant alleles, *pinhead* and *zwille* identified by forward genetic screens (Lynn et al., 1999, Moussian et al., 1998) are characterized by abnormal shoot apical meristems (SAM) development and yet do not display any other discernible phenotypes. The high levels of amino acid sequence similarity theoretically indicated a possibility of function redundancy between AGO1 and AGO10; however, *ago10* unlike *ago1* mutants still effectively carried out post transcriptional gene silencing and showed no reduction in the accumulation of miRNAs, tasiRNA and other RNAs associated with AGO1 (Morel et al., 2002, Takeda et al., 2008).

Recent observations have demonstrated the crucial need for AGO10 in the regulation of SAM by specifically interacting with miR165 and miR166 both of which regulate the expression of class III homedomain-Leucine Zipper (HD-Zip III) transcription factors (Liu, 2009, Zhu et al., 2011) which ultimately determine the fate of the SAM. AGO10 is thought to specifically sequester miR165/166 duplexes to prevent their incorporation into AGO1 and subsequent repression of the HD-ZIP III transcription factors (Zhu et al., 2011). It is therefore AGO10's strong binding capability and not its slicing activity that is the determinant of its interaction. By fusing the promoter sequence to a reporter gene, AGO10 was seen to be more limited to whole embryos, in the provascular strands and the adaxial side of cotyledons (Mallory et al., 2009b).

The AGO2/AGO3/AGO7 clade

AGO2 and AGO3 share a very high level of amino acid sequence homology although no functional redundancies have been reported between the two AGOs. All members of this clade share overlapping expression domains, with AGOs 2 and 3 being most highly expressed in developing seeds and fruits and at slightly lower levels in leaves and flowers (Schmid et al., 2005). Both AGOs 2 and 3 are expressed in the

nuclease as well as the cytoplasm (Takeda et al., 2008) and knockouts of these AGOs show no phenotype deviating from that expressed by the wild-type plants (Lobbes et al., 2006). Even though a northern blotting has shown accumulation of numerous short RNA species assessed in *ago2* and *ago3* mutants (Takeda et al., 2008, Katiyar-Agarwal et al., 2007), AGO2 is known to preferentially load short RNA species including viral RNA possessing a 5' terminal adenine residue (Mi et al., 2008a, Takeda et al., 2008).

AtAGO2 has been implicated in antiviral defense against *Turnip crinkle virus* (TCV) and *Cucumber mosaic virus* (CMV) (Harvey et al., 2011a). However, *ago2* mutants were not susceptible to any other viruses, indicative of its specificity. Harvey *et al* therefore proposed that the induction of AGO2 upon TCV and CMV infection may have been a result of decreased accumulation of the AGO1-dependent AGO2 regulating miRNA miR403 (Harvey et al., 2011a). This may indicate that the system could have evolved to provide backup protection against viruses that attack AGO1with their silencing suppressors for example 2b of CMV and P38 of TCV or it simply is an accidental consequence of reduced miR403 levels (Ki Wook Kim, 2011). Further details on the antiviral role of AGO2 will be discussed in the introductory section of Chapter III.

Alleles of *ago7* mutants exhibited accelerated juvenile-to-adult phase change in Arabidopsis (Hunter et al., 2003, Peragine et al., 2004, Yoshikawa et al., 2005) as well as floral morphogenesis defects characteristically associated with disruption of TAS3 biogenesis (Adenot et al., 2006, Garcia et al., 2006). AGO7 has since been demonstrated to function exclusively in the TAS3 tasiRNA biogenesis pathway (Montgomery et al., 2008) where miR390 is specifically loaded to AGO7 to direct its binding to two miR390 target sites within the Tas3 mRNA. AGO7 then cleaves the targeted transcript at the 3' target site marking the cleaved mRNA for RDR6-directed dsRNA synthesis (Montgomery et al., 2008, Yoshikawa et al., 2005). Some TAS3-specific tasiRNAs are subsequently loaded onto AGO1 to target the auxin response factor family members *Arf3* and *Arf4* for cleavage-based repression, and since ARF3 and ARF4 are necessary for specification of the adaxial fate of *Arabidopsis* rosettes (Fahlgren et al., 2006), AGO7-mediated miR390 directed regulation of gene expression is essential for normal plant

development. AGO7 is predominantly expressed in the vasculature of seedlings, in the tissues and cells surrounding the SAM (Montgomery et al., 2008) and in the adaxial-most cells of newly developing leaves further confirming its importance in proper leave development (Fahlgren et al., 2006, Garcia et al., 2006). Just like *ago2* mutants, the *ago7* mutants were only hyper-susceptible to TCV infection (Qu et al., 2008) but not any other virus furthermore indicating a very specific AGO-virus association. AGO7 besides miR390 does not show any 5' terminal nucleotide preference suggesting the presence of a specialized association mechanism.

The AGO4/AGO6/AGO8/AGO9 clade

AGO4 functions in the effector step of RNA-directed DNA methylation (RdDM) to maintain transposons in their epigenetically silent state through sRNA-directed DNA methylation of the repetitive genomic sequences (Zilberman et al., 2004, Xie et al., 2004). It preferentially binds repeat-associated (rasiRNAs) and heterochromatin-specific (hcsiRNAs) siRNAs. Although many of the rasiRNAs and hcsiRNAs posses varying 5' terminal adenine, cytosine, guanine and uracil residues, AGO4 preferentially binds short RNAs with a 5' terminal adenine residue (Mi et al., 2008a, Havecker et al., 2010a). The *ago4* mutants were first identified using forward genetics for mutants impaired in transcriptional gene silencing of the SUPERMAN locus along with the RdDM machinery proteins CHROMOMETHYLASES3 (CMT3) and KRYPTONITE (KYP) (Zilberman et al., 2004).

Array data (Schmid et al., 2005) illustrated in Figure 2.2 shows that *AGO4* is expressed ubiquitously throughout the plant tissue which was also consistent with the GUS reporter observations (Havecker et al, 2010). AGO4 appears to be exclusively located in the nucleolus where it co-localizes with the RdDM proteins RDR2, DCL3 and DOMAINS REARRANGED METHYLASE2 (DRM2) specifically in cajal bodies and AB bodies (Li et al, 2006, Pontes et al, 2006). The localization of AGO4 in these specialized nuclear bodies clearly indicates its importance in sRNA-directed DNA methylation and maintenance of heterochromatin integrity (Irvine et al., 2006). Even

though AGO4 has not been directly linked to any specific antiviral defense, *ago4* mutants were exceptionally susceptible to the bacterial pathogen *Pseudomonas syringae* suggesting its role in the activation of pathogen-specific defense mechanisms (Agorio & Vera, 2007). Kim *et al* however suggest that is also possible that epigenetic down regulation of other genes in the *ago4* mutant plant could account for the susceptibility observed (Ki Wook Kim, 2011).

AGO6, with similar expression patterns to AGO4 (Schmid et al., 2005, Havecker et al., 2010) appears to play a partially redundant or additive role with AGO4 as the level of transgene reactivation was demonstrated to be even higher in the *ago4/ago6/ros1* triple mutant when compared to either of the double *ago4/ros1* mutants (Zheng et al, 2007). These observations suggest that these two AGOs may act on a shared subset of repeat elements, and that their overlapping function occurs in similar tissues and at the same developmental time point.

Just like AGOs 2 and 3, AGO8 and 9 have very high amino acid sequence similarities and are therefore believed to have arisen due to a recent gene duplication event (Vaucheret, 2008) and also like AGOs 2 and 3 are located on the same chromosomes on the *Arabidopsis* genome. Microarray data (Figure 2.2) also shows that their expression patterns are very similar. AGO8 levels are however generally lower than AGO9 levels especially in reproductive and actively meristematic tissues. AGO8 contains a splicing-induced frame-shift which is predicted to render the AGO8 protein non-functional hence a pseudogene (Takeda et al, 2008). AGO9 has been loosely linked to siRNA-directed maintenance of the silencing state of repetitive DNA elements (Havecker et al., 2010a) as well as an apomixes-like fertilization-independent seed production phenotype (Olmedo-Monfil et al, 2010).

The 10 AtAGOs can therefore be classified as RNA slicers, RNA binders and chromatin modifiers. Members of the AGO1/5/10 clade are slicers, clade 2/3/7 bind although AGO7 has been demonstrated to direct *Tas3* cleavage), and the four remaining family members of the AGO4/6/8/9 clade are chromatin modifiers. Generally speaking therefore, AGOs regulate certain age-related as well as standard developmental

processes by acting upon specific tissues at specific times, hence the hypothesis that its abundance would vary as the plant develops, and under different prevailing situations in different tissues. A compilation of transcriptome array data (Figure 2.2 below) documenting the expression of *Arabidopsis* AGOs in different tissues during normal development shows that the different AGOs are constitutively expressed in roots, stems, leaves, apices, seeds and flowers as well as other floral organs. Its distribution and abundance among the different tissues is however quite diverse.

The commonly used plant model *Arabidopsis thaliana* is however not the most suitable host to study plant-virus interactions due to its recalcitrant susceptibility to a number of plant viruses, including our model virus TBSV. *N. benthamiana* on the other hand provides a proven model system used in the study of plant-virus interactions due to its susceptibility to a number of plant viruses and the availability of a completely sequenced genome. Furthermore, AGOs have only been extensively studied in *Arabidopsis*, yet *N. benthamiana*, member of the *Solanaceae* would provide more direct potential platform for translational research onto food crops such as potato, tomato and eggplant.

In light of the above indication that AtAGOs are expressed variably based on the type of plant tissue, developmental phase as well as prevailing conditions caused by both biotic and abiotic agents; my specific objective was therefore to determine the temporal abundance and distribution of the *AGO* transcripts in young (less than 4 weeks) and old (after flowering; over 7 weeks old) *N. benthamiana* roots, leaves and stems undergoing normal development.

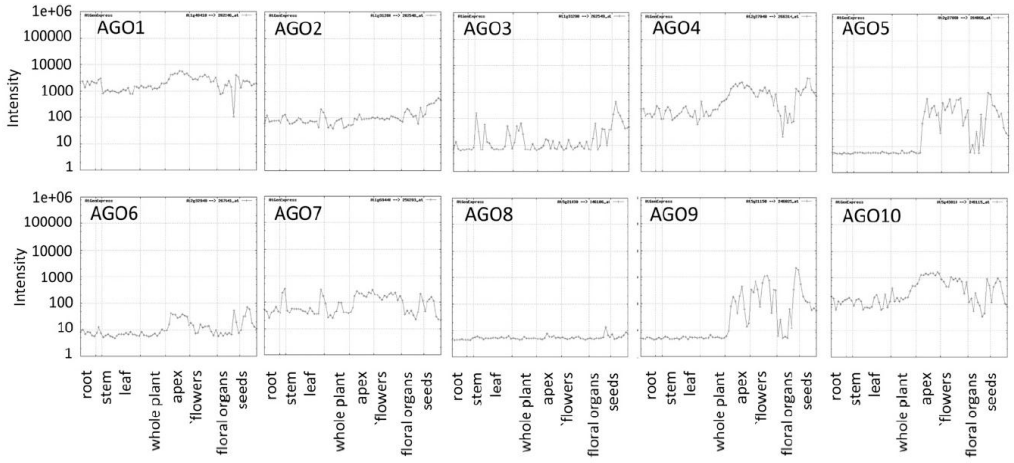

Figure 2.2. Transcriptome microarray analysis showing expression profiles of the 10 *Arabidopsis AGO* genes during normal growth and development (Schmid et al., 2005). *AtAGO1* is the most highly and consistently expressed throughout the whole plant meanwhile *AtAGO8* on the other hand is the least expressed. Expression of *AtAGO5* and *-9* follow a similar pattern; they are both very lowly expressed in vegetative parts of the plant but are 10 fold more expressed in the plants reproductive parts and apex. *AtAGO4* and *-10* also follow a similar pattern only with a less drastic increase in expression in actively dividing tissues. *AtAGO2*, *-3*, *-6* and *-7* are relatively less expressed and follow a similar pattern with occasional irregular peaks and lows within the same tissues at different time points.

Materials and methods

Extraction and purification of total RNA

N. benthamiana plants were grown in a growth chamber with 25/22°C day/night temperature cycles and 16-h-light/8-h-dark cycles. The plants sampled were 3, 4 and 5 week old plants as a representation of the young tissues and 10, 12 and 16 week old plants for older tissues. Prior to extraction of RNA, TLE buffer was prepared to a final concentration of 0.18 M Tris, 0.09 M LiCl solution, 4.5 mM EDTA adjusting final pH to 8.2, then addition of 1% SDS. Total RNA was then extracted by homogenizing approximately 0.5g of leaf, stem and root tissues in 1.5 mL of Extraction Buffer (made by mixing 10 mL of the previously prepared TLE Buffer, 0.9 mL of a 2 M sodium acetate, 10 mL of acidic phenol, 2 mL of chloroform and 10 uL of beta-mercaptoethanol) in a mortar and pestle. The resulting slurry was transferred to an RNase-free 1.5 mL eppendorf tube and centrifuged at 13000 g for 6 minutes at room temperature. The upper aqueous layer was transferred to a new eppendorf and mixed with an equal volume of a 1:1 phenol and chloroform, vortexed and centrifuged again at 13000 g for 6 minutes at room temperature. The resulting aqueous phase was mixed with an equal volume of chloroform, vortexed and centrifuged again at 13000 g for 10 minutes at room temperature. The aqueous phase was then transferred into a new 1.5 mL RNAse-free eppendorf tube and 1/3 of 8M LiCl was added and left to precipitate at -20^{o}C for at least 2 hours. Total RNA was pelleted by centrifuging at 15000 g for 20 minutes at 4^{o}C. The resulting pellet was washed with a 70% ethanol solution before briefly drying in a spin vac. The pellet was resuspended in nuclease free IX TE buffer.

Contaminant genomic DNA was degraded using Ambion TURBO DNA-free DNAse (Life Technologies, Carlsbad, CA). 10X TURBO DNAse buffer was added to a final concentration of 1X and 1 uL of TURBO DNAse is added to the resuspended RNA sample, mixed gently and incubated at 37^{o}C for 30 – 45 min. 0.1 volume of DNAse inactivation reagent was added and mixed well prior to incubating at room temperature and occasionally agitating for 5 minutes. The DNAse inactivation reagent was then

separated from the total RNA by centrifugal forces at 10000 g for 2 min at room temperature. Total RNA concentration was quantified using a NanoDrop (Thermo Fisher Scientific, Waltham, MA) with typical averages of 500 – 1500 ng/uL.

In order to verify the quality and integrity of the resulting total RNA, 5 uL (+1 uL of 5 X loading dye) electrophoresed through a 1% agarose gel, stained with ethidium bromide and visualized under UV light. The RNA loading dye used contains trace amounts of formaldehyde which helps to denature RNA that migrates through the agarose gel in a linear relation to the log of its molecular weight (similar to DNA). Figure 2.3 shows a sample of the RNA quality typically obtained using this method of RNA isolation. The remaining RNA was then either stored for future use at -20^{o}C or used straight away to make complementary DNA (cDNA) for PCR analysis.

Reverse transcription and the synthesis of cDNA from total extracted RNA

Reverse transcription was carried out using M-MLV Reverse Transcriptase (Life Technologies) reagent. *Moloney murine leukemia virus* Reverse Transcriptase (M-MLV RT), isolated from *E. coli* uses single-stranded RNA in the presence of a primer to synthesize a complementary DNA strand up to 7 kb (Kotewicz et al., 1985, Kotewicz et al., 1988, Gerard et al., 1997). First strand cDNA synthesis is carried out by adding 1 µL oligo-dT 12-18 bp (500 µg/mL), 4 µg total RNA and 1 µL 10mM dNTP in a nuclease-free 200 uL PCR tube. Sterile distilled water was added to achieve a total volume of 12 uL. It was then gently mixed and heated in a PCR machine at 65^{o}C for 5 minutes after which it was quickly chilled on ice. This step is critical for disruption of RNA secondary structures so as to facilitate oligo-dT or other gene specific priming. The PCR tube contents were then briefly centrifuged to collect the contents at the bottom of the tube.

To the above samples, a mixture of 4 µL 5X First-Strand Buffer, 2 µL 0.1 M DTT, 1 µL RNaseOUT Recombinant Ribonuclease Inhibitor (40 units/µl) and 1 µL M-MLV reverse transcriptase was added and gently mixed by taping the sides of the tube. The contents of the PCR tube are once more collected by a brief centrifugation.

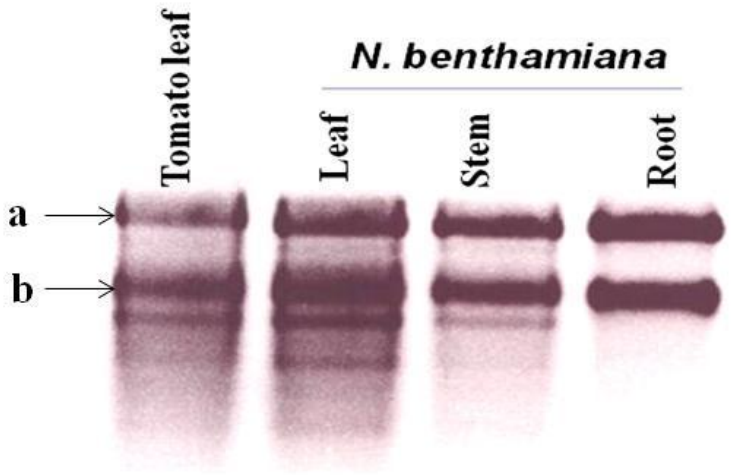

Figure 2.3. A sample of total RNA electrophoresed through a 1% agarose gel. Extracted from *S. lycopersicum* leaf, and *N. benthamiana* leaf, stem and root, DNAse treated to show quality of extracted RNA. Bands labeled '**a'** and '**b'** represent 28 and 18s, ribosomal RNAs respectively.

The tubes were then incubated in a PCR machine at 37^{o}C for 52 minutes, followed by a transcriptase inactivation step at 70^{o}C for 15 minutes. The synthesized cDNA was then either stored at -20^{o}C or directly used for PCR.

Semi-quantitative and Quantitative Real-Time PCR

Conventional/semi-quantitative as well as RT qPCR primers were designed to amplify sequences of endogenous *AGO* cDNA. The methods section of Chapter III explicitly explains the details as of how the primers for qRT PCR were designed. Utmost care was taken during primer design so as not to amplify sequences from other *AGOs* as well as avoid sequences inserted into the TRV virus vector to initiate endogenous gene silencing (see chapter III). Prior to primer design and synthesis, all known AGO sequences (*NbAGO-1, -2, -4, -5, -6, -7* and *–X)* were aligned using MUSCLE (MUltiple Sequence Comparison by Log- Expectation) online software (EBI, 2012). The output files were then customized for easy viewing using BOXSHADE 3.21 online software (ch.EMBNET.org, 2012) and unique sequence regions were selected for primer design. The alignment and BOXSHADE output files can be found in the Appendix data portion of this thesis.

Although the principles behind the primer designs were the same, the qRT PCR primers were designed to amplify between 75 and 150 bp of sequences while the conventional PCR primers between 350 and 1000 bp of AGO sequences. Initially, because of the flexibility associated with longer amplicon sequences, primer design for conventional PCR had been predicted to be much less tedious than its qRT PCR counterparts, however, it was quickly realized that it would not be the case since the primers designed from many regions of the sequences did not amplify the expected sizes and had to be redesigned in other regions of the sequence multiple times. While other primers were designed based on the above mentioned strategy, primers for *NbAGO1* were directly obtained from Jones (Jones et al, 2006) as well as those for *Actin*, our reference gene whose primers were obtained from Thangavelu (Thangavelu et al., 1993).

All the primers were designed such that their melting temperatures oscillated between 58 and 62^{o}C so that they could all be included in the same cycle run for a more precise comparison of results.

Conventional semi-quantitative PCR was set up in an Applied Biosystems 2720 Thermal Cycler, 2.5µl of DNA a 10X loading dye (30% glycerol, 0.25% bromophenol blue, 10 mM Tris pH 8.0 and 2.5 mM EDTA) was added to the samples and 15ul were run on a 1% agarose gel at 100 volts in 1X TBE (90 mM Tris, 90 mM Boric acid, 2 mM EDTA) for 30 min. These gels were then stained with ethidium bromide for 30 min, and viewed with a UV light box. Results obtained using the conventional PCR primers were verified using qRT PCR. The procedures for primer design and analysis for qRT PCR are explained in the Materials and methods section of chapter III.

After determining the efficiencies of the designed qRT PCR primers, the primers were then used to verify the amount of specific *AGO* transcript levels in the plant tissues. A comparative method (delta Ct) (Pfaffl et al., 2002, QIAGEN, 2004) was used, whereby the differences in C_t values between the target (*AGO*) and reference genes (*Actin*) are first calculated to normalize initial template concentrations. After normalization, the C_t values were then compared directly. The exponential data shown by the normalized C_t (delta C_t) values were converted to a linear scale by calculating the Log base 2 ^ - (delta Ct). The resulting values were the portrayed on 2D column charts complete with error bars so as to validate significance of the biological repeats.

The data obtained was further analyzed for statistical relevance using the standard student t-test, P-values range from zero to 1 and refer to the probability of observing data at least as extreme as that observed, given that the null hypothesis was true. If the obtained p-value was small (less than 0.05), then it was concluded that the null hypothesis was either false or an unusual event had occurred, hence results were significant. The data obtained from RT qPCR was then analyzed for statistical relevance based on the standard deviation values using the standard student t-test.

PCR setup		PCR conditions	
Template (cDNA)	2.0 µl	94°C ..... 5 min	
10X Thermopol Buffer	2.5 µl	94°C ..... 30 sec	40 cycles
10 mM dNTP	0.5 µl	55°C ..... 30 sec	
10 µM primer forward	0.5µl	68°C ..... 1 min	
10 µM primer reverse	0.5 µl	68°C .....10 min	
Taq polymerase	0.125µl	4°C ..... ∞	
H_2O	19.0 µl		
TOTAL	25 µl		

Figure 2.4. PCR parameters and conditions for conventional semi-quantitative PCR.

***N. benthamiana Actin* primers**

Actin-F: GCTTCAGTGAGTAGTACAGGGTGTTC
Actin-R: ATGGCAGACGGTGAGGATATTCA

***N. benthamiana AGO 1* primers**

Ex AGO1-F: CATACCCAGTGGCCTTGTCT
Ex AGO1-R: ATTCGATTGCCAAACTCC

***N. benthamiana AGO 2* primers**

Ex AGO2-F: GGATAGTTGCAGGTCGTAGC
Int. AGO2-R: TCTTCAGCCCGTACCATTTC

***N. benthamiana AGO 4* primers**

Ex AGO4-F: AAGGGCGTGTTCTGCCTGCC
Ex AGO4-R: GCCTGCATGGGCACACAGGT

***N. benthamiana AGO 5* primers**

Ex AGO5-F: GCCACCTGCCTATTACGCCCA
Ex AGO5-R: TCCGAAACCCACCATACAGTTGC

***N. benthamiana AGO 6* primers**

Ex AGO6-F: ATGCCATGCCTGGATGTCGGAA
Ex AGO6-R: AAGGATCCCACAACCGCAGCAA

***N. benthamiana AGO 7* primers**

Ex AGO7-F: CGGCCGGGATGTCAAAGGTGT
Ex AGO7-R:CGCTCGGGGAGTTTTAGAAGCTCC

***N. benthamiana AGO X* primers**

AGOX-F: ATGTCGGAACGTGGACGCGG
AGOX-R: TCCCGATCAGCAACACTCACGA

Figure 2.5. List of primers used for conventional PCR. The primers were designed to amplify between 350 and 1000 bp and have melting points between 58 and 62^{o}C. All primers labeled 'Ex-' denote that they amplify sequences of the endogenous gene not included in the TRV construct. *NbAGOX* and *AGO2* reverse primers however amplified parts of the sequences in their respective *TRV-AGO* constructs.

Results

Conventional semi-quantitative PCR

Generally, the primers designed for conventional PCR were able to amplify the expected size fragments. Amplicons from *AGOs 2, 4* and *6* were sequenced and confirmed to be the correct *AGO* sequences eliminating the probability of amplification of any other closely related *AGO*. Tissues were sampled were from 3 week old plants as a representation of the young tissues and 8 week old plants for old tissues.

The PCR primers used for semi-quantitative analysis were designed to amplify between 350 and 1000 bp of endogenous *NbAGO* cDNA. The resulting amplicons were of 300, 650, 750, 400, 650 and 600 bp for *NbAGOs 1, 2, 4, 5, 6* and *7* respectively. Numerous futile attempts were made at designing primers for conventional PCR amplification of endogenous *NbAGOX* (details about *NbAGOX* is discussed in the introductory section of Chapter III). Multiple primers were designed to amplify across varying regions of the available 814 bp sequence but none of them successfully amplified an expected size amplicon when used with complementary DNA template from either *N. benthamiana* or *N. tabacum*.

Semi-quantitative PCR results (Figure 2.6) showed varying levels of *NbAGO* expression in the tested tissues. However, by simply observing the amplicon intensity, *NbAGOs 1, 2*, *4* and *5* seemed to be more abundantly expressed across all tissues than *6*, *7* and *X*. More specifically however, the results indicate that *NbAGO1* transcripts were expressed ubiquitously throughout plant leaves, stems and roots of both young and old plants. Except for the consistently observed reduction of the transcript levels in leaves of young plants, *NbAGO2*, just like *NbAGO1* was seen to be expressed fairly uniformly in all tested plant tissues. *NbAGO4* mRNA levels were noticeably reduced in the stems of young plants, but seemed to remain ubiquitously expressed in leaves and roots irrespective of age. *NbAGO5* transcripts were clearly and consistently reduced in the leaves of the young as well as older plants. However, its expression in stems and roots were observed to be similar irrespective of plant age.

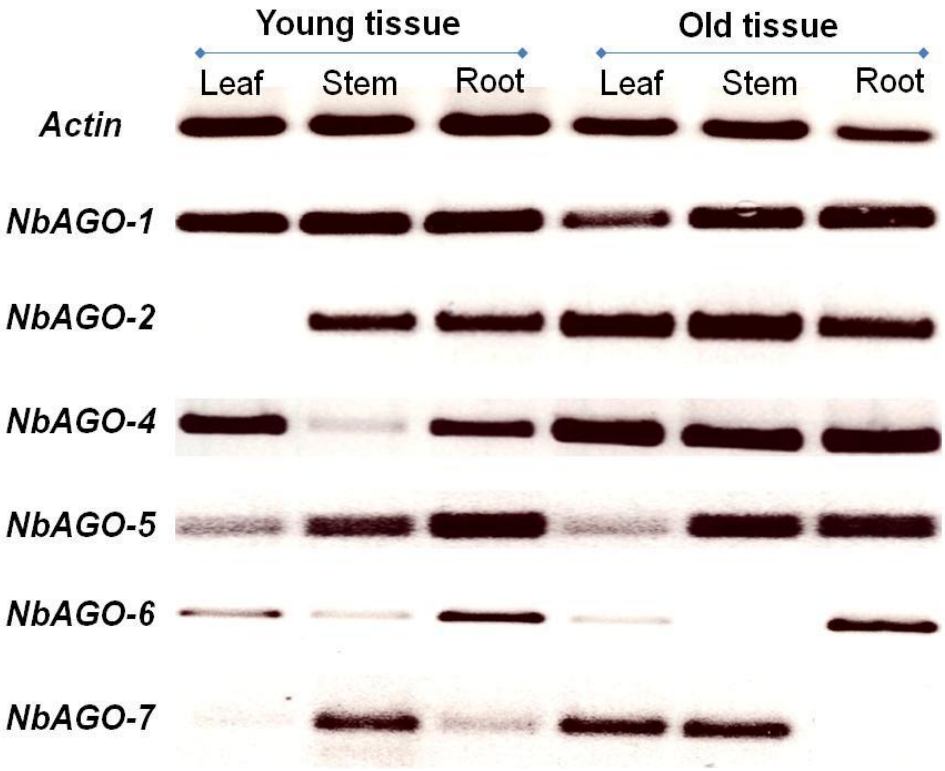

Figure 2.6. Semi-quantitative PCR results illustrating the general distribution pattern of *N. benthamiana AGO* genes in young and old leaves, stems and roots. These experiments were repeated at least 3 times with slightly varying results and the results shown here represent the most consistent observations.

NbAGO6, one of the least abundantly expressed transcripts was fairly highly expressed only in the roots of both 3 and 8 week old plants. In both young and old plant leaves and stems, *NbAGO6* expression was drastically reduced when compared to its expression in root tissues.

NbAGO7 expression varied depending on plant age. It was observed that in the younger plants, the stems expressed the highest transcript levels whereas in older leaves and stems both had comparable levels of *NbAGO7* transcripts.

Conventional or semi-quantitative PCR results merely present a qualitative analysis and apart from the inability to test for individual primer efficiencies for impartial comparison, one of its biggest limitations is its inconvenience when precise quantification or comparison of amplicon levels are required, hence the need for a more quantitative analysis system provided by quantitative Real-Time PCR.

Quantitative Real-Time PCR Results

The designed qRT-PCR primers were first subjected to a preliminary test run and PCR products were electrophoresed through a 1% agarose gel to ensure correct amplification of endogenous AGO cDNA. Details are discussed in Materials and methods section of chapter III. Here, only results of the successfully tested primers with proven efficiencies used in qRT-PCR are presented.

Unlike conventional PCR, a quantitative PCR analysis is able to amplify and simultaneously quantify a given target intensity at any given PCR cycle. The quantity is then assigned either an absolute number of copies or a relative amount when normalized to a given normalizing gene which has to be stably expressed in a given set of tissues (Vandesompele et al., 2002, Perez-Novo et al., 2005). The *actin* gene, highly conserved among all eukaryotes (Thomas et al., 2003, Langer et al., 2002, Bezier et al., 2002) was chosen as a normalizing gene because it is abundantly and universally expressed throughout *N. benthamiana* cells in roots, stems as well as leaves (data not shown). After normalization to the gene of reference and linearization of the C_t values, target

abundance was then directly compared on a 2D column chart fitted with error bars as shown in Figures 2.7 and 2.8 below. Tissues were sampled were from 3 week old plants as a representation of the young tissues and 8 week old plants for old tissues. Samples were obtained from three biological replicates, and additionally three technical replicates were set up. The experiments were repeated at least 2 times and all results showed similar tendencies.

The overall results shown in Figure 2.7 illustrate that largely, *NbAGOs 1, 2* and *4* were the most abundantly expressed, irrespective of the plant tissue or age. Likewise, the expression of *NbAGOs 6, 7 and X* in all tissues regardless of plant age were observed to be very low; generally more than a 2 fold decrease when compared to *NbAGO1*, four-fold when compared to *NbAGO2* and approximately 7 fold less than *NbAGO4*. These observations were comparable to results reported with semi-quantitative PCR analysis shown in the previous section. Furthermore, it is safe to speculate that these arbitrary comparative expression values may indicate the importance of each AGO in the particular plant developmental stage.

The individual *AGO* qRT-PCR results shown in Figure 2.8 illustrate close-ups of the expression levels of the specific *NbAGOs* in particular tissues thereby providing a clearer picture of the specific distribution of a given *NbAGOs* in leaves, roots and stems of both the old and young plants.

NbAGO1 transcripts generally appeared to be more abundantly expressed in the older plants. However, also notable is the significant abundance of *NbAGO1* in 3 week old *N. benthamiana* stems when compared to its leaf and root tissues. In the 8 week old plants however, levels of *NbAGO1* seem to be comparable to each other. Similarly, the expression pattern of *NbAGO2* transcripts in all tissues mirror the expression of *NbAGO1* transcripts in that the older tissues show higher mRNA levels than its younger counterpart. Quite distinct, however is the significant low expression of *NbAGO2* in the 3 week old leaves, when compared to its roots and stems which show transcript levels of more than 10 times the amount observed in leaves. In comparison, in the older leaves,

the levels of *NbAGO2* mRNA were also higher in stems and roots when compared to its leaves by about 1.5 and 2.2-fold.

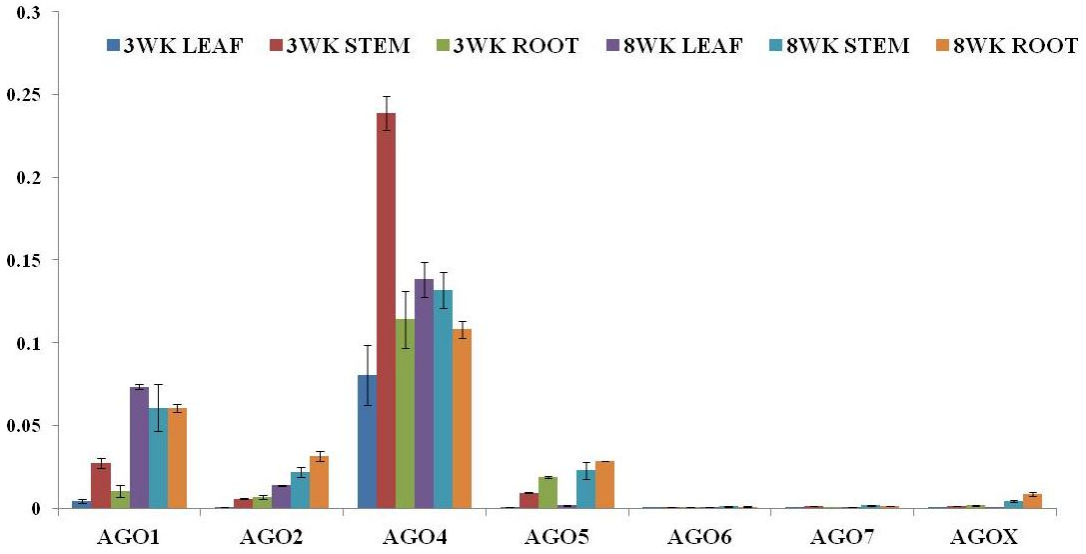

Figure 2.7. qRT PCR results illustrating the general distribution pattern of *N. benthamiana AGO* genes in 3 and 8 week old plant leaves, stems and roots. Overall, *NbAGOs 1, 2, 4* and *5* appear to be the most abundant. With the exception of *NbAGO4* in 3 week plant stems, the older 8 week *N. benthamiana* plants appear to generally express more *AGO* mRNA irrespective of the *AGO* and tissue in question. Furthermore, with the exception of AGO4 in 8 week old plants, leaves of both young and older plants quite distinctly appear to express the least amount of any of the *AGO* transcripts. Also quite discrete is the similarity in expression pattern between *NbAGO5* and *X*, as well as among *NbAGOs 4, 6* and *7*. Values on the y-axis represent the relative abundance of each *AGO* transcript.

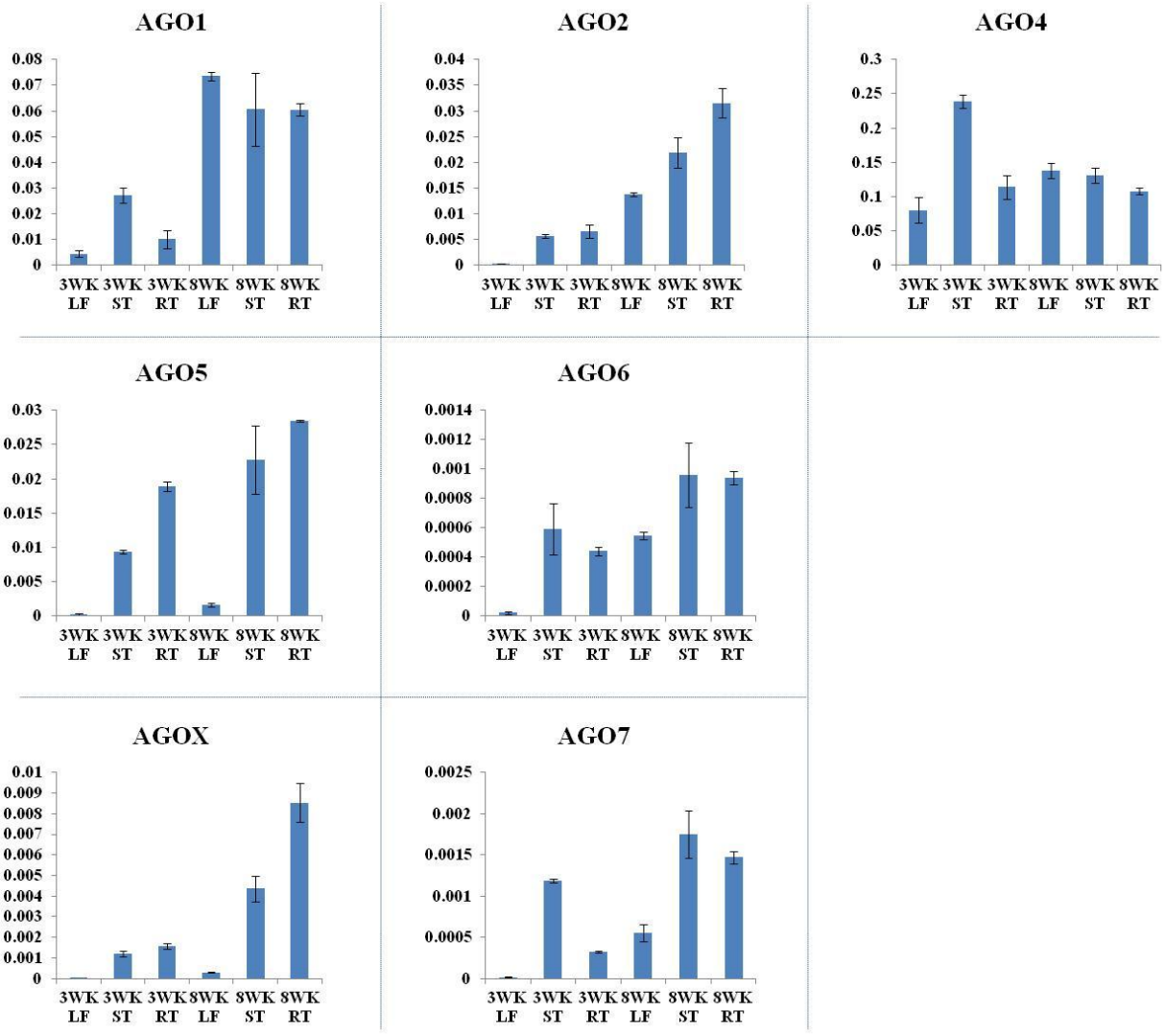

Figure 2.8. Quantitative RT-PCR results illustrating the distribution pattern of individual *N. benthamiana AGO* transcripts in young and old leaves, stems and roots. The values on the y-axis indicate the relative abundance of the AGO transcripts.

With the exception of the significantly high expression seen in 3 week old stems, *NbAGO4* transcripts were observed to be expressed at similar levels in all tissues irrespective of the difference in plant age. The expression pattern of *NbAGO5* is quite distinctly similar to that observed in *NbAGO2*. In both 3 and 8 week old plants, the expression of *NbAGO5* is quite noticeably low in leaves, and highest in roots. It is also important to note that although the expression levels of *NbAGO2* and *5* follow a similar pattern and appear to be at comparable levels of abundance; *NbAGO5* appears to be more abundant than *NbAGO2* in young roots and *NbAGO2* appears to be more highly expressed in older leaves than *NbAGO5*.

NbAGO6, just like *NbAGO4* also seem to be fairly equally expressed in older plant tissues and young stems and roots. An exception was observed in the 3 week old leaf where its expression was observed to be drastically low. *NbAGO7* mRNA levels were also observed to be significantly low in young leaves, and just as observed with *NbAGO6* higher in corresponding stems. This trend was also observed in older plants, although the levels of *AGO* transcripts in corresponding leaves were not as dramatically low as observed in the younger plants when compared to stems and roots. *NbAGOX*, although expressed at much lower levels also follows a similar distribution pattern observed with *NbAGO2* and *5* transcripts where the leaves show remarkably low levels of mRNA when compared to corresponding roots and stems.

In summary, both conventional semi and –quantitative real-time PCR analysis results consistently showed that the most abundantly expressed *AGOs* in *N. benthamiana* are *1, 2, 4* and *5* irrespective of plant tissue and age. Both PCR analyses also consistently showed the low expression levels of *NbAGO2* in young plant leaf tissues and the generally higher abundance of *NbAGO2* transcripts in older tissues. A striking discrepancy is however observed in levels of *NbAGO4* where conventional PCR showed distinctly low levels of transcript while the inverse is observed in qRT-PCR. Both PCR results also distinctly show low levels of *NbAGO5* mRNA in both young and old leaves.

Generally speaking therefore, the results obtained by the two PCR methods largely concur with each other and the observations made herein can be deemed trustworthy.

Discussion

As hypothesized, the expression profiles of the different *NbAGOs* were seen to vary depending on plant tissue and age. In the model plant *Arabidopsis*, microarray data showed that of the 10 different *AGOs*, *AGO1* was the most abundantly and consistently expressed throughout the whole plant (Schmid et al., 2005). AtAGO1 is known to play critical roles in the proper development in multiple tissues, translational repression as well as post transcriptional gene silencing hence its antiviral defense role (Baumberger & Baulcombe, 2005b, Vaucheret, 2005, Brodersen et al., 2008, Yoshikawa et al., 2005). Given its importance in the plant system, it is only expected that it be abundant and consistently expressed throughout the plant. Our results also show that transcripts of its *N. benthamiana* homologue *NbAGO1* are also generally expressed abundantly and fairly consistently especially in the older plant tissues. When *NbAGO1* was silenced using a TRV VIGS system, numerous developmental abnormalities were observed in *N. benthamiana* leaves, flowers and apical meristems (Jones, 2006). Further experiments also determined that the *NbAGO* is required for full systemic silencing further highlighting its importance and justifying its abundance and ubiquitous expression levels.

In *Arabidopsis, AtAGO1* was found to be most active in meristematic cells and vascular tissue (Vaucheret, 2006). Our results show significantly high levels of *NbAGO1* in young stems compared to its leaves and roots. This was in accordance to the prior predictions since the stem tissues harvested contained regions of actively differentiating cells that forming new leaves and branches. However, the older plant tissues expressed significantly more *NbAGO1* possibly due to the fact that in the 3 week old plants, the vasculature was not yet fully developed and therefore was not apt for the localization of NbAGO1. Furthermore, this assertion may be supported by the fact that during the purification of total RNA, when using the young stems, the whole stems was chopped and homogenized whereas when using the older stems, only the fleshy bark was used

and the fibrous woody interior discarded. This action may have resulted in the concentration of vascular tissues where the AGO is localized, hence the observed significant spike in *NbAGO1* transcripts in the older stems when compared to the younger ones.

Just like *NbAGO1*, *NbAGO2* transcripts were also observed to be more generally abundant in older plant tissues. In *Arabidopsis*, array data shows that under normal stress-free conditions *AtAGO2* was very highly expressed in developing seeds and fruits, but in comparison, lowly in roots, stems and leaves (Schmid et al., 2005). Following the same analogy therefore, the tissues used for analysis were expected to express uniformly transcript levels. The young leaves however, distinctly show reduced amounts of *NbAGO2* transcripts compared to corresponding stems and roots. Although this atypical observation cannot be explained at this time, it sheds more light on previous observations made in our laboratory that *N. benthamiana* plants were more resistant to TBSV infection caused by inoculation of its roots than its leaves (publication in preparation), possibly due to the abundance of the anti-TBSV NbAGO2 in roots.

Also, similar to the plant model *Arabidopsis*, our results show that in *N. benthamiana*, the *NbAGO4* transcripts were abundantly expressed in all tested tissues in spite of their age difference. AtAGO4 has been implicated in sRNA-directed DNA methylation, maintenance of heterochromatin integrity (Irvine et al., 2006) as well as specific transcriptional gene silencing (Zilberman et al., 2004). *AtAGO4* has also been linked to the general *Arabidopsis* defense mechanism not necessarily involving gene silencing (Agorio & Vera, 2007). These vitals roles justify its abundance in expression throughout the plant. Jones *et al* suggest that both *NbAGO1* and *NbAGO4* act on silencing pathways, but at different stages. They specifically suggest that the short interfering RNA amplification step required for full systemic silencing is dependent upon a nuclear event requiring the activity of *NbAGO4* (Jones, 2006).

NbAGO5, also highly expressed in stems and roots of both young and old tissues also showed a similar trend in expression to *NbAGO1* and *2* transcripts. In *Arabidopsis*, array data showed that *AtAGO5* found on the same clade as *AtAGO1* showed a decent

spike in expression levels in sites of active cell division such as the apex, flowers, floral organs and seeds (Schmid et al., 2005); However, within the tissues used for analysis in *N. benthamiana* (roots, stems and leaves), irrespective of plant age, the leaves consistently showed the lowest levels of *NbAGO5* transcripts. Although not yet empirically confirmed, in *Arabidopsis, AtAGO5* is speculated to be involved in regulation of gene expression, giving a possible explanation to it similarity in expression with *NbAGO1* confirmed to be involved in regulation of gene expression. The high transcript levels shown in stems and roots can be attributed to fact that both stem and root tissue harvested were sites of active cell division, hence hotspots for localization of AGOs involved in regulation of gene expression.

Our qRT-PCR results show that *NbAGOs 6, 7,* and *X* were the least expressed transcripts in *N. benthamiana*; at least 10-fold less expression than *NbAGOs 1, 2, 4* and *5*.

The overall expression pattern of *NbAGO6* almost exactly mirrors that of *NbAGO4*. In *Arabidopsis,* AtAGO6 seems to have a partially redundant role with AtAGO4 hence may be involved in some aspect of DNA-methylation and heterochromatin remodeling to a certain degree. We therefore also speculate that its N. benthamiana homologue *NbAGO6* may also play a partially redundant role in DNA-methylation and heterochromatin remodeling just like *NbAGO4*. *AtAGO7* on the other hand is involved in the TAS3 tasiRNA biogenesis pathway ultimately affecting proper leaf and seed development (Montgomery et al., 2008). Array data shows inexplicably erratic levels of expression of both *AtAGOs 6* and *7* depending on tissue and age (Schmid et al., 2005). The expression of *NbAGO7* also quite distinctly mirrors that of *NbAGO1* in 3 week old tissues which may be attributed to its functional similarity to NbAGO1. *NbAGOX* and *NbAGO5* previously speculated to the same show similar expression patterns and therefore may be the same, or have very similar roles in *N. benthamiana*.

The results shown above although not decisive help give us a better understanding of *NbAGOs* in *N. benthamiana* a great plant model to study the

involvement of the ARGONAUTE family of proteins in RNA silencing. *NbAGOs 1, 2, 4* and *5* were observed to be the most abundantly expressed in all tissue. Generally, *NbAGOs 1, 2, 5, 7* and *X*, while more abundant in older tissues, were also expressed significantly highly in stems and roots than in corresponding leaves. It is fairly evident therefore, that even though the *N. benthamiana* AGOs are homologues of the *Arabidopsis* AGOs, their distribution and abundance within the different tissues at different developmental stages vary slightly hence their possible function may be expected to vary as well. It is also possible that AGOs in *N. benthamiana* posses different *cis*-regulatory motifs that regulate their expression in a different manner than those observed in the plant model *Arabidopsis*.

CHAPTER III

IDENTIFICATION OF AN ARGONAUTE FOR ANTIVIRAL SILENCING IN *N. BENTHAMIANA*

Introduction

The RNA silencing mechanism among other functions has an antiviral defense role. ARGONAUTE proteins (AGOs) are known to be principal components of this mechanism hence indirectly play a critical role in antiviral defense. RNAi models predict that AGOs form the key catalytic units of RNA induced silencing complex (RISC) that directly cleaves RNA or indirectly by means of translational repression (Baulcombe, 2004, Ding & Voinnet, 2007).

The *Arabidopsis* AtAGO1 has been shown to be involved in the generation of transitory siRNA from sRNA cleaved transcripts (Chen et al., 2010, Cuperus et al., 2010). It is also known to mediate siRNA-directed RNA silencing with siRNA sources being from an infecting virus or an introduced transgene. AtAGO1 is the main AGO family member involved in antiviral defense and *ago1* mutants are seen to be extremely susceptible to various viruses including the *Cucumber mosaic virus* (CMV) (Morel et al., 2002, Zhang et al., 2006) and members of the *Polerovirus* family (Baumberger et al., 2007, Bortolamiol et al., 2007, Bortolamiol et al., 2008), in fact these viruses encode suppressors that directly target the action of AGO1. And, although AtAGO1 also seems to function in both the cytoplasm and nucleus of the plant cell, it appears to be process viral RNA only in the cytoplasm (Fang & Spector, 2007, Song et al., 2007).

Just like the Arabidopsis AtAGO1, AtAGO2 has also been implicated in antiviral defense, only this time against *Turnip crinkle virus* (TCV) and *Cucumber mosaic virus* (CMV). AtAGO2 was upregulated upon infection by these viruses and it was further observed that *ago2* mutant plants were extremely susceptible to TCV and CMV (Harvey et al., 2011a, Wang et al., 2011a). However, *Atago2* mutants were not susceptible to any

other viruses indicative of its specificity. Just like *Atago2* mutants, *Atago7* mutants were only hyper-susceptible to TCV infection (Qu et al., 2008) but not any other virus, furthermore indicating a very specific AGO-virus association.

Even though the *Arabidopsis* AtAGO4 has not been directly linked to any specific antiviral defense, *Atago4* mutants were exceptionally susceptible to the bacterial pathogen *Pseudomonas syringae* suggesting its role in the activation of a pathogen-specific defense mechanisms (Agorio & Vera, 2007). Kim *et al* however suggest that is also possible that epigenetic down regulation of other genes in the *ago4* mutant plant could account for the susceptibility observed (Ki Wook Kim, 2011). In *N. benthamiana*, observations on the *Potato virus X* (PVX) suggest that the contribution of AGO4-like proteins in the specific translational control of viral transcripts is a key factor in virus resistance mediated by NB–LRR proteins (Bhattacharjee et al., 2009).

AtAGO6 found on the same clade as AtAGO4 appears to play a partially redundant or additive role with AtAGO4 as the level of transgene reactivation was demonstrated to be even higher in the *ago4/ago6/ros1* triple mutant when compared to either of the double *ago4/ros1* mutants (Zheng et al., 2008). Although not empirically verified yet, this observation may suggest that AtAGO6 just like AtAGO4 is also directly linked to an antiviral role.

Although, only one of these examples with At*ago1* mutant and CMV, provides direct evidence that an AGO protein protects against a fully virulent virus (Morel et al., 2002), the role of AGOs in antiviral defense is clearly unmistakable. Given that so little is known about the antiviral defense role of the ARGONAUTE family of proteins in plant species other than *Arabidopsis*, and that knock-out lines are only available for *Arabidopsis*, our specific objective therefore was to use the VIGS system to individually silence known *AGOs* in *N. benthamiana* and later challenge the silenced plants with a wide array of viruses with or without their silencing suppressors and make observations on virus accumulation as well as the phenotypic effects of silencing the different AGOs. VIGS offers the advantage of rapidity with phenotypes being observed in as little as 3 weeks and since it does not require full-length cDNA sequences to function (Scofield,

2009), we are able to initiate our experiments even in the absence of complete gene sequence information.

The *Tobacco rattle virus* (TRV) is a suitable candidate for use as a virus vector in *N. benthamiana*, our model plant system, because it replicates abundantly and moves systemically without causing symptoms that deter normal plant growth and development (Baulcombe et al., 2001, Ratcliff et al., 2001, Burch-Smith et al., 2004). As discussed in chapter 1, TRV is a viral vector commonly used to silence endogenous genes in a wide range of plants species (Ratcliff et al., 2001, Burch-Smith et al., 2004). The original form of TRV used in this study was constructed for infiltration into the host plant using *Agrobacterium*. It was based on a construct generated by Ratcliff and colleagues (Ratcliff et al., 2001).

The *TRV-NbAGO* constructs were generated by inserting the PCR-generated fragments into the *SmaI* site of pBinTra6 a *Tobravirus* vector (Jones et al., 2006). The viral cDNAs constructs were inserted behind CaMV 35S promoters, with a self-cleaving ribozyme from the satellite viroid of *Subterranean clover mottle virus* at the 3' end (see also Chapter I). RNA1 remains pretty much intact, with only minor alterations before insertion into the pBIN19 binary vector T-DNA plasmid but in RNA2 the 29 and 32 kDa nematode transmission factors are removed to create a multiple cloning site (MCS) for insertion of cDNA fragments in this case, the sequences of the different *NbAGOs* named *NbAGO1*, *2*, *4*, *5*, *6*, *7* and *X*. All the numbered AGOs were named based on their similarity to known *Arabidopsis* AGO proteins. *NbAGOX* however, had no significant similarity to any of the known *AtAGOs* hence was named '*X*'. However, sequence comparison between the newly released *Solanum lycopersicum* genome with the available 800 bp sequence of *NbAGOX* showed over 90% sequence similarity to *SlAGO5a* (Bai et al., 2012) indicating that it may be an AGO5 homologue as well. Figure 3.1 shows a schematic representation of a generic AGO protein illustrating the relative positions of the corresponding cloned *AGO* cDNA fragments along the different domains. An attempt to make a comparison of the known complete sequences of *N. benthamiana* AGOs 1, 2 and 4, *Solanum lycopersicum* 2 and *Arabidopsis* 1, 2 and 4

AGO proteins is also shown in Figure 3.2. Furthermore, a list of all currently known *NbAGO* sequences and the sequences inserted in the TRV virus vector can be found in the supplemental section of this thesis.

In our effort to investigate the effects of silencing of the individual *NbAGOs* on the accumulation of viruses other than TBSV, our collaborators facilitated us with various virus-GFP chimeric constructs also capable of being delivered by agroinfiltration. Below is a summary of the viral constructs used in this study in addition to the TBSV constructs discussed in Chapter I.

Tobacco mosaic virus (TMV)

TMV, a type member of the *Tobamovirus* genus is a positive-sense single-stranded, rod-shaped RNA virus that causes mosaic symptoms in tobacco and similar symptoms on other *solanaceous* species. It encodes four products: two replicase-associated proteins that are directly translated from the TMV RNA, the movement protein and a coat protein that are translated from subgenomic RNAs (Scholthof, 2004). The 126 kDa replicase protein is also believed to posses silencing suppressor roles (Csorba, 2007), the 30kDa movement protein directs cell-to-cell spread while the capsid protein is also involved in systemic spread.

Dr. John Lindbo a senior scientist at Campbells Soup Company/Campbells Seeds graciously provided us with two TMV-GFP chimeric constructs; the pJL 24 and the pJL TURBO-G illustrated in Figure 3.3. The pJL 24 consists of a GFP sequence inserted in the entirety of the TMV genome between the movement and coat protein. In the pJL TURBO-G however, GFP replaces the removed CP hence the virus is rendered incapable of systemic spread.

Both constructs are driven by the 35S CaMV promoter and were designed to transiently express foreign recombinant proteins in plants at levels of up to 3 to 5 mg/g fresh weight of plant tissue (Lindbo, 2007). Both constructs can be agroinfiltrated in *N. benthamiana* leaves and accumulate substantial amounts of GFP even when not co-inoculated with the suppressor P19.

Figure 3.1. A schematic representation of a generic ARGONAUTE protein illustrating the position of the corresponding cloned *AGO* cDNA fragments along the different domains. The positions of the domains were predicted using NCBI's online Conserved Domain search program (Marchler-Bauer et al., 2011).

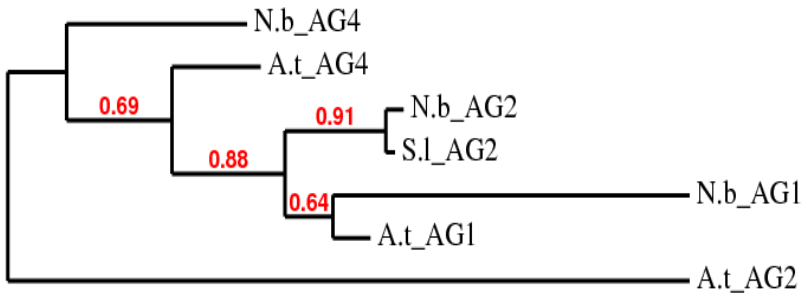

Figure 3.2. A non- rooted phylogenetic tree comparing known complete sequences of *N. benthamiana* AGOs 1, 2 and 4, *Solanum lycopersicum* 2 and *Arabidopsis* 1, 2 and 4 AGO proteins. Using the online 'Méthodes et Algorithmes pour la Bio-informatique' software (Dereeper et al., 2008) at *phylogeny.fr*, bootstrapping was performed with 1,000 bootstrap replicates, and percentage of bootstrap support is shown by values at the branch nodes of the tree.

Sunn-hemp mosaic virus (SHMV)

Sunn-hemp mosaic virus (SHMV) is a member of the *Tobamovirus* genus and *Virgaviridae* family of plant viruses. It is pathogenic to most leguminous plants (Silver, 1996). Just like TMV, it encodes four genes: two replicase-associated proteins that are directly translated from the gRNA, the movement protein and a coat protein that are translated from sgRNAs and carry out similar functions as in TMV. The SHMV construct was provided by Dr. Christopher M Kearney from Baylor University. The coat protein has been eliminated and replaced with a GFP sequence signal in the SHEC-GFP construct (Liu, 2010b). Systemic spread is therefore contained, but since the CP also has silencing suppressor functions, unless co-infiltrated with TBSV P19 silencing suppressor, GFP is not seen to accumulate in *N. benthamiana* leaves. Also driven by the CaMV 35S promoter, SHEC-GFP was designed to transiently express foreign proteins in plants. Co-infiltration with P19 has been shown to yield up to 25% of GFP per fresh weight of leave tissue (Liu, 2010b).

Foxtail mosaic virus (FoMV)

Although its experimental host range includes *Nicotiana spp.* and the *Chenopodium* plant genera, FoMV is mainly considered to be a virus of *Poaceae* plant family. It is a non-enveloped, flexous, filamentous virus of the *Potexvirus* genus and *Alphaflexiviridae* family whose type member is the *Potato virus X*. It is a single-strand positive-sense RNA virus and encodes five proteins. The RNA-dependent RNA polymerase (RdRp) is translated directly from the gRNA. ORF1 (152 kDa) encodes a protein with the RNA-dependent RNA polymerase, followed by methyltransferase and helicase motifs; ORFs 2 , 3 and 4 consists of a 26, 11.3, and 5.8 kDa protein respectively and encode the triple gene block (TGB) of movement proteins, of which TGB1 is believed to function as a silencing suppressor. ORF 5 encodes the 25 kDa coat protein also needed for systemic spread (ViralZone Expasy, 2008, Robertson, 2004)

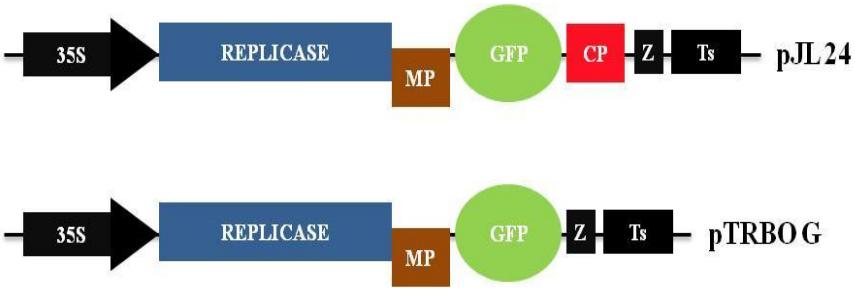

Figure 3.3. Maps of the TMV pJL24 and TRBO-G plasmids. Expression in both constructs is driven by the 35S promoter. The dark box labeled 'z' at the 3' end represents the self cleaving ribozymes; 'Ts' refers to the CaMV polyA signal sequence/terminator.

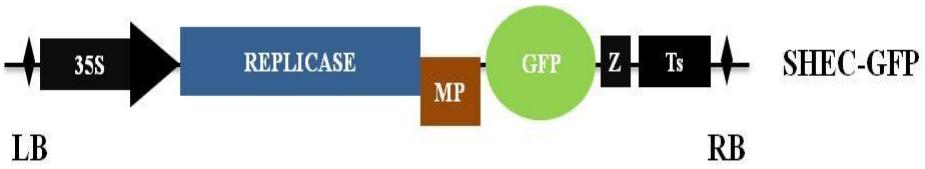

Figure 3.4. Map of the SHEC-GFP plasmid (Liu, 2010b). The dark box labeled 'z' at the 3' end represents the self cleaving ribozymes; 'Ts' refers to the CaMV polyA signal sequence/terminator.

Dr. Kearney also kindly provided us with his FECT vector series where both the coat protein (CP) and triple gene block (TGB) are eliminated from the original FoMV and replaced with GFP as can be seen in Figure 3.5. The modified FoMV vector retained the full-length replicase and 40 bases of TGB1 ORF representing a 29% deletion of its entire genome. In *N. benthamiana*, co-inoculation of FECT40 with P19 expressed GFP at 40% of the total soluble protein (Liu, 2010a).

Turnip crinkle virus (TCV)

TCV, a member of the *Tombusviridae* family and *Carmovirus* genus, has a positive-sense single-strand RNA, packaged in icosahedral capsids, with five major open reading frames. The p28 and p88 proteins are translated from gRNA by ribosomal read-through of the p28 terminator, and encode the replication components of the virus. The overlapping p8 and p9, termed MP1 and MP2 respectively are expressed from sgRNA1 and are required for cell-to-cell movement and systemic spread of the virus The 3′-proximal ORF encodes for a multifunctional capsid protein which plays an essential role in cell-to-cell movement of TCV in *N. benthamiana* (Cohen, 2000) and also acts as an effective suppressor of RNA silencing and systemic infection (Qu, 2003, Thomas, 2003). Figure 3.6 shows the TCV GFP-chimeric construct whose CP has been replaced by the GFP, thereby impeding systemic spread. GFP accumulation is only observed when the construct is co-infiltrated with a silencing suppressor (Powers, 2008). The TCV constructs were kindly provided by Dr. Steven Lommel from the Department of Plant Pathology at North Carolina State University.

Figure 3.5. Schematics of the FECT vector (Liu, 2010a). In FECT 40-GFP, the CP has been replaced with GFP but the construct retains 40 bases from the start of the TGB. The dark box labeled 'z' at the 3' end represents the self cleaving ribozymes; 'Ts' refers to the terminator signal.

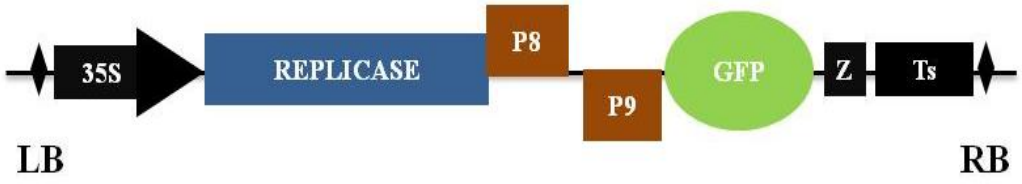

Figure 3.6. Schematics of the TCV GFP-chimeric virus vector (Powers, 2008) driven by a 35S CaMV promoter. The dark box labeled 'z' at the 3' end represents the self cleaving ribozymes; 'Ts' refers to the terminator signal.

Materials and methods

Obtaining and cloning *NbAGO* segments

N. benthamiana ARGONAUTE homologues were obtained by searching the publicly available tobacco sequences for similarity with other known plant AGOs, the 10 and 18 AGOs from *Arabidopsis* and rice (*Oryza sativa*), respectively. The obtained *AGO* cDNA fragments were then cloned into the MCS of TRV and the *virus-AGO* cassettes were then transformed into *Agrobacterium* to be able to launch an infection through agroinfiltration. Meticulous care was taken to ensure that the cloned segments were unique to avoid cross-silencing. The clones and constructs were already available at the onset of this study (Scholthof et al, 2011).

More specifically however, TRV constructs of *N. benthamiana AGO1* and *-4* were acquired from colleagues (Jones et al., 2006). *NbAGO1* and *-4* share a 74 and 71% similarity in nucleotide sequence to *AtAGO1* and *AtAGO4*. For *AGO2*, a *Nicotiana tabacum* homologue was first identified by searching available databases. Then, using primers based on the identified sequences, a 0.6 kb fragment was amplified from *N. benthamiana* and cloned into the TRV system. Sequence analysis showed it to be over 96% similar to the *N. tabacum AGO2* nucleotide sequence, and approximately 65% nucleotide and 50% amino acid identity with *AtAGO2* (Scholthof et al, 2011). *NbAGOX*, with no significant similarity to any known *AtAGOs* were identified in available *N. benthamiana* databases. Primers were then designed to amplify approximately 400 bp unique sequences which were then cloned into the TRV vector system. *NbAGOs 5, 6* and *7* with approximately 66%, 50% and 69% similarities in nucleotide sequences to their corresponding *Arabidopsis* homologues were synthetically generated (GenScript, Piscataway NJ) based on bioinformatic analyses of *N. benthamiana* and *N. tabacum* sequences in available databases.

As discussed in Chapter I, for controls we use TRV-OO, an empty vector hence a negative control as well as *TRV-Mg-Chelatase* which shows a conspicuous

photobleaching phenotype as an experimental positive control. Our positive control gene, the *Magnesium-protoporphyrin IX chelatase* (*Mg-Chelatase*) acts at the branchpoint of tetrapyrrole biosynthesis, and is therefore vital in the formation of chlorophyll (Papenbrock et al., 2000). Effective silencing of the *Mg-Chelatase* gene causes a loss of leaf green pigment starting from the newly emerging leaves but gradually spreading to the older leaves. The silencing of the green pigment directly corresponds to the virus movement thus the silencing signal.

Silencing *AGO* genes

Agrobacterium transformed with the *TRV-AGO*, *TRV-MgChelatase*, *TRV-OO* and RNA1 constructs were prepared for infiltration as described by Jones *et al* (Jones et al, 2006) with minor modifications. The cells were grown for 12 – 18 hours in liquid Luria broth with a kanamycin selection of 50 ug/mL in a constantly agitating 28^{o}C incubator. The cells were then pelleted and resuspended in 10 mM $MgCl_2$ solution to a final optical density of 0.5. TRV-RNA1 and TRV-RNA2 (containing one of the *AGOs* or *Mg-Chelatase*) were then mixed in a ration of 1:5 (RNA1:RNA2), and using a needle-less 1 or 3 mL syringe was infiltrated into the abaxial surface of a three week old *N. benthamiana* leaf. Usually, a single infiltration was sufficient to cover the entire leaf. Two leaves per plant were infiltrated. 4 – 5 weeks are allowed for the virus to replicate and accumulate within the host as silencing of its endogenous genes is occurring.

Total RNA extraction and cDNA synthesis

Total RNA was then extracted from the newly developed leaves as described in the Materials and methods section in Chapter II. Correspondingly, cDNA was also generated as described and quantitative Real-Time PCR was used to determine the success of silencing by determining the amount of specific *AGO* RNA transcripts in the silenced plants and comparing these to that in non-silenced plants.

Designing and use of the semi-quantitative/conventional PCR Primers

Conventional PCR was carried out using the exact primers and PCR conditions mentioned in the Materials and Methods section of Chapter II.

Verification of TRV vector infectivity and systemic spread

Furthermore, in order to verify the infectivity, integrity and ability for systemic spread of the TRV-constructs throughout the plant, cDNA was also made from total RNA extracted from the newly emerged leaves. However, since TRV does not possess a *Poly-A* tail, instead of using oligo dT primers, the TRV-MCS reverse primers were used to synthesize the required cDNA.

Conventional semi-quantitative PCR was then carried out using TRV MCS primers (*TRV MCS Forward Primer*: GAGTGGAGGTCCGATACGTC and *TRV MCS Reverse Primer*: CAGTGAGCGCGCGTAATA).

Designing of the quantitative Real-Time PCR Primers

The q-RT PCR primers were designed to amplify regions of the endogenous *AGO* genes that were not part of fragment inserted into the TRV vector so as to accurately represent silencing of the plant *AGO* genes by not amplifying the genes contained in the systemic virus vector. Secondly, the q-RT PCR primers were designed to only amplify unique regions of the multiple known *AGO* genes so as to eliminate the possibility of amplifying crossed silenced regions of the AGO genes. For this, currently known sequences of *NbAGO-1, -2, -4, -5, -6, -7* and *–X* were aligned using MUSCLE (MUltiple Sequence Comparison by Log- Expectation) online software (European Bioinformatics Institute, 2012). The output files were then customized for easy viewing using BOXSHADE 3.21 online software (ch.EMBNET.org, 2012) and unique sequence regions were selected for primer design. The following q-RT PCR primers were ultimately designed using Primerquest online program (IDT, 2012) based on BIORAD real-time PCR and MIQE (Minimum Information for Publication of Quantitative Real-Time PCR Experiments) (Bustin et al., 2009, BIORAD, 2006) guidelines. A list of the primers (purchased from Integrated DNA Technologies Inc. San Jose, CA) used is shown in Figure 3.7.

A preliminary PCR test to ensure the amplification of single correct size fragments was carried using conventional PCR on genomic and complementary DNA extracted from 4 week old virus free *N. benthamiana* leaves using the designed qRT PCR primers. The PCR conditions, parameters and results are shown in Figure 3.8 and 3.9. PCR was set up in an Applied Biosystems 2720 Thermal Cycler. Then 2.5µl of DNA a 10X loading dye (30% glycerol, 0.25% bromophenol blue, 10 mM Tris pH 8.0 and 2.5 mM EDTA) was added to the samples and 15 ul were electrophoresed through a 1% agarose gel at 100 volts in 1X TBE (90 mM Tris, 90 mM Boric acid, 2 mM EDTA) for 30 minutes. These gels were then stained with ethidium bromide for 30 min, and viewed on a UV light box. As shown in Figure 3.9, amplicons from genomic DNA using *NbAGO5* and *6* primers clearly show a marked increase in fragment size when compared to cDNA amplicons due to the fact that the designed primers amplified across an intron. All other amplicons corresponded to their expected sizes using both genomic and complementary DNA.

After the preliminary primer test to verify primer integrity using conventional PCR, qRT PCR was then carried out using SYBR Green Master Mix reagent (Life Technologies, Carlsbad, CA). The SYBR dye intercalates with double-stranded DNA causing the dye to fluoresce. The qPCR instrument then detects the fluorescence and the program software calculates Ct values from the intensity of the fluorescence. Using a 7500 Fast Real-Time PCR SDS v 1.41 System (Applied Biosystems) qRT PCR reactions were performed under the conditions indicated in Figure 3.10 and primer efficiencies were calculated. The original template DNA (both genomic and complementary) were diluted 0, 2, 4, 6 and 8 times resulting in arbitrary concentrations of 1, 0.5, 0.25, 0.125 and 0.0625 units. Using the newly designed primers, the samples of varying concentrations were then set up for qPCR in a 96-well plate in triplicates following the conditions mentioned in Figure 3.10. A dissociation cycle starting at 60^{o}C was also included.

***N. benthamiana Actin* primers**

rtActin-F: CCGGTGTCCTGAGGTCCTTT
rtActin-R: CTCGTGGATTCCTGCAGCTT

***N. benthamiana AGO 1* primers**

rtAGO1-F: TTCCTGGTGGTGCTGAGAGTTTGA
rtAGO1-R: CTTGCTGATGCTGATGTTGCTGCT

***N. benthamiana AGO 2* primers**

rtAGO2-F: AGCAGTGCCTGTGCTAGATTTCCT
rtAGO2-R: AAGGTCGCGAGTCATCTCATCAGT

***N. benthamiana AGO 4* primers**

rtAGO4-F: TGGATGAAGTTCGAGGACGCATCA
rtAGO4-R: AAGTCGAGGCAACTGAGGAACAGT

***N. benthamiana AGO 5* primers**

rtAGO5-F: GGAAGAAATGGACGCAATCCGCAA
rtAGO5-R: ACAGGGAACAGACGTGTATGGTGT

***N. benthamiana AGO 6* primers**

rtAGO6-F: AACTATCTGCCACTGGAGCTGTGT
rtAGO6-R: ATTCGTTCTCGAGGCTTCTGCCTT

***N. benthamiana AGO 7* primers**

rtAGO7-F: TCTTCAAGCACGATGGTCCGGTTA
rtAGO7-R: TGGCTGCTGGCCAATTCACATTAC

***N. benthamiana AGO X* primers**

rtAGOX-F: TCGATAGCAATGTCGGAACGTGGA
rtAGOX-R: GGTGGAGCATTGAAAGACGGCAAA

Figure 3.7. A list of the qRT PCR primers used to amplify *N. benthamiana* endogenous AGOs. *Actin* primers were also designed to amplify *Actin* as an internal reference gene.

PCR setup		PCR conditions	
Template (genomic DNA/cDNA)	2.0 µl	94°C ..... 5 min	
10X Thermopol Buffer	2.5 µl	94°C ..... 30 sec	32 cycles
10 mM dNTP	0.5 µl	55°C ..... 30 sec	
10 µM primer forward	0.5µl	68°C ..... 45 sec	
10 µM primer reverse	0.5 µl	68°C ..... 5 min	
Taq polymerase	0.125µl	4°C ..... ∞	
H_2O	19.0 µl		
TOTAL	25 µl		

Figure 3.8. Preliminary test PCR setup and conditions.

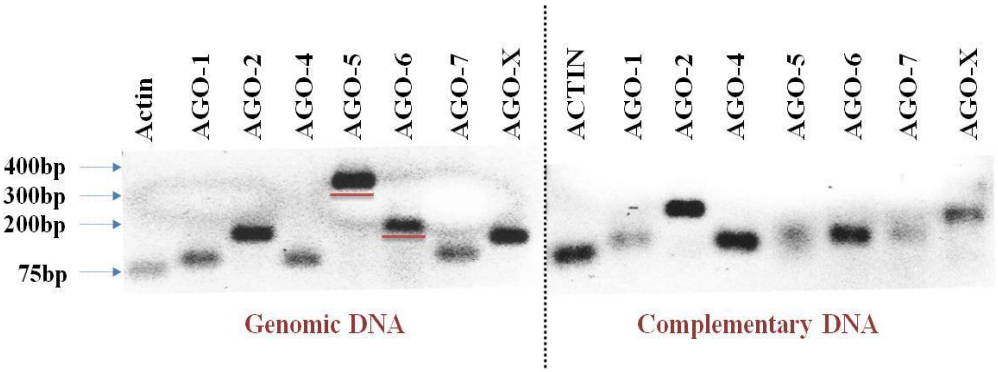

Figure 3.9. Results of a preliminary primer test using designed qRT PCR primers for conventional PCR to ensure correct size single amplicons from genomic and complementary DNA.

qRT PCR setup		qRT PCR conditions	
Template (genomic DNA/cDNA)	6.0 µl	50°C ..... 5 min	
2X SYBR Green Mix...	7.5 µl	95°C ..... 10 min	
10 µM primer forward	0.75µl	95°C ..... 15 sec	40 cycles
10 µM primer reverse	0.75 µl	60°C ..... 1 min	
TOTAL	15.0 µl	60°C (Dissociation Curve starting Temperature)	

Figure 3.10. qRT PCR setup and conditions.

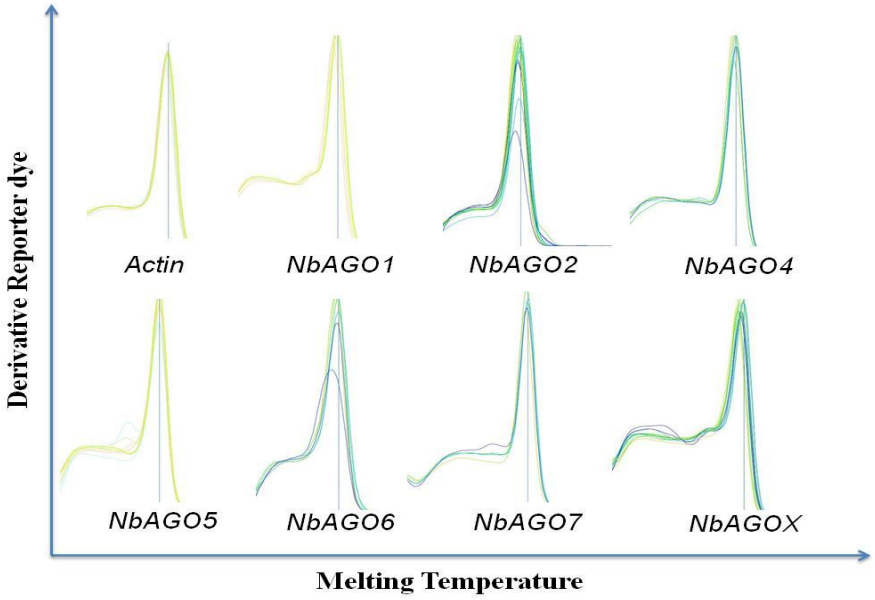

Figure 3.11. Melt curve analysis. Dissociation curves obtained from primer efficiency test.

The resulting melting curves shown in Figure 3.11 obtained by plotting '*Amplicon Melting Temperature (X-axis) against Intensity of Reporter dye (Y-axis)*' showed single peaks indicative of the desired single PCR product with all the different primers used at various template concentrations. The lateral displacement to the left observed in the resulting amplification curves also uniformly corresponded to the concentration of the template with the more concentrated sample clearly showing a lower C_t (threshold cycle) values.

A log base 10 of the initial template concentration (the independent variable) is plotted on the *x* axis and average C_t values (the dependent variable) is plotted on the *y* axis (Figure 3.12). Note that the original and averaged Ct values can be reviewed in the Appendix section. The theoretical maximum value of coefficient of determination (R^2) of 1.00 (or 100%) indicates that the amount of product doubles with each cycle. A linear trendline is then created so as to calculate the slope of the line from the simple regression equation $Y=mx+b$ (where m is the slope and b is the y intercept). The efficiencies of the primers are the calculated from the equation 'Efficiency $=10^{-(1/\text{slope})}$ -1 (Taylor et al., 2010) as shown in Table 3.1.

Use of the designed qRT-PCR primers to verify silencing of transcripts

After determining the efficiencies of the designed qRT PCR primers, the primers were then used to verify the amount of specific *AGO* transcript levels in the plant tissues. Precise qPCR assays are usually correlated with high PCR efficiency. PCR efficiency is especially important when reporting transcript concentrations for target genes (*NbAGO*) relative to those of reference genes (*Actin*) (Bustin et al., 2009). A comparative method (delta Ct) (Pfaffl et al., 2002, QIAGEN, 2004) was used, whereby the differences in C_t values between the target and reference genes are first calculated to normalize initial template concentrations. After normalization, the Ct values can then be compared directly. The normalized Ct values are then converted to a linear scale by calculating the 2^ - (delta Ct values).

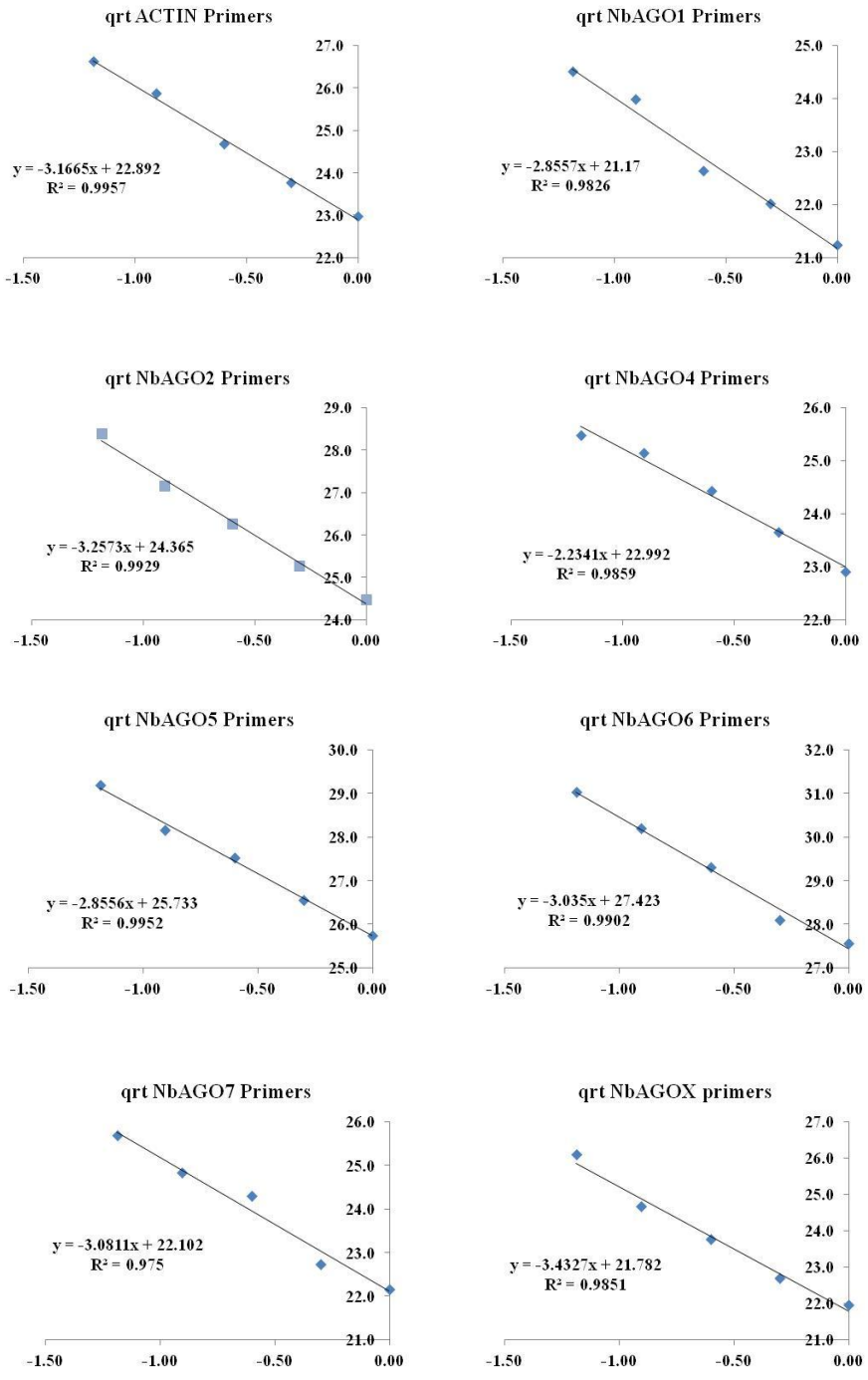

Figure 3.12. Calculation of individual qRT-PCR primer efficiency. Log base 10 of the initial template concentration (the independent variable) is plotted on the *x* axis against C_t values (the dependent variable) is plotted on the *y* axis.

Table 3.1. Calculation of individual qRT-PCR primer efficiency. The high qRT-PCR primer efficiency values (>1.0) observed for all but *NbAGOX* primers can be possibly attributed to intercalation of the SYBR dye to primer dimers, template saturation of PCR at higher concentrations or could have been reduced by use of more dilution factors. These results therefore show that the primers can be adequately used for qRT-PCR.

Primer	Slope	1/slope	PCR Eff (10^-(1/slope) - 1
qrtActin	3.1665	0.315806095	1.069217273
qrtNbAGO1	2.8557	0.350176839	1.239632904
qrtNbAGO2	3.2573	0.307002732	1.027695477
qrtNbAGO4	2.2341	0.447607538	1.802899575
qrtNbAGO5	2.8556	0.350189102	1.239696143
qrtNbAGO6	3.035	0.329489292	1.135449432
qrtNbAGO7	3.0811	0.324559411	1.111346004
qrtNbAGOX	3.4327	0.291315874	0.955761415

PCR setup		PCR conditions	
Template (cDNA)	2.0 µl	94°C ..... 5 min	
10X Thermopol Buffer	2.5 µl	94°C ..... 30 sec	32 cycles
10 mM dNTP	0.5 µl	55°C ..... 30 sec	
10 µM primer forward	0.5µl	68°C ..... 1 min	
10 µM primer reverse	0.5 µl	68°C ..... 5 min	
Taq polymerase	0.125µl	4°C ..... ∞	
H_2O	19.0 µl		
TOTAL	25 µl		

Figure 3.13. PCR setup and conditions using TRV MCS primers to test for integrity and ability for systemic spread of the TRV constructs.

This is conducted to convert the 'Exponential Amplification' values to a linear scale. The resulting values were portrayed on 2D column charts with error bars so as to validate significance of the biological and technical repeats. The data obtained was further analyzed for statistical relevance as discussed in Chapter I.

Testing activity against GFP-chimeric viruses

Agrobacterium transformed with the GFP-chimeric virus as well as the P19 constructs were prepared for infiltration as described in Liu *et al (Liu et al., 2002a)* with minor modifications. The cells were grown for 16 – 18 hours in liquid Luria broth with a kanamycin selection of 50 ug/mL in a constantly agitating 28^{o}C incubator. The cells were then pelleted and resuspended in 10 mM $MgCl_2$ solution to a final optical density of 0.5, and using a needle-less 1 or 3 mL syringe was infiltrated into one half of the abaxial surface of the silenced leaf. The other half of the leaf was co-infiltrated with P19 and GFP-chimeric virus construct mixed in a ratio of 1:5 respectively to serve as a positive control. The plants were then visually assayed for virus accumulation by observing GFP signal under a 488 nm UV-light, and pictures were taken with 4 second exposures without flash. GFP accumulation in the leaves was often noticed as early as 2 days post infiltration.

Results

Accumulation of the TRV constructs was verified through semi-quantitative PCR. Using TRV MCS primers (results shown in Figure 3.14), the presence of an intact insert was detected as early as 5 days post initiation of silencing in the newly emerging leaves verifying its stability and capability for systemic spread. Further PCR analysis at 10, 15 and 45 days after initiation of silencing yielded similar results demonstrating the persistence of the TRV constructs.

About 8-12 days after initiation of silencing, newly emerging leaves on the *TRV-Mg-Chelatase* infiltrated plants started showing signs of photobleaching which gradually spread into the nearby leaves. The oldest leaves were the last to show signs of photobleaching. In 3 - 4 weeks, more than 75% of the plant aerial tissues exhibited a

severe loss of its green pigment as discussed in Chapter I. As also mentioned in Chapter I, a TRV infection in *N. benthamiana* does not cause any discernible phenotypes when compared to its virus-free counterpart. It was also observed that, with the exception of silencing using the *TRV- NbAGO1*construct, all the other tested *TRV-AGOs* did not cause any observable abnormality in *N. benthamiana* tissues. Both above and below ground tissues were keenly observed but no particularly salient phenotypic changes were witnessed as seen in Figure 3.15.

The silencing of *NbAGO1* on the other hand caused very conspicuous deformations on the aerial parts of the plant, specifically on leaves, flowers and leaf petiole as seen in Figure 3.16 below. These phenotypes persisted throughout the lifetime of the plant. The silenced plant did not produce any seeds since its flowers were aborted for the most part and the few surviving ones were severely deformed. The silencing of *NbAGO7* was initially observed to cause a slight deformation in leaf shape almost reminiscent of the phenotype caused by silencing of *NbAGO1*; however the phenotype disappeared after a few days of its appearance.

Verification of *AGO* transcript silencing

Apart from *AGO1* in *N. benthamiana*, the silencing of all the other known *NbAGOs* cannot be visibly confirmed since they produce no noticeable phenotype. An analysis of transcript levels is therefore eminent in order to be completely sure that the silencing of a particular gene has successfully occurred. Both semi and quantitative Real-Time PCR were intended to be used to verify transcript levels of the individual *AGO* genes in *N. benthamiana*.

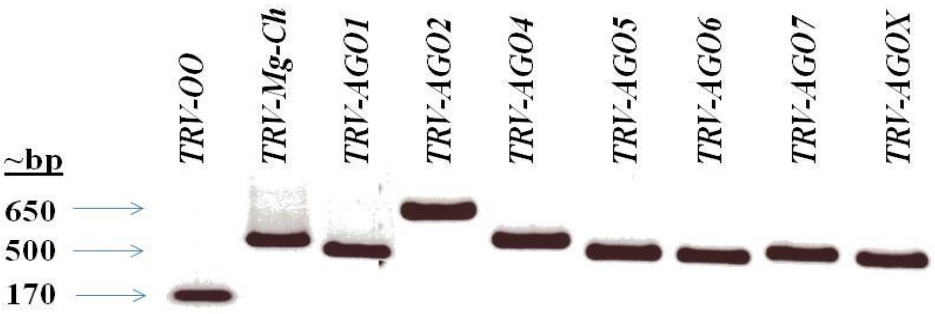

Figure 3.14. PCR results using TRV MCS primers showing integrity and ability for systemic spread of the TRV constructs with intact inserts.

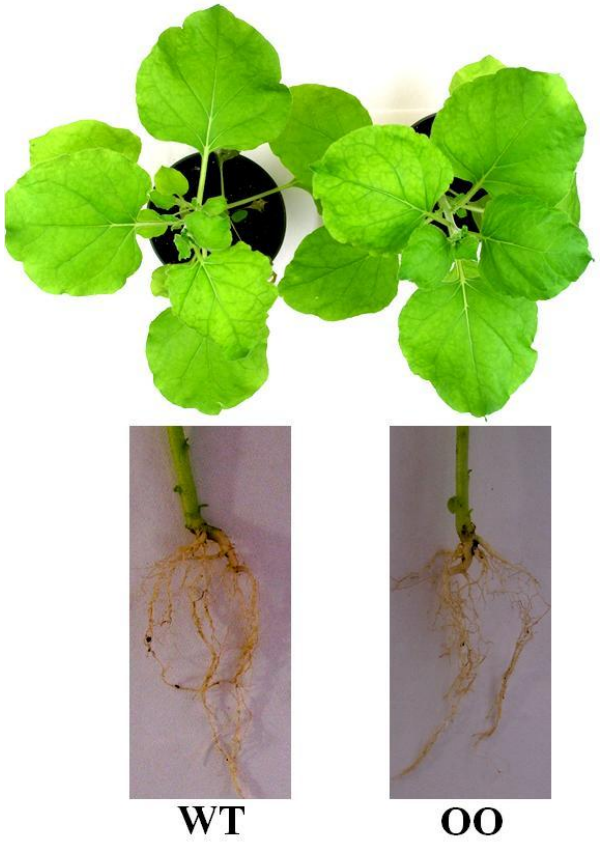

Figure 3.15. Aerial and subterraneal *N. benthamiana* tissues exposed to reveal the lack of phenotype caused by infection with the *Tobacco rattle virus* construct used for induction of *AGO* gene silencing. Here a healthy virus free plant (**WT**) is compared with a plant infiltrated with an empty TRV vector construct (**OO**) about 28 days after initial agroinfiltration of TRV-OO.

For conventional PCR the primers designed to amplify endogenous *AGOs* as mentioned in Chapter II were used according to the specifications stated previously. However, after multiple technical and biological repeats, the results were not consistent for most of the *AGOs*. Nonetheless, as an example, Figure 3.17 clearly shows a decrease in *NbAGO2* mRNA levels when *NbAGO2* silenced plants were compared to a healthy non-TRV infiltrated plant (H), empty TRV vector (OO) and *NbAGO1* silenced plants. The use of qRT-PCR was therefore preferred over conventional semi-quantitative PCR. However, even with qRT-PCR analysis, the results obtained from the putative *NbAGOX* silenced plants were never consistent hence are not shown here. Also included as control were a non-TRV infiltrated plant (WT) and a plant infiltrated with an empty TRV vector (OO). These experiments were repeated with at least 3 biological replicates, with three technical replicates each time a run was set up. The results shown in Figure 3.18 represent the most consistent observations from the biological repeats.

By simply comparing the levels of *NbAGO* transcript expression in non-AGO silenced TRV infiltrated (OO) plants with those from a virus free (WT) plants, the upregulation of the *AGOs* 1, 5, 6 and X was clearly observed indicating a possible induction of these *NbAGOs* due to the virus infection. Furthermore, quantitative Real-Time PCR results (Figure 3.18) show that except for *NbAGO2*, the silencing of all the other *N. benthamiana AGOs* resulted in a decrease in the specific *AGO* transcript levels when compared to the control plants infiltrated with the empty vector.

The most drastic reduction in transcript levels was seen for *NbAGOs 4* and *6* silenced plants while the least by *NbAGOs 1, 5* and *7* silenced plants. The surprisingly stable or elevated levels of *NbAGO2* transcripts in the putative silenced plant are thought to be caused by a number of factors that shall be elaborated upon in the discussion session of this Chapter. *AGO2* transcript levels are also seen to be elevated in the *TRV-NbAGO5* silenced plants. Curiously however, the levels of *AGO2* mRNA were dramatically reduced in *AGOs 6* and *7* silenced plants.

Figure 3.16. Close-up pictures of developmental defects caused by silencing *NbAGO1*. **A**. Leaf midrib emerging from leaf surface. **B**. Pine leaf-like leaves **C**. Deformed flowers

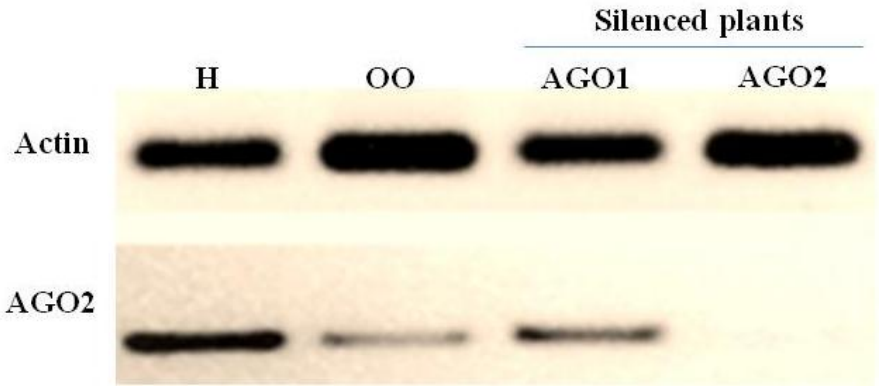

Figure 3.17. Semi-quantitative PCR results. The expression of *NbAGO2* transcripts in non-TRV infiltrated wild-type plants (**H**), empty TRV vector (**OO**), *TRV-AGO1* and *TRV-AGO2* agroinfiltrated silenced plants. The expression of *Actin* mRNA was used as a reference gene.

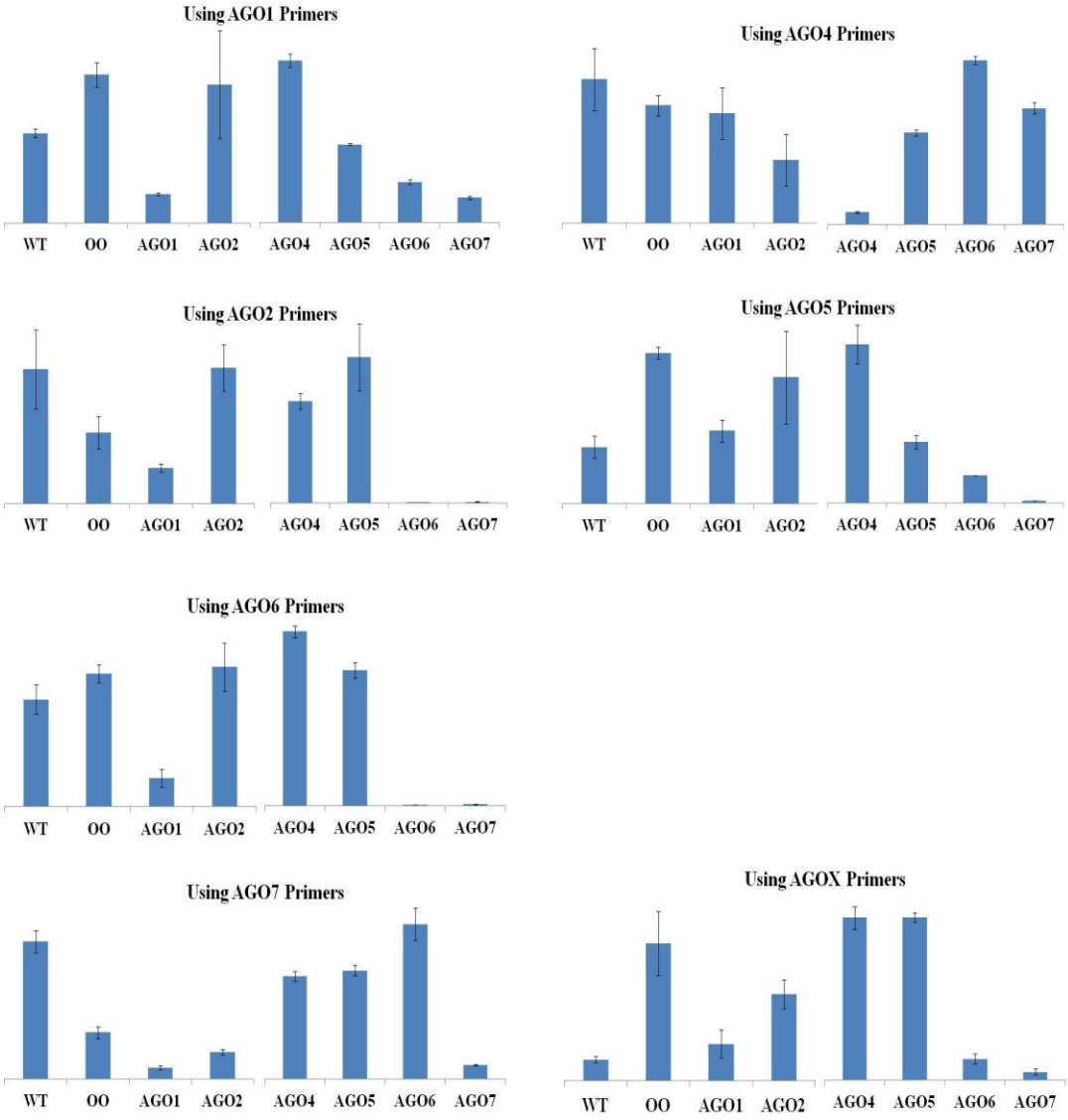

Figure 3.18. qRT-PCR analysis of individual *NbAGO* transcript levels in silenced plants. The relative *AGO* transcript levels based on qRT-PCR with indicated primers are plotted on the *y-axes* and the sampled plants (WT for virus-free plants, OO for control plants infiltrated with an empty TRV virus vector, and the specific-*AGO* silenced plants) on the *x-axes*. Results from *AGOX* silenced plants are not shown because of the lack of consistency in the repeats.

NbAGO1 mRNA levels in *NbAGOs 5, 6* and *7* silenced plants are also seen to be significantly reduced when compared to the control OO plant levels. Cross silencing of these AGOs is not suspected due to low sequence similarity between the *AGOs* in question.

The silencing of *AGO1* however, may have affected a downstream pathway involved in the regulation of the other *AGOs*. Interestingly however, whenever each of the *NbAGOs 5, 6* and *7* were silenced, the levels of *NbAGO1* transcripts also seemed to be significantly reduced. The corresponding phenotype associated with the silencing of *NbAGO1* as described in Figure 3.16 were however not witnessed when *NbAGOs 5, 6* and *7* were silenced.

NbAGOX transcript levels are seen to be greatly induced by a TRV infection, but also equally significantly reduced when *NbAGOs 1, 5* and *6* are silenced. Despite the lack of observable phenotype associated with TRV-mediated silencing of *NbAGOs 2, 4, 5, 6, 7* and *X*, the combined results of both semi- and quantitative Real-Time PCR analysis show that there was a significant reduction in the specific *AGO* transcript levels indicating the success of the gene silencing procedure.

Activity against GFP-chimeric viruses

After four to six weeks of silencing, half-leaf assays were carried out where half of the leaf is infiltrated with GFP virus constructs (FECT, SHEC, TG, TGdP19, TCV and SHMV) and on the other half, the GFP-virus chimeric construct is complemented with P19. Observations were made on accumulation or disappearance of the GFP signal starting at 2 and up to15 days.

The results shown in Figure 3.19 consistently illustrated that only when P19 was coexpressed as in TG, or co infiltrated with SHEC and FECT constructs, was there noticeable accumulation of GFP. The TMV construct (TURBO) however, encodes a silencing suppressor in its replicase hence accumulates to comparable levels whether or not co-infiltrated with P19. Just as observed in the non-silenced plants in Figure 3.19, TRV-mediated silencing of *NbAGOs 1*, *4*, *5* and *6* did not seem to alter the accumulation

of GFP in any of the silenced plants during any time point and the silenced plants showed the same tendencies in GFP accumulation as the non-*AGO* silenced plants (data not shown). Curiously however, *NbAGO1* silenced leaves seemed to exhibit almost no necrotic lesions as a result of virus accumulation in contrast to what was observed in other *AGO* silenced as well as the non-silenced control plants.

In *NbAGO2* silenced leaves shown in Figure 3.19, TGdP19 consistently accumulated GFP to levels comparable to TG (Scholthof et al, 2011) indicative of the anti-TBSV role played by this *AGO*. Results with all other virus-GFP chimeric constructs (except TMV) were nonetheless similar to observations made on non-*AGO* silenced plants also indicative of the specificity of this antiviral defense role of *NbAGO2* against TBSV and its interaction with the silencing suppressor P19.

The TMV TURBO-G construct encoding its own silencing suppressor was seen to accumulate whether or not co-infiltrated with P19. However, when closely examined, TURBO-G was seen to accumulate to a lesser extent in the non-silenced leaf when not co-infiltrated with P19. Furthermore, in an *NbAGO2* silenced leaf, TURBO-G was seen to accumulate to comparable amounts whether or not co-infiltrated with P19, and in both cases its accumulation was higher than in the non-silenced leaf infiltrated without P19 indicative of a possible need for *NbAGO2* in TMV antiviral silencing. As observed in Figure 3.22, in *NbAGOX* silenced plants, 75% of the time, although to a lesser extent, TGdP19 accumulated in the leaves in visible amounts just like in *NbAGO2* silenced plant suggesting its possible defense role in specifically silencing TBSV. Observations made on *NbAGO7* silenced plants suggest that it may play a role in the silencing of TBSV and FoMV. As shown in Figure 3.19, at approximately two days after inoculation with the GFP-virus, there is a notable accumulation of GFP (not witnessed in silencing of other AGOs). However, when observed another 8 days later, the GFP signal was no longer present.

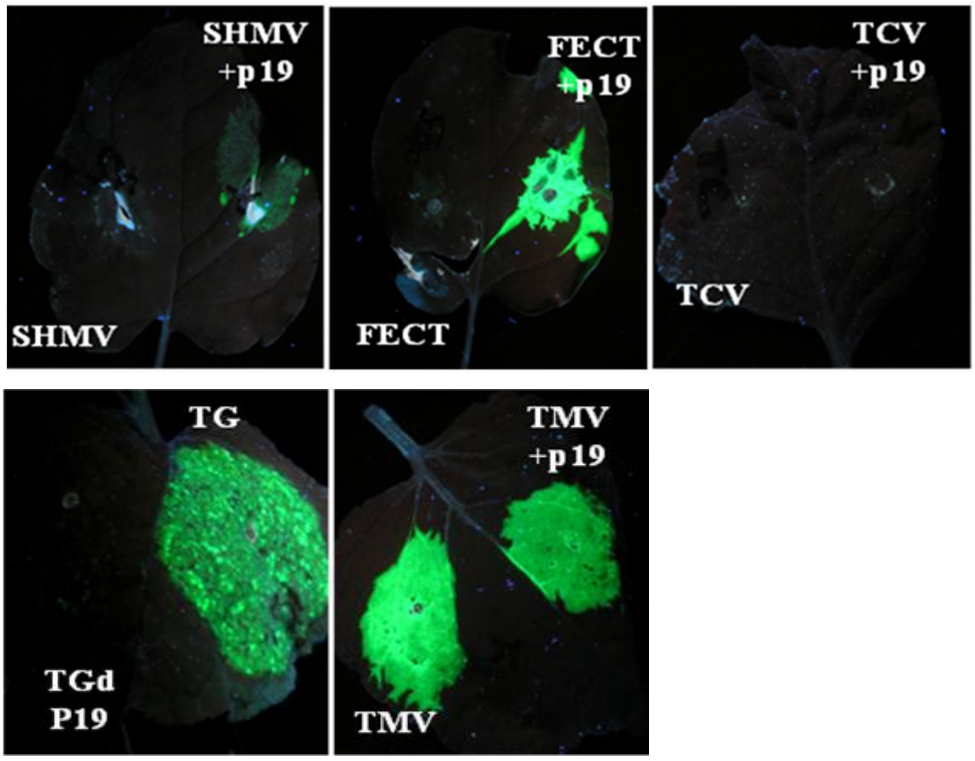

Figure 3.19. Half leaf assays on non-silenced *N. benthamiana* leaves using TBSV, TMV, SHMV, FoMV and TCV GFP-chimeric constructs. Agroinfiltrated leaves were observed under UV light 12 days after initial inoculation.

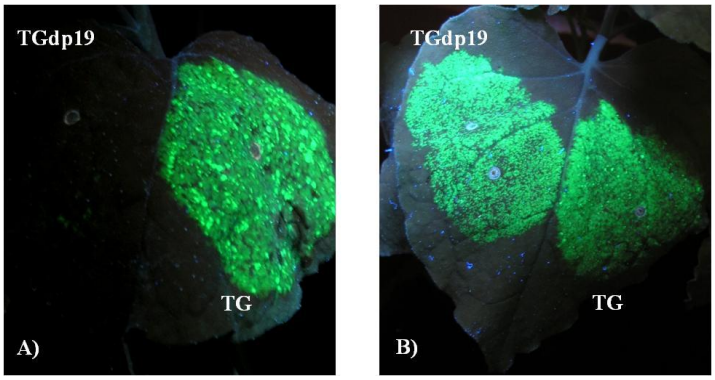

Figure 3.20. Half-leaf assays using TBSV constructs on **A)** *TRV-OO* agroinfiltrated and **B)** *TRV-NbAGO2* agroinfiltrated plant. TBSV GFP-chimeric constructs were agroinfiltrated approximately 4 weeks after initiation of TRV based gene silencing. Observations were made under UV light at 10 days after TBSV inoculation.

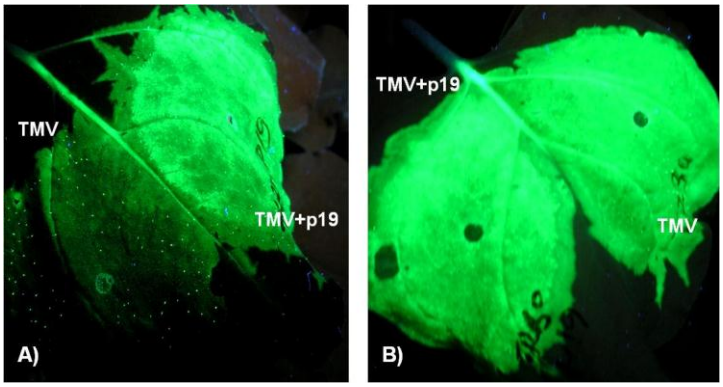

Figure 3.21. Half-leaf assays using TMV constructs on **A)** *TRV-OO* agroinfiltrated and **B)** *TRV-NbAGO2* agroinfiltrated plant. TMV GFP-chimeric constructs were agroinfiltrated approximately 4 weeks after initiation of TRV based gene silencing. Observations were made under UV light at 10 days after TMV inoculation.

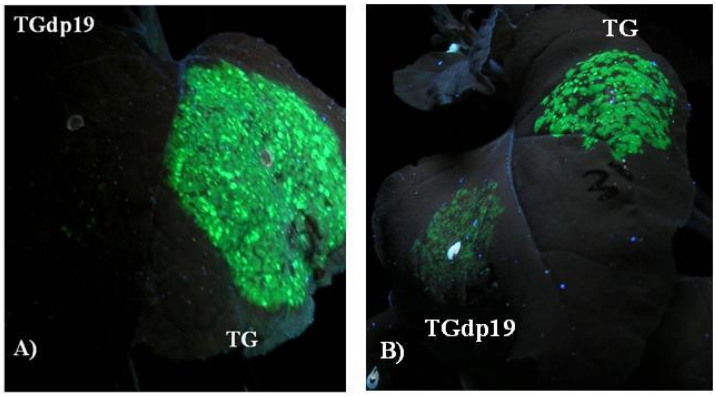

Figure 3.22. Half-leaf assays using TBSV constructs on **A)** *TRV-OO* agroinfiltrated and **B)** *TRV-NbAGOX* agroinfiltrated plant. TBSV GFP-chimeric constructs were agroinfiltrated approximately 4 weeks after initiation of TRV based gene silencing. Observations were made under UV light at 10 days after TBSV inoculation.

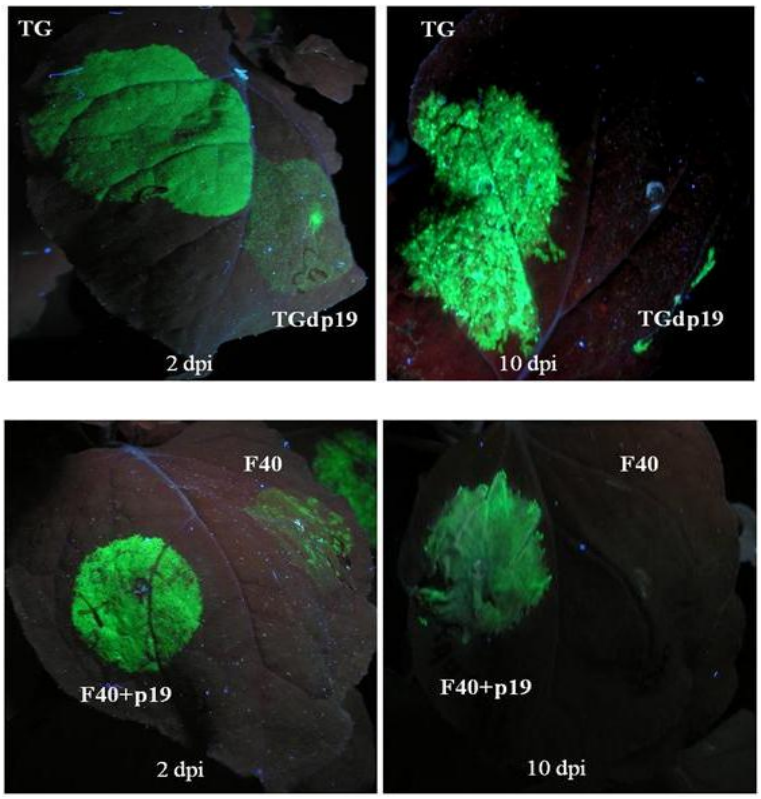

Figure 3.23. Half-leaf assays *TRV-NbAGO7* agroinfiltrated plant. TBSV and FoMV GFP-chimeric constructs were agroinfiltrated approximately 4 weeks after initiation of TRV based gene silencing. Observations were made under UV light at 2 and 10 days after GFP-chimeric virus inoculation.

Table 3.2. A summary of results obtained from single knockouts of the different *N. benthamiana AGO* genes

	WT	OO	AGO1	AGO2	AGO4	AGO5	AGO6	AGO7	AGOX
TGdP19	-	-	-	+	-	-	-	-/+	+
FECT40	-	-	-	-	-	-	-	-/+	-
SHEC	-	-	-	-	-	-	-	-/+	-
TURBO	-	-	-	-/+	-	-	-	-/+	-
TCV	-	-	-	-					

In summary therefore, as indicated in the table above, our results indicate that the only ARGONAUTE proteins implicated in antiviral defense against TBSV, FoMV, SHMV, TMV and TCV viruses were *AGOs 2, 7* and *X*. Virus-induced gene silencing of *NbAGO2* consistently led to the accumulation of TBSV without its silencing suppressor, and occasionally led to higher accumulation of the TMV construct TURBO-G when compared to a non-silenced plant. The silencing of *NbAGOX* also led to the accumulation of TGdP19 more than 75% of the time the test was carried out. When *NbAGO7* was silenced, TBSV, FoMV and SHMV not con-infiltrated with P19 constructs were seen to accumulate GFP earlier than in the non-silenced controls. However, the observed GFP accumulation was not persistent and completely disappeared within the next 5 days indicating that *NbAGO7* may play a partial role in antiviral defense.

Discussion

Semi-quantitative PCR analysis using primers designed to amplify the MCS of the TRV vector showed that the agroinfiltrated TRV constructs were able to accumulate, move systemically and remain intact for up to 45 days after the initiation of silencing.

Gene expression analysis of the plants silenced for individual *NbAGO* genes effectively confirmed the downregulation (to different degrees) of transcripts levels of the silenced gene, but also led to some very peculiar observations not previously reported. It was consistently noticed that the agroinfiltration of the TRV vector led to an upregulation of *N. benthamiana AGOs 1, 5* and *6.* Although this is a novel observation, it was not completely unexpected since *AGO1* has also been implicated in several antiviral defense roles, a notable example being where the *Potato virus X* silencing suppressor P25 was observed to interact with AGO1 in *N. benthamiana* and degrade it through the proteasome pathway so as to perpetuate its systemic spread (Chiu et al., 2010). Schott et al also recently observed that P19, the gene silencing suppressor of TBSV was able to prevent miRNA loading onto AGO1 in *Arabidopsis* primarily by sequestration of siRNA (Schott et al, 2012). Anti-TRV defense roles of *AGOs 5* and *6* have not been previously reported in *N. benthamiana*. It is therefore plausible to assume that the *N. benthamiana AGOs 1, 5* and *6* either play an antiviral defensive role in a TRV infection or somehow interact with the components of the pathogen to facilitate its replication and systemic spread.

Despite its numerous advantages, one of the arguments against the use of the virus-induced gene silencing system is its lack of specificity in that it has been known to inadvertently result in the suppression of other closely related non-target genes. This is especially common when working with host species that do not have completely sequenced genomes as in our case with *N. benthamiana* (Ekengren et al., 2003, He et al., 2004, Liu et al., 2004b). Indeed, our transcriptome analysis results using qRT-PCR hint towards such an observation; *NbAGO1* mRNA levels in *NbAGOs 5, 6* and *7* silenced plants were seen to be significantly reduced when compared to the *NbAGO1* transcript levels in control OO plant levels. Interestingly enough, whenever each of the *NbAGOs 5, 6* and *7* were silenced, the levels of *NbAGO1* transcripts also seemed to be significantly reduced. In order to eliminate cross silencing of the *AGO* genes as a possible explanation, the sequences inserted into the TRV vector were aligned against each other to match percentage similarities. NCBI's nucleotide sequences alignment BLAST suite

web based program was used to perform the alignments (NLM, 2012). Results show that the *AGOs 5, 6* and *7* sequences cloned in the TRV vector show a mere 8, 15 and 17% similarity to the cloned *NbAGO1* sequences. This essentially discards the possibility of cross silencing of these *AGOs*; instead, each of these *AGOs* may be involved in other pathways regulation the expression of the other(s). The possibility of cross silencing can be further discarded since the characteristic developmental deformation phenotype typically associated with the silencing of *NbAGO1* was not seen when *AGOs -5* and *-6* were silenced. However, a remarkably similar phenotype (only to a lesser extent) was observed about 2 to 3 weeks upon initiation of *NbAGO7* silencing, but the phenotype was non persistent and was no longer perceived after 3 weeks.

The surprisingly stable levels of *NbAGO2* mRNA in the putative *NbAGO2*-silenced plants observed in qRT-PCR analysis (although not reassuringly consistent with semi-quantitative PCR as shown in Figure 3.17) can possibly be attributed to a number of factors. First and probably most importantly, when the designing of the qRT-PCR primers to amplify endogenous *NbAGO2* was carried out, just like in the case with other *N. benthamiana AGOs*, we had a very limited sequence of only about 800 bp, approximately 600 bp of which were part of the sequence inserted into the TRV vector. Initially, attempts were made to design the *NbAGO2* qRT-PCR primers to amplify regions outside of the 600 bp fragment inserted the TRV vector. Multiple attempts at this design contemplation were painfully unsuccessful. Later on, it was deduced that even if the primers were designed to amplify regions within the 600 bp sequence inserted in the TRV vector, when only oligo dT to synthesize the cDNA, theoretically, only mRNA of plant origin would be used to synthesize cDNA because TRV RNA does not have a polyA tail. These speculations may have been wrong and the *NbAGO2* sequence inserted in the TRV vector may have been amplified explaining the stability or slight upregulation of *NbAGO2* transcript levels observed in the putative *NbAGO2* silenced plants. However, if the observations that the amplicons were of viral origin were absolutely certain, due to the massive accumulation of TRV virus upon a successful infection in *N. benthamiana*, a much higher transcript level would have been observed

through qRT-PCR analysis. A second explanation may lie in the possibility of a currently unidentified *N. benthamiana AGO*, possibly *NbAGO3* with very similar sequences to our currently known *NbAGO2*. Therefore *NbAGO2* may have been successfully silenced but the designed primers amplified its close homologue the putative *NbAGO3*. In *Arabidopsis*, AtAGO2 and AtAGO3 are known to share a very high level of amino acid sequence similarity and are located adjacently in the *Arabidopsis* genome. Both AtAGOs fall in the same clade and are thought to have arisen from a recent duplication event (Ki Wook Kim, 2011). It is not completely far-fetched to speculate that a similar situation may exist within *N. benthamiana AGOs*.

In the commonly used plant model *Arabidopsis*, AtAGO1, the most abundant and consistently expressed AGO not only regulates expression of miRNAs involved in proper plant development (Baumberger & Baulcombe, 2005a, Vaucheret, 2005), but is also heavily involved in multiple antiviral defense against CMV and other member of the *Polerovirus* family (Morel et al., 2002, Zhang et al., 2006). AtAGO1 silenced plants exhibited multiple developmental defects and showed extreme susceptibility to the above name viruses (Baumberger et al., 2007, Bortolamiol et al., 2007, Bortolamiol et al., 2008). As previously reported by Jones et al (Jones et al, 2006), and confirmed in the present study, the silencing of *NbAGO1*, just like its *Arabidopsis* homologue also caused several developmental defects on the aerial parts of the *N. benthamiana* plant. It led to the deformation of both emerging and older leaves; leaf veins were misaligned, leaf midrib emerged from leaf surface, flowers were malformed and aborted to mention but a few developmental defects. NbAGO1, just like AtAGO1 is therefore possibly involved in the regulation of developmentally related miRNAs. Surprisingly therefore, silencing of NbAGO1 did not cause any enhanced susceptibility to any of the viruses tested. If anything, the leaves that showed the characteristic phenotype associated with NbAGO1 silencing were observed to be more resistant to necrosis caused by accumulation of TMV and TBSV. This may also indicate that in *N. benthamiana*, AGO1 possibly regulates the defense mechanism associated with program cell death to fight off a viral invasion, hence when AGO1 is silenced, limited or no necrosis was perceived on plant

leaves. Multiple attempts were carried out to verify this by attempting to silence *AGO1* in *N. tabacum* Glurk. Upon a TMV infection, Glurk leaves show very distinct necrotic local lesions, demonstrating the classical Holmes' N-gene resistance limiting virus accumulation and spread (Beijerinck, 1898, Scholthof, 2004). My hypothesis therefore was that AGO1 was somehow involved in this (Nucleotide-Binding Site Leucine-Rich Repeat) NBS-LRR class of disease resistance and silencing it would cripple the resistance mechanism. However, unfortunately all attempts to silence AGO1 in *N. tabacum* were unsuccessful. On the other hand, one may argue that the N-gene resistance mechanism does not exist in *N. benthamiana*; hence the observations made had no relation to this resistance mechanism therefore attempts should have been made at studying other components of the defense mechanism. We did not have any constructs or viruses previously tested on AtAGO1 silenced *Arabidopsis* and so at this moment can only confirm that in *N. benthamiana*, the limited number of viruses we tested, NbAGO1 was not involved in antiviral defense. The silencing of NbAGO1 could have possibly led to an epigenetic down regulation of other genes actually involved in the defense mechanism causing leaf necrosis explaining the limited necrosis observed on NbAGO1 silenced plants despite the massively evident accumulation of virus.

The *Arabidopsis* AtAGO2 has also been implicated in antiviral defense, specifically and only against TCV and CMV (Harvey et al., 2011a, Wang et al., 2011a) and no other viruses indicative of its specificity. Virus-induced gene silencing of AGO2 in *N. benthamiana* just as in *Arabidopsis* did not result in any observable phenotype providing evidence that it may not play a critical role in regulation of plant developmental process. My observations as well as those reported by Scholthof *et al* however indicate that NbAGO2 (Scholthof et al, 2011), and NbAGOX are consistently observed to be necessary in the silencing of the P19 defective TBSV.

The present study also indicates that NbAGO2 may be loosely associated with anti-TMV defense. Just like in *Arabidopsis* where the precise mechanism explaining the observed specific *virus-AGO* interactions are not known, the particular interactions observed in *N. benthamiana* with TBSV and AGOs 2 and X cannot be fully explained at this time.

Although the *Arabidopsis* AGO7 has only been linked to anti-TCV defense (Qu et al., 2008), our observations indicate that its *N. benthamiana* homologue may be loosely involved in a general antiviral defense evident in that the TBSV, SHMV and FoMV constructs without their silencing suppressors accumulated to substantial levels earlier on in NbAGO7 silenced leaves. The GFP accumulation however later disappeared indicating that probably another mechanism, kicked in to carry out the antiviral defense later on, or that NbAGO7 has a limited antiviral defense role that has to be complemented by another system in order to be completely effective.

Our observations with the limited number of viruses also indicate that just like in *Arabidopsis*, AGOs 4, 5 and 6 have no reported antiviral defense role. The AtAGO4 although not directly linked to any specific antiviral defense is seen to be involved in defense against *Pseudomonas syringae* suggesting its role in the activation of certain pathogen-specific defense mechanisms (Agorio & Vera, 2007) or possibly due to epigenetic down regulation of other genes actually involved in this defense mechanism (Ki Wook Kim, 2011). In *N. benthamiana*, observations on the *Potato virus X* (PVX) suggest that the contribution of AGO4-like proteins regulate virus resistance mediated by NB–LRR proteins (Bhattacharjee et al., 2009) furthermore confirming the specific-AGO-pathogen interaction by modulating a particular defense pathway.

Although, the GFP-chimeric virus constructs used in our system do not represent what exactly occurs in a natural infection, the role of AGOs in antiviral defense and more specifically, the distinct interaction between a particular AGO and a given pathogen is clearly unmistakable. It is also quite clear that much as there are some very striking similarities between the AGOs of *Arabidopsis* and its *N. benthamiana* homologues, they do not always play the same regulatory or antiviral defense role. Additionally, it is clearly understood that only a very limited number of viruses have been tested to come to any universal conclusion about entire virus families raising the need for further widespread experiments.

CHAPTER IV

SILENCING OF MULTIPLE *N. BENTHAMIANA ARGONAUTES* TO INVESTIGATE ADDITIVE EFFECTS OR FUNCTIONAL REDUNDANCY IN ANTIVIRAL SILENCING

Introduction

ARGONAUTES (AGOs) represent a highly conserved, ubiquitously expressed gene family present in almost all eukaryotes, bacteria and archaea (Hock & Meister, 2008, Hutvagner & Simard, 2008). As mentioned in the previous chapters, AGOs are extremely diversified in abundance and function within different species; *C. elegans* for example encode as many as 27 known AGO proteins (Kim et al., 2005), while *Schizosaccharomyces pombe* on the other hand has only one AGO solely involved in both RNAi and transcriptional silencing (Sigova et al., 2004).

The plant model *Arabidopsis* encodes 10 known AGOs (Hutvagner & Simard, 2008, Zhang, 2011, Benning, 1998, Manavella, 2011, Morel et al., 2002), and yet phylogenetic analysis of the diploid *Musa acuminata* ssp. Malaccensis (a wild relative of the modern commercialized banana) sequences revealed an estimated 15 *AGO* genes or loci containing PIWI domain sequences in its genome (Teo et al., 2011). The common rice (*Oryza sativa*) genome contains 18 copies of genes of the AGO family (Nonomura et al., 2007, Wu et al., 2009b, Fujita et al., 2010, Itoh et al., 2005, Raghavan, 1988) while in a recent paper, 15 *AGO* genes were indentified in the tomato (*Solanacearum lycopersicum*) genome (Bai et al., 2012). Members of the AGO protein family therefore seem to play important roles in RNA-mediated silencing during plant development as well as to mitigate effects of abiotic and biotic stress.

The sheer number of identified AGOs compared to the roles generally played by AGO proteins leads to the speculation that there may exist certain overlapping, redundant or additive roles among AGOs within the same species. Hence when one member of the AGO family is silenced, only a small effect is observed or another orthologue of the same family takes over the role previously carried out by the silenced

AGO, therefore a delayed or non-persistent phenotype may develop as was observed when NbAGO7 was silenced in Chapter III. In *Arabidopsis* it was observed that *Plantacyanins* of phytocyanin family of blue copper proteins (Cupredoxins) (Dong et al., 2005) are regulated through either AGO1 or AGO2 via the miR408. In fact, neither single mutations of *ago1* nor *ago2* individually impeded the regulation of *Plantacyanin*, rather only an *ago1*/*ago2* double mutant appears compromised in miR408-mediated regulation of *Plantacyanin*, suggesting that AtAGO1 and AtAGO2 have redundant roles in this regulation (Maunoury, 2011).

Both the *Arabidopsis* AGOs 4 and 6 are speculated to direct the RNA silencing pathway at the transcriptional level through heterochromatin silencing (Zheng et al., 2007, Havecker et al., 2010a). Zheng *et al* showed that when the expression of a transcriptionally-silent transgene was reactivated in the *ros1* mutant background; the level of transcriptional reactivation was higher in the *ago4/ros1* double mutant background than in the *ago6/ros1* mutant. This suggests that although AtAGO6 plays a role in sRNA-directed heterochromatin RNA silencing, it is not as widespread as that directed by AGO4 in Arabidopsis. The level of transgene reactivation was demonstrated to be even higher in the *ago4/ago6/ros1* triple mutant, compared to either of the analyzed double mutants. Furthermore, array and reporter gene expression data reveal that the expression domain of AGO6 overlaps that of AGO4 (Schmid et al., 2005). Taken together, these observations suggest that these two *Arabidopsis* AGO family members act on a shared subset of repeat elements, and that their overlapping function occurs in analogous tissues and at the similar developmental time points (Ki Wook Kim, 2011).

The *Drosophila melanogaster* genome encodes five AGO protein family members: Aubergine (Aub), Piwi, DmAGO1, DmAGO2, and DmAGO3 (Carmell et al., 2002, Kataoka et al., 2001, Williams & Rubin, 2002) each of which has been assigned to distinct role in RNA silencing pathways. For example, while DmAGO1 is required for miRNA function, DmAGO2 is a crucial component of the RNA-induced silencing complex in siRNA-triggered RNA interference. DmAgo2 however, contains an unusual

amino-terminus with two types of imperfect glutamine-rich repeats (GRRs) now known to be essential for the normal growth and microtubule-based organelle transport. Using loss of function mutants, Meyer *et al* (Meyer et al., 2006) showed that the ensuing defects do not appear as a result of disruption of siRNA-dependent process but rather suggest an interference of the mutant *ago2* proteins in an AGO1-dependent pathway. They also further demonstrate that DmAGO1 and DmAGO2 act in a partially redundant manner to control the expression of the segment-polarity gene *wingless* in the early embryo furthermore validating the argument against a strict separation of AGO1 and AGO2 functions in gene regulation (Meyer et al., 2006).

Members of the AGO protein family are also known to regulate the expression and function of each other. In *Arabidopsis*, AtAGO10 regulates shoot apical meristems (SAM) by specifically interacting with miR166/165. AtAGO1 is also capable of binding to miR166; however AtAGO10 has a higher binding affinity for miR166 than does AtAGO1. It therefore acts as a decoy for miR166/165 to be able to maintain the SAM in the required tissues preventing their incorporation into AGO1 complexes and subsequent repression of the class III HOMEODOMAIN-LEUCINE ZIPPER transcription factors, targets of the mi166/165 (Zhu et al., 2011).

In light of these observations, I therefore specifically proposed that *N. benthamiana* AGOs, just like most other AGO proteins in the eukaryotic taxa may have overlapping, redundant or additive roles therefore silencing of only one of the AGOs may not result in any observable effects against a given virus. My specific objective therefore was to explore the possibility of silencing various combinations of *NbAGOs* and test them for antiviral activity.

Materials and methods

Computation of possible combinations

All possible combinations were manually computated by rearranging all the different TRV-AGO constructs in an MS Office Excel file resulting into combinations ranging from those that include all 7 constructs to single knockouts. For purposes of

simplifying data registry, each combination was given a number which was used to label the individual plant pots. The resulting total of 126 TRV-AGO construct combinations were all agroinfiltrated and this experiment was repeated at least three times. For results that were thought to be interesting, a fourth and fifth repeat were set up as well. The identification number and combinations of TRV-AGO constructs used to silence multiple *NbAGO* genes using the TRV VIGS system are detailed in the Appendix section (A.5) of this thesis.

Agroinfiltration

TRV-AGO constructs were prepared and infiltrated according to specifications stated in the Materials and methods section of Chapter III. All the cultures were adjusted to an optical density of 0.5 prior to agroinfiltration. Each constructs was individually infiltrated so that each leaf at least received all TRV-NbAGO constructs being tested. Two leaves per plant were infiltrated but when necessary for example when a total of more than 4 constructs needed to be infiltrated, a maximum of four leaves were used. The *N. benthamiana* plants were then placed on growth shelves with 25/22°C day/night temperature cycles and 16h-light/8h-dark cycles. A period of 3 – 5 weeks was allowed for the TRV-AGO virus to replicate and accumulate within the plant as silencing of its endogenous genes is occurring.

Testing activity against GFP-chimeric viruses

GFP-chimeric virus and P19 constructs were prepared for infiltration as described in the Materials and methods section of Chapter III above. Agroinfiltration was also carried out as previously mentioned. Starting from about 2 days after agrofiltration, the plants were visually assayed for virus accumulation by observing GFP signal under a 488 nm UV-light, and pictures were taken with 4 second exposures without flash. GFP was monitored for the next 12 days and results were documented for further analyses.

Results

After the silencing combinations were set up, it was clearly evident that the pleiotropic developmental phenotypes characterized by leaf deformations and flower abortions associated with *AGO1* silencing in *N. benthamiana* were always prominent in all silencing combinations including the *TRV-NbAGO1* construct. Furthermore, when *TRV-NbAGO2* was included in a silencing combination that also included the *TRV-NbAGO1* construct, The TBSV GFP-chimeric construct without its P19 silencing suppressor (TGdP19) was expected to accumulate to high levels as shown in Chapter III; however more than 90% of the times this experiment was repeated, this was not observed indicative that *NbAGO2* had not been silenced in these leaves. Similar observations were witnessed with silencing combinations that included both *TRV-NbAGO1* and *TRV-NbAGOX* constructs. When these leaves were agroinfiltrated with the GFP-chimeric viruses they showed characteristics similar to those shown by plants silenced only for *NbAGO1*: none of the GFP-chimeric viruses accumulated if not co-infiltrated with P19 and the leaves showed resistance to necrosis due to virus accumulation. These observations then incited the proposition that the other constructs were probably not replicating and moving systemically within the plant due to suppression by the *TRV-NbAGO1* construct.

In order to prove that the other constructs were not being spread systemically, RNA was extracted from the upper newly emerging leaves and cDNA was synthesized using TRV-MCS reverse primers. PCR was carried out using the TRV-MCS primers to determine virus-construct systemic spread. All the procedures for RNA purification, cDNA synthesis and PCR followed are listed in the Materials and methods section of Chapters II and III.

Semi-quantitative PCR results showed that irrespective of the silencing combination being used; whenever the combination including *TRV-NbAGO1* construct, only the *TRV-NbAGO1* was observed to be moving systemically in the *N. benthamiana* plant (data not shown). In order to visually document this phenomenon, TRV constructs that caused a clearly discernible phenotype were used. Conventional semi-quantitative

PCR using TRV MCS primers was then performed to determine the systemic spread of the individual constructs. For this, an experiment was conducted whereby in one plant the *TRV-NbAGO1* construct was solely infiltrated, in another both *TRV-NbAGO1* and *TRV-MgCh* and in a third plant only *TRV-MgChelatase*. Observations were made starting at about 5 days after initiation of silencing.

The resulting phenotypes coupled with the semi-quantitative PCR results shown in Figure 4.1 indeed confirmed that an infection with *TRV-NbAGO1* somehow suppresses the systemic accumulation of *TRV-MgCh* just as observed with the other *TRV-AGO* constructs.

The experiments were repeated at least 3 more times with the same outcomes. These plants were kept for approximately 10 more weeks during which the plants were keenly observed for the appearance of the slower moving TRV construct. At about 6 weeks after the initiation of silencing, the conspicuous photobleaching phenotype associated with silencing of *N. benthamiana* leaf *Magnesium Chelatase* was seen on one branch of the plant. This slowly spread to other parts of the plant as well showing less distinct leaf and flower deformations associated with the silencing of *NbAGO1*. After approximately 6 days, in a few plants, as shown in Figure 4.2, the photobleaching phenotype was observed to completely take over the previously *AGO1* silenced *N. benthamiana* leaves. Note however that unlike the previous plants mentioned in Chapters II and III, these plants were kept at 19^{o}C under a 12/12 hour light/day conditions. This way the *N. benthamiana* plants were able to survive long enough to be able to make the observations here mentioned.

In order to confirm some of the observations made at 60 days after initiation of silencing shown in Figure 4.2, semi-quantitative PCR (Figure 4.3) was carried out using the TRV-MCS primers following the specifications previously stated in Chapter II and III. Also included in the PCR analysis were co-infiltrations of *TRV-NbAGO1* and *TRV-NbAGO2*.

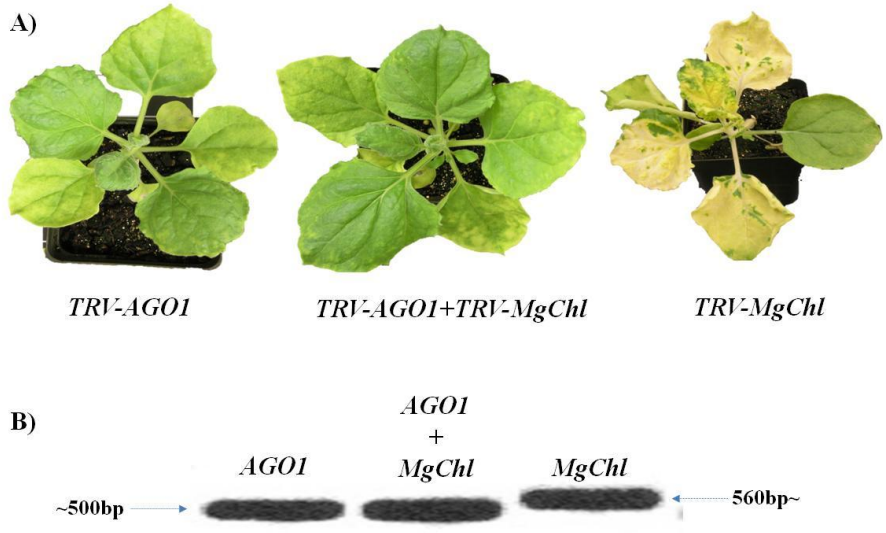

Figure 4.1. Results of co-infiltration of TRV-NbAGO1 and TRV-MgChl after 10 days. **A**) Phenotypes observed 10 days after initiation of gene silencing. It is clearly evident that the TRV-NbAGO1 construct is somehow suppressing the systemic spread hence impeding silencing of the *Magnesium Chelatase* gene. **B**) Semi-quantitative PCR analysis to amplify an approximately 500 or 560 bp fragment from *NbAGO1* or *MgChl* sequences inserted in the TRV vector upon systemic infection. Results showed that when co-infiltrated with *TRV-NbAGO1*, the *TRV-MgChl* construct does not move systemically further confirming the lack of photobleaching phenotype observed in the co-infiltrations.

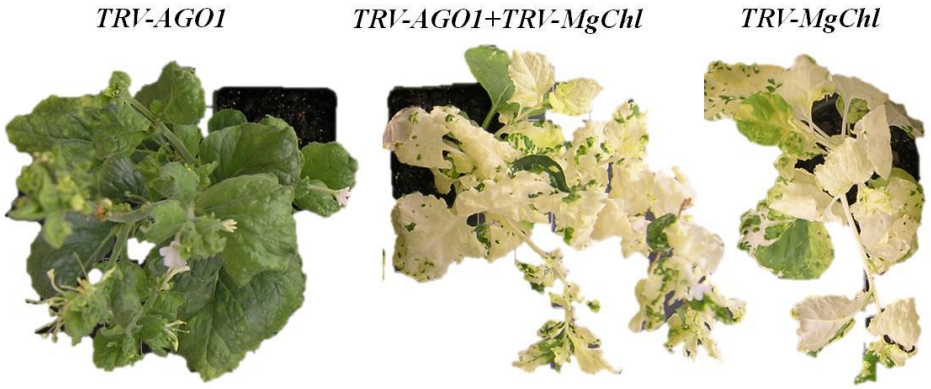

Figure 4.2. Results of co-infiltration of *TRV-NbAGO1* and *TRV-MgChl* after 60 days. Phenotypes observed 60 days after initiation of silencing. The photobleaching phenotype associated with *Magnesium Chelatase* gene silencing is recovered indicating that the *TRV-MgChl* virus constructs although initially suppressed was able to recover and move systemically in the plant or the phenotype observed was due to the slow movement of the silencing signal and not the viral construct.

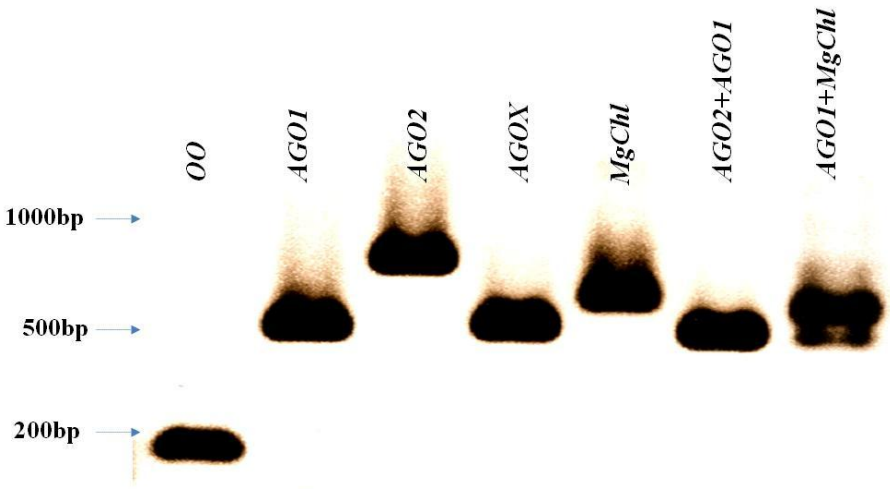

Figure 4.3. Results of semi-quantitative PCR from *N. benthamiana* leaves 60 days after initiation of silencing. As seen in the phenotype, both *TRV-NbAGO1* and *TRV-MgChl* viral constructs are present in the double co-infiltrations. However, when *TRV-NbAGO1* is co-infiltrated with *TRV-NbAGO2*, even at 60 dpi, *TRV-NbAGO2* viral construct was still not present in the newly emerging leaves, indicative of its inability to spread systemically in the presence of *TRV-NbAGO1* viral construct.

Other silencing combinations were also repeated with widely varying observations. However, in all *TRV-AGO* viral construct combinations that included either or both *TRV-NbAGOX* and *TRV-NbAGO2* but not *TRV-AGO1*, the GFP-chimeric TBSV construct defective of its silencing suppressor showed accumulation of GFP further confirming the role of *NbAGO2* and *NbAGOX* in the silencing of the TBSV.

Another fairly consistent observation (also mentioned in Chapter III) was that in combinations including both the *TRV-NbAGO2* and *TRV-NbAGOX*, leaf necrosis due to virus accumulation appeared to be more rapid and severe when compared to the individually silenced plants or the healthy virus-free controls. It is important to note that the observed necrosis was more severe compared to the controls irrespective of which type of virus was being used for inoculation (data not shown).

Discussion

The results clearly suggest that upon co-inoculation of *N. benthamiana* with various TRV vector constructs, there is an uneven systemic accumulation of the viral constructs. The explanation of the mechanism behind these findings is still unclear and this concept has not been previously reported. Wu *et al* documented the effect of insert size on the development of symptoms caused by using TRV as a vector in tomato (*Solanacearum lycopersicum*) and found that the empty vector caused far more extensive symptoms of virus infection than other silencing constructs (Wu et al., 2011). This suggested that the viral systemic spread hence symptom development may be influenced by the size of the viral vector. Along the same train of thoughts therefore, our *TRV-NbAGO1* with a smaller (about 300 bp) insert is then logically more capable of systemic spread than *TRV-NbAGO2* with a much larger insert of about 590 bp. However, this does not explain why the *TRV-NbAGO1* viral construct is still seen to outcompete and suppress even the empty vector *TRV-OO* as observed in our experiments (data not shown).

Another possible explanation of the efficiency in systemic spread of the *TRV-NbAGO1* viral construct may lie in its long-range RNA-RNA interactions (Miller &

White, 2006, Serrano et al., 2006, Hu et al., 2007, Diviney et al., 2008, Song et al., 2008). RNA viruses have been traditionally viewed as linearized sequences or localized structures such as hairpins. It is now known that functional viral RNA elements that are formed by long-range RNA–RNA interactions spanning significant distances. These interactions may usually regulate both translation and transcription. Wu *et al* reported that in the TBSV genome replication requires a long-range RNA–based interaction spanning approximately 3000 nucleotides. Observations from in vivo and in vitro analyses suggest that the discontinuous RNA platform formed by the interaction facilitates efficient assembly of the viral RNA replicase (Wu et al., 2009a). A functional viral RNA genome is therefore a three-dimensional molecule with multiple interactions occurring which may hinder or facilitate virus replication. It is therefore not too far-fetched to propose that the insertion of the approximately 320 bp *NbAGO1* sequences into the TRV vector may have modified its three dimensional structure to fold in a way that favors replication giving it a competitive edge over the other constructs.

The consistently evident predominance of the *TRV-NbAGO1* viral construct over the rest of the constructs verified both by phenotype observation and semi-quantitative PCR analysis substantiates that even though it is possible to concurrently silence multiple *N. benthamiana AGO* genes using the TRV vector system, the fact that one construct may suppress the systemic spread of another would make this system quite impractical for silencing of multiple genes. Although the TRV-VIGS system may not be the most adequate for multiple genes silencing in plants, there exists several tools for identification of loss-of-function of gene(s) such as, Targeting Induced Local Lesions in Genomes (TILLING), chemical and physical mutagenesis, T-DNA and transposon insertion techniques (Unver & Budak, 2009), as well as the use of inverted hairpins which will be discussed in the next chapter.

CHAPTER V

THE USE OF A VIRUS-FREE SYSTEM FOR DETERMINATION OF THE ANTIVIRAL SILENCING ROLES OF ARGONAUTES IN *N. BENTHAMIANA*

Introduction

In spite of the numerous undisputable advantages of the use of the virus-induced gene silencing (VIGS) approach, the method also entails various limitations. A complete loss-of-function by VIGS is normally not achieved partially due to the fact that maximum down-regulation in the expression level of the targeted gene does not exceed 75–90% (Pflieger et al., 2008, Orzaez et al., 2006). In many cases the low levels of gene expression may be enough to produce functional protein and expected phenotypes are not witnessed even if there is a considerable reduction in expression of the gene of interest. Furthermore, some viral infection can not only cause symptoms on plants but also manipulate host functions and mask the expected phenotype or even interfere with it manifestation. In *N. benthamiana* however, the problem is slightly minimized since the VIGS vector *Tobacco rattle virus* (TRV) only causes very minor symptoms that do not appear to alter the normal plant physiology (Ratcliff et al., 2001). Another main argument against the use of a virus vector is that unexpected synergistic or antagonistic interactions between the viruses in the host system may mar results and lead to false experimental observations and conclusions. In nature, mixed infections of plant viruses are common, and a number of important virus diseases of plants are the outcomes of interactions between distinct causative agents. Multiple infections often lead to a variety of unexpected intrahost virus–virus interactions, creating usually unpredictable biological and epidemiological consequences in the host plants (Syller, 2012, Garcia-Marcos, 2009). The mechanisms behind these interactions are still largely unknown and so their occurrence and nature cannot be predicted.

Viral-viral interactions have been reported since the early 1950's. The classical work on the nature of viral interactions was first reported on experiments focused on the synergy between *Potato virus X* (PVX) and *Potato Virus Y* (PVY) viruses by Ross and

colleagues between 1950 and 1974 (Loebenstein et al, 2006). The experiments showed that the levels of PVX and not PVY increased during a double infection. A co-infection of PVX and PVY led to an even greater accumulation of PVX when PVX or PVY was inoculated prior to carrying out the co-infections (Rochow et al, 1954, Rochow et al 1955). The increase in disease severity was observed to correspond to the increase in PVX levels which were dependent on the plant growth stage as well as environmental conditions under which they were being grown, further demonstrating the complexity of these inter viral interactions.

A number of viral synergisms which do not involve a member of the potyvirus group have been reported. In a mixed infection of the *Begomoviruses Pepper golden mosaic virsus* (PepGMV) and the *Pepper huasteco yellow vein virus* (PHYVV), a double infection was seen to induce more severe symptoms than those observed in single viral infections (Renteria-Canett et al., 2011). Since both single stranded DNA viruses belong to the same genus, the authors speculate that the exacerbation of the infection was as a result of an increased DNA concentration.

The unpredictability and host dependence of these interactions can be further appreciated in a report by Alves-Junior *et al* where in *S. lycopersicum* (tomato), the *Tomato rugose mosaic virus* (ToRMV) negatively interferes with *Tomato yellow spot virus* (ToYSV) during the initial stages of infection. However once systemic infection is established this interference ceases. On the other hand, in *N. benthamiana*, ToYSV invades the mesophyll, while ToRMV is phloem-restricted, and therefore during dual infection in this host, ToYSV releases ToRMV from the phloem seriously exacerbating symptoms due to the double infection (Alves-Junior et al., 2009).

These virus-virus interactions are not only limited to similar viruses as can be witnessed in the synergistic pathogenicity of a phloem-limited DNA *Begomovirus* the *Abutilon mosaic virus* (AbMV) and RNA *Tobamovirus Tobacco mosaic virus* (TMV). Despite the fact that the RNA virus caused a substantial decrease in accumulation of the DNA virus, the overall pathogenicity was more severe in a mixed than in a single infection. The authors implicate that the observation may be explained by simultaneous action of the

two viruses on different host pathways, which in combination provokes an overall enhanced host response witnessed by the exaggerated symptoms produced (Pohl & Wege, 2007). Isolate-specific synergy in disease symptoms has also been observed in a *Cauliflower mosaic virus* and *Turnip vein-clearing virus* mixed infection (Hii et al., 2002). Observations in our laboratory also show that TBSV infections are more severe in *N. benthamiana* plants that are already infected with TRV (unpublished data). These and many of the observations reported in mixed infections led us to re-evaluate some of our observations using a virus-free system.

As previously discussed in Chapter I, double stranded RNA (dsRNA) can effectively trigger gene silencing in plant systems (Waterhouse et al., 2001, Sharp, 2001) by sequence-specific RNA degradation. When using hairpin-RNAi, gene silencing is achieved by use of constructs that express a self-complementary gene construct encoding a hairpin consisting of an inverted repeat of a fragment of the gene sequence separated by an intron (Wesley et al., 2001, Smith et al., 2000). The hairpin stem (separated by its intron loop) designed with fragments of the targeted endogenous genes provides a source of the dsRNA trigger needed to initiate the PTGS process (Helliwell & Waterhouse, 2003). The generic hairpin vector pHELLSGATE from Australia's National Science Agency Commonwealth Scientific and Industrial Research Organization (CSIRO) was used to design the required hairpin vectors.

Materials and methods

The pHELLSGATE hairpinRNAi vector

The concept of the pHELLSGATE hairpin vectors is based on Invitrogen's Gateway recombination cloning technique. PCR products for the target gene are generated with flanking attB1 and attB2 sites and then in a single reaction using BP clonase, the products are simultaneously recombined into a vector carrying two attP1 and attP2 cassettes separated by a PDK intron sequence. As shown in Figure 5.1, the presence of a negative selection marker, the toxic ccdB gene ensures that both halves of the hairpin are present in the construct.

Prior to the construction of the hairpin vectors, the primers used to amplify the endogenous *NbAGO2* were designed with flanking attB1 and attB2 sites as shown below. In order to generate PCR products with flanking *aat*B sites, the *aat*B1 and *aat*B2 sequences were added onto the 5' ends of the primers designed to amplify endogenous gene fragment which to be inserted into the vector. However, besides the 12 bp sequence of the *aat*B sites, at least 6 more random nucleotides were added at the 5' end so as to improve the stability of the primers.

A 2-step PCR reaction was then carried out to optimally achieve the gene fragments required for the BP clonase reaction. In the first step template specific primers containing the 12+ nucleotides of the *att*B sites plus the gene specific primers were first used in a 10 cycle PCR run to amplify the target gene under the conditions stated in Figure 5.2.

Because of the sequence precision required in this reaction, Vent DNA polymerase (Life Technologies) which has exonuclease proof reading activity was used. In the second step 10 uL of the reaction mixture from the first PCR was used as the DNA template. Here the *att*B adapter primers (Figure 5.2) are used to amplify the full *att*B PCR product. Note that the adapter primers have 4 additional guanine (G) nucleotides at the 5' ends. These are known to make the reaction more efficient. The reaction setup conditions are also listed in Figure 5.2.

Approximately 10 uL of the resulting products from the second PCR were electrophoresed through a 1% agarose gel to confirm amplification of the correct size fragment. The gel was then stained in an Ethidium bromide solution and visualized under UV light.

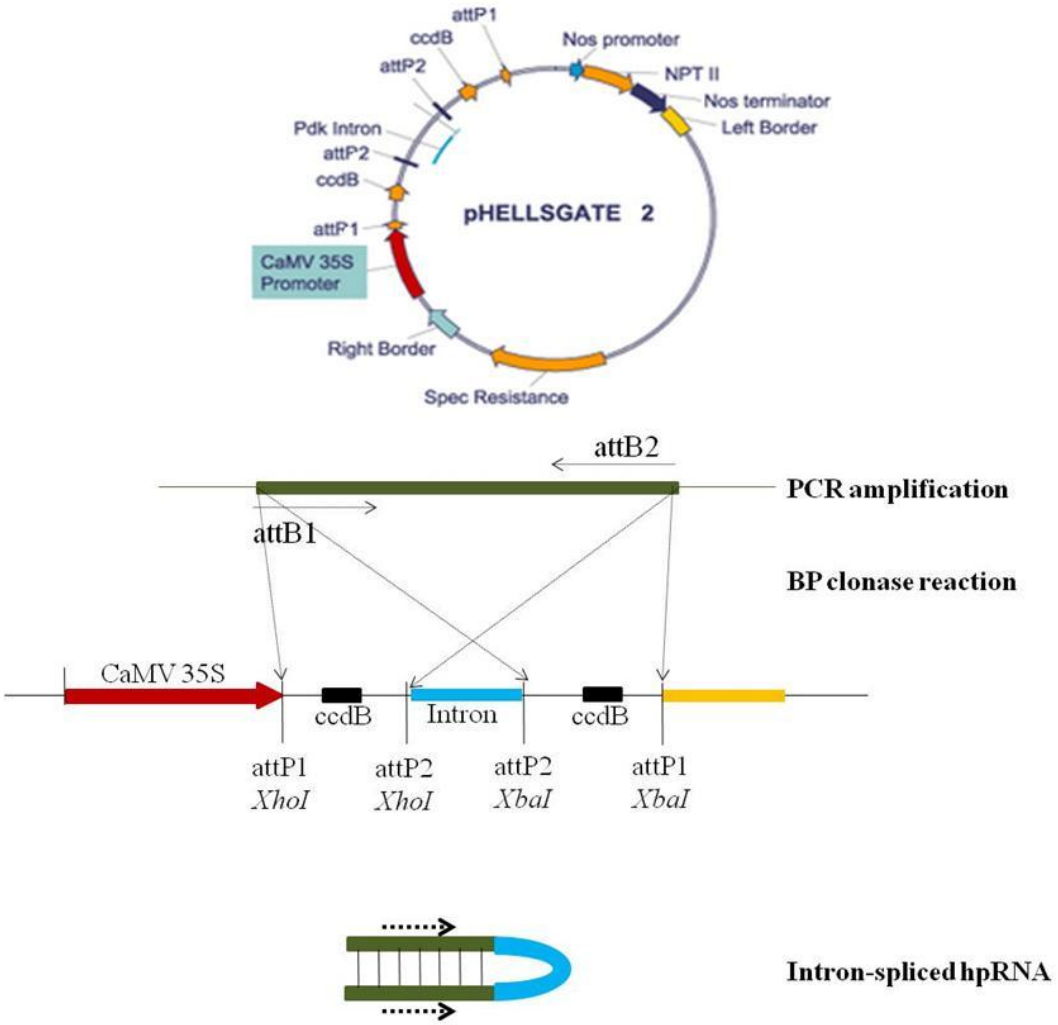

Figure 5.1. Designing a pHELLSGATE hairpin vector. Schematics of the pHELLSGATE vector and BP clonase recombination reactions with pHELLSGATE vectors to produce the hairpinRNA. Hairpin vector diagrams have been modified from CSIRO plant web page (CSIRO, 2007).

Template specific primers

*aat*B1:NbAGO2 Forward Primer:
5'- TTGTACA AAAAAGCAGGCTNN GAGCACTTGGCTGAACATGA-3'

*aat*B1:NbAGO2 Reverse Primer:
5'- TTTGTACA AGAAAGCTGGGTN TCTTCAGCCCGTACCATTTC-3'

Adapter primers

*aat*B1 Adapter Forward Primer:
5'-GGGACAAGTTTGTACAAAAAAGCAGGC T-3'

*aat*B2 Adapter Reverse Primer:
5'-GGGGACCACTTTGTACAAGAAAGCTGGGT-3'

First PCR setup		**PCR conditions**	
Template (DNA)	1.0 µl	95°C ..... 2 min	
10X Thermopol II Buffer	2.0µl	95°C ..... 30 sec	10 cycles
50mM MgSO4	1.0µl	55°C ..... 30 sec	
10 mM dNTP	0.5 µl	72°C .....1 min	
10 µM attB1+NbAGO2	0.5µl	72°C 5min	
10 µM attB2+NbAGO2	0.5 µl	4°C ..... ∞	
VENT polymerase	0.125µl		
H_2O	13.3 µl		
TOTAL	20 µl		

Second PCR setup		**PCR conditions**	
Template (DNA)	10.0 µl	95°C ..... 2 min	
10X Thermopol II Buffer	5.0 µl	95°C ..... 30 sec	25 cycles
50mM MgSO4	2.5 µl	55°C ..... 30 sec	
10 mM dNTP	1.0 µl	72°C .....1 min	
10 µM attB1 adapter F	4.0 µl	72°C .....10 min	
10 µM attB2 adapter R	4.0 µl	4°C ..... ∞	
VENT polymerase	1.0 µl		
H_2O	22.5 µl		
TOTAL	50 µl		

Figure 5.2. Primers and PCR conditions used to amplify the endogenous *NbAGO2* with flanking attB1 and attB2 sites prior to BP clonase reaction.

Upon satisfactory confirmation of fragment size, the remaining 40 uL were then subjected to a PCR cleanup to remove enzyme buffers and other impurities from the resulting PCR product. DNA was purified using Qiagen's QIAquick gel extraction kit following manufacturers (QIAGEN Valencia, CA) suggested protocol and eluted in 40 uL of IX TE buffer.

BP clonase reaction

The Gateway BP Clonase enzyme mixes contains both INTEGRASE and INTEGRATION HOST FACTOR proteins that catalyze the in vitro recombination of PCR products or DNA segments containing *att*B sites and a vector containing *att*P sites such as pHELLSGATE 2 in our case (CSIRO Clayton South Vic, Australia). The BP clonase reaction was then carried out by mixing approximately 150 ng of the pHELLSGATE vector, 25 ng of purified aatB PCR product and 1uL of BP clonase enzyme (Invitrogen). A total volume of 8 uL was achieved by adding 1X TE buffer of pH 8.0. The mixture was gently agitated and incubated at 25^{o}C overnight.

Transformation into bacteria

A mixture of 2 uL of the BP clonase reactions were mixed with 25 uL of the DH10β strain of *Escherichia coli*. Transformation was performed in a BIORAD Electroporator with the capacitance extender at 960 uFD, Gene Pulser at 25 uFD and the pulse controller at 200 OHMS in disposable 1mm generic cuvettes using 1.5 mV of current. The transformed bacteria were vigorously agitating in a 37^{o}C incubator for 2 hours after which they were sparsely spread on a selection medium containing 50 ug/mL spectinomycin antibiotics and once again incubated at 37^{o}C for at 16-18 hours. About 15 of the resulting individual colonies were picked out and grown in liquid Luria Broth containing 50 ug/mL spectinomycin the selection antibiotic for approximately 6 hours. DNA was isolated and purified from the transformed bacteria using Qiagen's QIAprep Spin Miniprep Kit (QIAGEN Valencia, USA) following the manufacturer's suggested protocol.

Validation of successful BP clonase reactions

In order to investigate the validity of the resulting clones, restriction digestions as well as PCR reactions using primers specially designed to amplify parts of the PDK intron as well as the inserted gene were used. Restriction digestions were carried out separately using *XbaI* and *XhoI* enzymes in order to ensure that the gene fragment had been inserted in both sides of the PDK intron. Digestions were carried out overnight at the recommended temperatures and later 10 uL of each was run on a 1% agarose gel at 100V for 45 minutes and later visualized on a UV light box. Semi-quantitative PCR was also intended to be used for plasmid integrity validation. The PCR primers used to ensure that both halves fragments had been inserted in the vector were designed as shown in Figure 5.3. Further validation of the construct integrity was carried out through a sequencing reaction and analysis.

Transient silencing of *NbAGO2*

After satisfactory validation of the *pHELLSGATE-NbAGO2* plasmid construct, it was then transformed into GV3101 (also known as strain pMP90RK) strain of *Agrobacterium tumafaciens* so as to be agroinfiltrated into leaves in a transient assay. Here, an empty pHELLGATE vector (with a mutated ccdB gene) was also transformed into *Agrobacterium* to serve as an experimental control. Transformation of *Agrobacterium* was carried out following the same procedure previously mentioned in *E. coli* transformation. The *Agrobacterium* colonies however were grown at 28^{o}C instead, and the resulting individual colonies were cultured in liquid LB with a 50 ng/mL of spectinomycin.

Cultures were prepared and agroinfiltration was carried out following the procedures already mentioned in Chapter III and IV. New fully developed leaves of 5 or 6 week old plants were used for this procedure. The constructs were infiltrated onto 3 sets of plants.

Primer 1 (NbAGO2 Fwd): GAGCACTTGGCTGAACATGA

Primer 2 (PDK IN): GTTTACATAAACAACATAGT

Primer 3 (PDK OUT): CTTGTAGTTTTATTAACTTCT

PCR setup		PCR conditions		
Template (Plasmid)	2.0 µl	94°C	5 min	
10X Thermopol Buffer	2.5 µl	94°C	30 sec	30 cycles
10 mM dNTP	0.5 µl	55°C	30 sec	
10 µM (Primer 1 or Primer3)	0.5µl	68°C	1 min	
10 µM (Primer 2 or Primer1)	0.5 µl	68°C	10 min	
Taq polymerase	0.125µl	4°C	∞	
H_2O	19.0 µl			
TOTAL	25 µl			

Figure 5.3. Designing and use of primers in a PCR reaction to used ensure that both gene fragments stems of the hairpin loop had been inserted in the pHELLSGATE vector.

To avoid premature leaf senescence and yellowing probably caused by the spectinomycin antibiotics used for selection, the *Agrobacterium* cultures had to be washed and rinsed at least three times in the infiltration buffer which consisted of 10 mM MgCl. Ten days after the infiltration, TGdP19 the GFP-chimeric *Tomato bushy stunt virus* not expressing its P19 silencing suppressor was agroinfiltrated onto the same leaf, and also on another nearby non-infiltrated leaf to determine whether the silencing signal had moved through the plant into the adjacent leaf. An empty pHELLSGATE vector was also agroinfiltrated for use as a negative control. Observations were then made at 5, 10 and 15 days on accumulation of GFP in the originally pHELLSGATE infiltrated leaf as well as the adjacent non-infiltrated leaf.

Transgenic silencing of *NbAGO2*

After confirmation of plasmid integrity by sequencing and success with the transient assays, the plasmids were sent to our collaborators. The generation of *NbAGO2-silenced* transgenic plants was carried out by Dr. Jintao Zhang at the Texas A&M AgriLife Research Station in Weslaco, TX. The protocol used for transformation can be found in the appendix section of this thesis. He reported difficulties in generating *NbAGO2*-silenced transformants when compared to the empty vector controls, but seemingly successful transgenic events had occurred and viable plants were obtained.

Verification of successful plant transformants and endogenous *NbAGO2* transcript levels in the plants

Both RNA and DNA were extracted and purified from the putative transgenic plants. RNA extraction was carried out following protocols mentioned in the previous chapters.

DNA was isolated from fully developed young leaves following a protocol originally obtained from the *iprotocol web page* and has been slightly modified for optimal DNA isolation from *N. benthamiana* leaves. [The iprotocol web page has been deleted as of September 2008 although the original author(s) of the protocol appear to be

from the Meyerowitz laboratory in California Institute of Technology (CALTECH)]. In essence, approximately 200 mg of leaf tissue was thoroughly macerated in 750 uL of Extraction buffer (100 mM Tris pH 8.0, 50 mM EDTA pH 8.0, 500 mM NaCl, 10 mM β-mercaptoethanol) using a mortar and pestle. 35 uL of a 20% SDS solution was added and incubated in a 65^{o}C heat block for 5 minutes. Then 130 uL of potassium acetate (CH_3CO_2K) was added, mixed and incubated on ice for 5 minutes. The resulting debris was then pelleted by centrifuging at 15000 g for 10 minutes at room temperature. Subsequently, 750 uL of absolute isopropyl alcohol and 75 uL of sodium acetate were added to the supernatant and incubated in a -20^{o}C freezer for at least 1 hour. DNA was then pelleted by centrifugation at 15000 g, the supernatant was discarded and 70% ethanol was used to wash the resulting pellet. Excess ethanol was evaporated in a spin vacuum centrifuge for approximately 30 minutes. The DNA was then resuspended in 30 uL of 1X TE buffer containing 20 ug/mL RNAse. The mixture was incubated at 37^{o}C for 15 minutes and then centrifuged at 15000 g for 5 minutes and diluted to a final volume of 60 uL for immediate usage or storage at -20^{o}C.

The presence of the insert was verified by carrying out a PCR reaction using the primers 1, 2 and 3 (Figure 5.3) previously used to validate the integrity of the *pHELLSGATE-NbAGO2* plasmid on the isolated DNA. The conditions used for PCR amplification were also identical to those stated in Figure 5.3.

Results

Initially attempts were made to design the hairpins using the pHANNIBAL system (CSIRO, 2007). The first (sense) PCR fragment was always easily inserted into the hairpin vector, however, the subsequent cloning of the antisense fragment proved impossible despite multiple attempts. The pHELLSGATE hairpin vector was then chosen by default to generate the hairpin vector necessary for transient and transgenic silencing of the *NbAGO2* gene. Initially, semi-quantitative PCR using the primers mentioned in Figure 5.4 was used to confirm the validity of the plasmid constructs. The results were however not consistent with even the empty vector showing faint amplicons

of the expected size on a 1% agarose gel. This method of construct validation was therefore discarded in favor of the use of restriction digests.

Flanking both recombination sites are *XbaI* and *XhoI* restriction enzyme sites. Confirmation of successful gene insertion and replacement of the ccdB gene was therefore carried out by an enzymatic digest using the above named restriction endonucleases. The results in Figure 5.5 show that of the 13 surviving colonies, only 4 had the gene fragment inserted during the BP clonase reaction, the other 9 either had recombination of the *aat*P sites or a mutated ccdB gene was simply not replaced hence showed patterns similar to the empty vector upon digestion. When using the pHELLSGATE-2 vector, during the BP clonase reaction, the PDK intron has been known to become inverted. To ensure that only the correctly oriented clones would be selected, the plasmids were sequenced in order to confirm the correct both the PDK intron gene fragment orientation.

Transient silencing of *NbAGO2*

Once confirmed to be correctly oriented, the plasmids as well as the empty vector were transformed into *Agrobacterium* GV3101 and agroinfiltrated into new fully developed leaves of 5 and 6 week old plants to initiate post transcriptional gene silencing of the endogenous *N. benthamiana* AGO2 transcripts. Ten days were allowed for silencing to occur prior to agroinfiltration of the TGdP19 construct. The results of monitoring GFP expression every 5 days for the next 15 days are presented in Figure 5.5.

At 5 days after agroinfiltration of the TGdP19 construct, there is a clear abundance of GFP in the leaf where the *pHELLSGATE-NbAGO2* construct was infiltrated much more than in the leaf infiltrated with just the empty pHELLSGATE vector.

In the adjacent non-infiltrated leaf, accumulation of GFP is comparable to that seen in empty pHELLSGATE infiltrated leaf. At 10 and 15 days after TGdP19 agroinfiltration however, no GFP signal is visible on the empty pHELLSGATE agroinfiltrated plants. There was an abundance of GFP in the *pHELLSGATE-NbAGO2* agroinfiltrated leaf as well as the adjacent leaf that was not infiltrated with the leaf at 10 days. Curiously however, although the GFP signal was persistent on the actual construct infiltrated leaf, it explicably diminished in the adjacent leaf at 15 days after TGd19 inoculation. The results showed that the hairpin construct effectively silenced *NbAGO2* which then allowed TGdP19 to accumulate.

Verification of plant transformation success and endogenous *NbAGO2* transcript levels

Upon reception of the putative transgenic plans from our collaborators, DNA was isolated from plant leaves and subjected to semi-quantitative PCR to analyze for the presence of the *pHELLSGATE-NbAGO2* construct in the plant genome. RNA was also extracted, cDNA synthesized and both semi-quantitative and quantitative Real-Time PCR were carried out to determine the levels of *NbAGO2* in the *pHELLSGATE-NbAGO2* transgenic plants versus the *pHELLSGATE* empty vector controls. The results are shown in Figures 5.6 and 5.7.

Semi-quantitative PCR analysis of the plant genomic DNA analysis showed that out of the 40+putative *pHELLSGATE-NbAGO2* transgenic plants, 11 of the putative transformants expressed the desired hairpin construct in their genomes showing over 25% transformation success rate. The results from the transcriptome analysis shown in Figure 5.7 also effectively illustrated that the transcript levels of *N. benthamiana AGO2* gene were significantly reduced in at least 4 of the 6 plants subjected to semi and quantitative Real-Time PCR analysis.

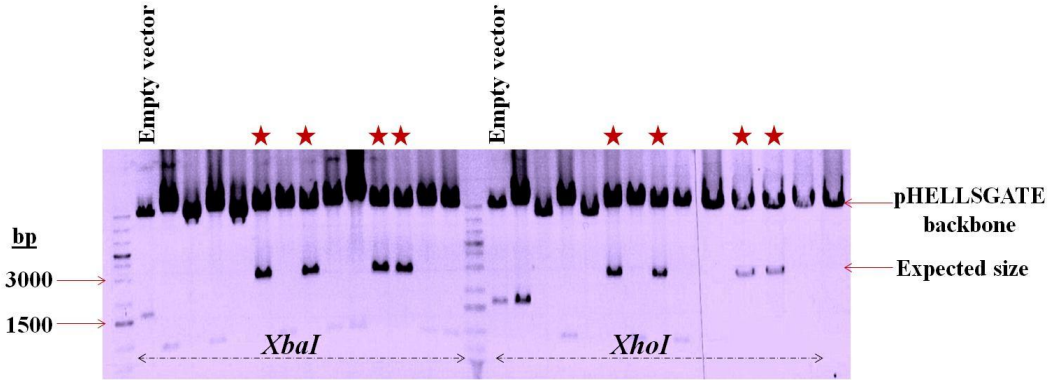

Figure 5.4. Restriction digests results using *XbaI* and *XhoI* endonucleases to confirm BP clonase success. The lanes marked with a red star denotes the putative successfully cloned plasmids that were sent for further sequencing to validate PDK intron orientation.

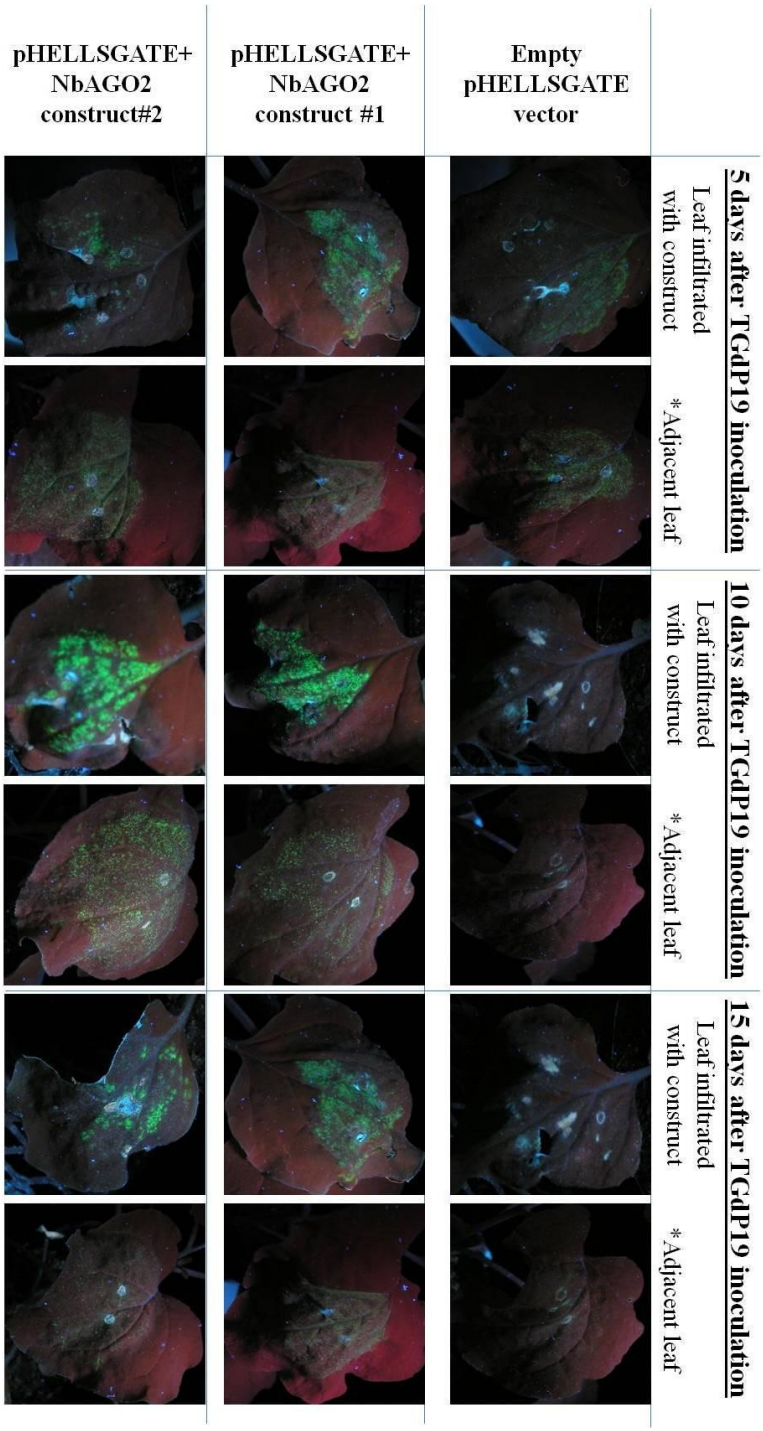

Figure 5.5. Transient silencing of *NbAGO2* using the pHELLSGATE hairpin vector. The pHELLSGATE agroinfiltrated and non-vector infiltrated *adjacent leaves were inoculated with TGdP19 and GFP accumulation was monitored over a 15 day period.

Seeds from the T0 plants have been harvested and planted, Southern blot analysis are being carried out to determine gene copy numbers of the T0 plants. Further semi- and qRT-PCR analysis will be carried out on the T1 generation to determine whether or not the pHELLSGATE constructs have remained intact in the plant genome and whether *NbAGO2* mRNA levels are still being down regulated through gene silencing. Efforts to regenerate T0 plants from stem cuttings in order to carry out further tests on the sustenance of the inserted vector and corresponding *NbAGO2* transcript repression activity have been unsuccessful thus far.

Discussion

Results from the transient assays performed by agroinfiltration of the pHELLSGATE constructs confirmed the observation previously made using VIGS that *NbAGO2* plays an anti-TBSV defensive role. The difference in GFP accumulation in the empty pHELLSGATE vector and *pHELLSGATE-NbAGO2* construct infiltrated leaves upon TGdP19 agroinfiltration was evident as early as 5 days and lasted up to 15 days after hairpin vector inoculation.

Through observations of silencing phenotypes and grafting experiments, RNA silencing has been shown to be non-cell-autonomous, with the capability of being induced locally and then spread to distant sites throughout the plant (Boerjan et al, 1994, Palauqui et al, 1996).

Other evidence for the involvement of a systemic signal in RNA silencing has come from the observation that systemic silencing can be induced in transgenic tobacco species by agroinfiltration or particle bombardment to deliver exogenous DNA sequences homologous to the transgene (Voinnet et al, 1997, Voinnet et al, 1998, Palauqui et al, 1999). Neither *Agrobacterium* nor T-DNA was detected in systemically silenced tissue of the agroinfiltrated plants indicating that the silencing must have been propagated by means of some ‘mobile signal’.

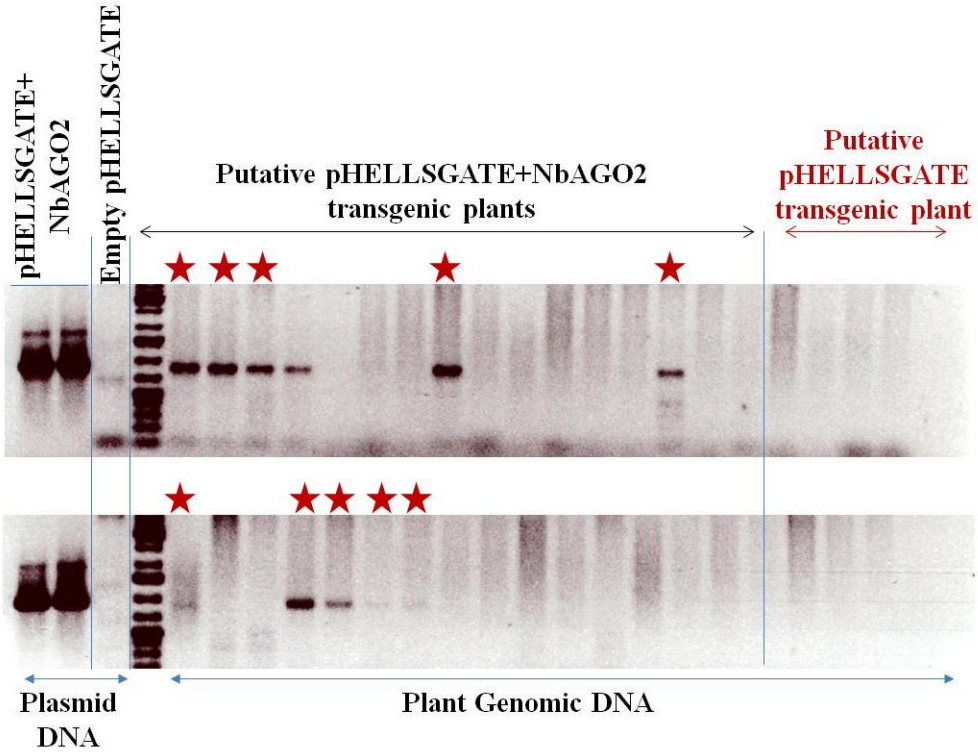

Figure 5.6. Semi-quantitative PCR analysis of plant genomic DNA for the presence of the *pHELLSGATE+NbAGO2* construct. Star-marked lanes denote the presence of the *pHELLSGATE+NbAGO2* construct and these plants were picked for further analysis. Plasmid DNA from *pHELLSGATE+NbAGO2* and empty *pHELLSGATE* transformed bacteria were used as PCR negative and positive controls.

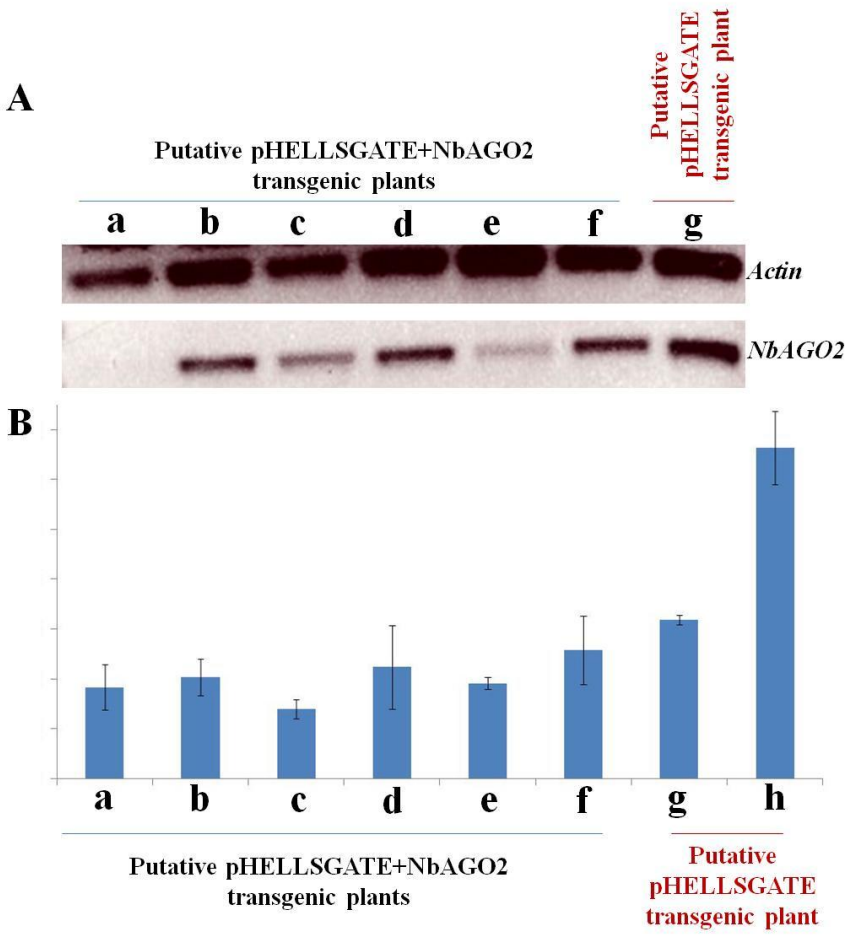

Figure 5.7. Transcript levels of *N. benthamiana AGO2* in selected putative transgenic plants. A: Semi-quantitative PCR results B: Quantitative Real-Time PCR results showing the relative amounts of *NbAGO2* transcripts.

Various candidates have been proposed as the 'mobile silencing signal' such as siRNAs already previously associated with RNA degradation processes in animal systems (Hammond et al, 2000, Yang et al, 2000). The characteristics of siRNAs make them ideal candidates for the mobile signal: consistent association with RNA silencing, perfectly long enough to convey sequence specificity and yet small enough to move easily through plasmodesmata. The possibility therefore that siRNAs are involved in systemic signaling is an attractive and popular model (Hamilton & Baulcombe, 1999) . Howevere, there is still no direct evidence that siRNAs actually play a role in systemic silencing (Mlotshwa et al, 2002).

Another candidate for the mobile silencing signal is the aberrant RNA transcript from a silenced locus (or a derivative of that mRNA), which may in some way trigger RNA silencing upon arrival in a new cell. In fact, mRNA cell-to-cell and systemic movement is not uncommon as reviewed by Jorgensen *et al* (Jorgensen et al, 1998). Several endogenous mRNAs have been observed to move through the plasmodesmata presumably using endogenous mechanisms for RNA trafficking. Examples include the maize *KNOTTED1* (Lucas et al, 1995) and *SUT1*in tobacco, tomato, and potato (Kuhn et al, 1997). Systemic movement of endogenous RNAs across graft junctions has also been known to occur as was observed in the Pumpkin *NACP* mRNA which moved from a pumpkin rootstock into the apex of cucumber scions (Ruiz-Medrano et al, 1999). These observations raise the possibility that the mobile silencing signal could be an mRNA or mRNA/protein complex that moves via normal pathways during macromolecular trafficking.

Double-stranded (dsRNA) molecules (with far less evidence) may provide another possible candidate for the mobile signal that induces systemic RNA silencing. Viroid genomes, with several hundred bases in length and possessing complex secondary structure and content can be conceived as a model for dsRNA movement. They are effectively capable of entering a series of transport pathways, exiting from the nucleus into the cytoplasm, cell-to-cell movement through plasmodesmata, as well as autonomous systemic movement (Gomez et al, 2001, Zhu et al, 2001).

In our transient experiments, we also observed that the silencing signal had spread to the adjacent non-hairpin construct infiltrated leaf at about 10 days after initiation of silencing as witnessed by the accumulation of GFP. However, when examined at about 5 days later, the GFP signal in the adjacent non-*pHELLSGATE-NbAGO2* infiltrated leaf has significantly diminished indicating the non persistence of the silencing signal in the absence of the source of its dsRNA trigger. In the hairpin silenced leaves, GFP accumulation was observed to persist.

Our observations not only proved the effectiveness of the use of hairpinRNA as a tool for silencing of *N. benthamiana AGO* genes, but also at efficiency levels comparable to the commonly used TRV-virus induced gene silencing systems. One added advantage of the hairpin RNA system is that it can be used not only in transient assays as in the VIGS system, but also in the generation of transgenic and more stable gene knockouts.

The post-transcriptional silencing of *NbAGO2* through both VIGS and transient hairpin RNA approach was not associated with any noticeable phenotype. Although difficulties were reported in the regeneration of plants transformed with the *pHELLSGATE-NbAGO2* hairpin vector, the seeds harvested from the putative transgenic T0 plants appeared to be viable and germinated at rates comparable to the wild-type and empty pHELLSGATE vector transformed plants. *NbAGO2* therefore does not appear to be involved in the regulation of normal plant development.

CHAPTER VI

FINAL SUMMARY AND DIRECTIONS

Earlier observations in our laboratories showed that young plants, unlike their older counterparts were incapable of silencing the *Tomato bushy stunt virus* GFP construct deficient of its silencing suppressor P19 (TGdP19) resulting in a persistent accumulation of GFP.

Furthermore, it was also consistently observed that upon inoculation of *N. benthamiana* roots with the TGdP19 construct, minimal accumulation of GFP was witnessed indicating the viral infection had been subdued; however, when the same plant leaves were inoculated, GFP was seen to accumulate abundantly and fairly persistently. These results seem to partially indicate that the root systems possessed a more effective antiviral defense mechanism than the leaves.

In Chapter II, my results showed that the distribution of *ARGONAUTE (AGO)* mRNA in *N. benthamiana* varied with plant age and tissue specificity. The older plants were observed to posses significantly higher quantities of most the *AGO* transcripts. We also noted that plant leaves also consistently contained the least amount of *AGO* mRNA when compared to stems and roots of corresponding ages. Our results coupled with earlier experimental observations hinted the antiviral defense roles played by these AGOs.

In Chapter III, I successfully carried out virus induced gene silencing (VIGS) of endogenous *AGO* genes using the *Tobacco rattle virus* vector system with more than 70% of the targeted transcripts reduced in all cases. We subsequently noticed that the knockdown of *NbAGO1* transcripts resulted in a distinct phenotype characterized by a malformation of leaves, aborted flowers and development of inflorescent structures on the leaf petiole. However, just like in the *N. benthamiana* plants infected with an empty TRV vector, knockdown of all other *NbAGO* mRNA did not result in any discernible phenotype. Upon agroinfiltration of the *Tomato bushy stunt virus* construct deficient of its P19 silencing suppressor, accumulation of GFP was witnessed on *N. benthamiana* plants silenced for *NbAGOs 2* and *X*, but not in control *N. benthamiana* plants suggesting

their role in antiviral defense. Similar results were observed when *Tobacco mosaic virus* GFP chimeric constructs were infiltrated on *NbAGO2* silenced plants. Agroinfiltration of *Foxtail mosaic virus*, *Sunnhemp mosaic virus*, and *Turnip crinkle virus* GFP chimeric constructs on *NbAGO2* silenced *N. benthamiana* plants however did not result in accumulation of GFP indicating the specificity of the antiviral defense to TBSV and TMV.

These observations suggest that in *N. benthamiana*, NbAGOs 2 and X may be involved in antiviral defense against TBSV and TMV. It is critical to note that since the use of the VIGS technique does not lead to a total knockdown of the targeted gene, the reduced mRNA quantities observed may have still been sufficient to effectively contribute towards the antiviral defense roles played by the AGO in question. Other gene knockdown/knockout strategies with higher levels of efficacy should also be used to repeat these experiments.

In Chapter IV, while attempting to silence of multiple *AGO* genes using the TRV-VIGS systems, we quickly noticed that silencing was not as effective as previously observed with individual gene knockdowns. Upon co-infiltration, the *TRV-NbAGO1* construct inexplicably seemed to suppress all other *NbAGO* as well as the *MgChl* constructs and limit their accumulation and systemic spread rendering the VIGS technique impractical for silencing of multiple genes. A possible way of circumventing this dilemma would also be to insert multiple sequences of the AGO genes in tandem in the TRV multiple cloning site while of course taking into account the size limitations required for stability of the constructs. Other methods that could be possibly used to this effect include; chemical and physical mutagenesis, T-DNA transposon insertion techniques and the use of inverted hairpins.

In Chapter V, gene silencing of *NbAGO2* was achieved by use of pHELLSGATE hairpin vector constructs expressing self-complementary *AGO2* gene fragments. Our results from transient assays using agroinfiltration of the constructs confirmed previous observations using the TRV VIGS system that upon silencing of NbAGO2, GFP accumulation was observed following TGdP19 agroinfiltration. Plants agroinfiltrated

with an empty vector control however successfully silenced the TGdP19 GFP chimeric construct. Transgenic plants expressing the *NbAGO2* hairpin construct and its corresponding controls were generated; the protein and mRNA expression levels of *NbAGO2* in the putative transgenic plants are currently being analyzed while pending further experimentation.

In summary, therefore, although the GFP-chimeric virus constructs used in our studies do not represent what accurately occurs in a natural infection, the role of AGOs in antiviral defense and the distinct interactions between a particular AGO and a given virus are clearly unmistakable.

REFERENCES

Adenot X, Elmayan T, Lauressergues D, Boutet S, Bouché N, Gasciolli V, Vaucheret H. (2006). DRB4-dependent TAS3 trans-acting siRNAs control leaf morphology through AGO7. *Curr Biol* 16: 927-32.

Agorio A, Vera P (2007). ARGONAUTE4 is required for resistance to *Pseudomonas syringae* in *Arabidopsis*. *Plant Cell* 19: 3778-90.

Allen E, Xie Z X, Gustafson A M, Carrington J C (2005). MicroRNA-directed phasing during trans-acting siRNA biogenesis in plants. *Cell* 121: 207-21.

Alvarado V, Scholthof H B (2009). Plant responses against invasive nucleic acids: RNA silencing and its suppression by plant viral pathogens. *Semin Cell Dev Biol* 20: 1032-40.

Alves-Junior M, Alfenas-Zerbini P, Andrade E C, Esposito D A, Silva F N, F da Cruz A C, Ventrella M C, Otoni W C, Zerbini F M (2009). Synergism and negative interference during co-infection of tomato and *Nicotiana benthamiana* with two bipartite begomoviruses. *Virology* 387: 257-66.

Bai M, Yang G S, Chen W T, Mao Z C, Kang H X, Chen G H, Yang Y H, Xie B Y (2012). Genome-wide identification of Dicer-like, Argonaute and RNA-dependent RNA polymerase gene families and their expression analyses in response to viral infection and abiotic stresses in *Solanum lycopersicum*. *Gene* 501: 52-62.

Baulcombe D, (2004). RNA silencing in plants. *Nature* 431: 356-63.

Baulcombe D C, Havecker E R, Wallbridge L M (2010). The *Arabidopsis* RNA-Directed DNA methylation ARGONAUTES Functionally diverge based on their expression and interaction with target loci. *Plant Cell* 22: 321-34.

Baulcombe D C, Ratcliff F, Martin-Hernandez A M (2001). *Tobacco rattle virus* as a vector for analysis of gene function by silencing. *Plant J* 25: 237-45.

Baulcombe D C, Voinnet O, Vain P, Angell S (1998). Systemic spread of sequence-specific transgene RNA degradation in plants is initiated by localized introduction of ectopic promoterless DNA. *Cell* 95: 177-87.

Baumberger N, Baulcombe D C (2005). *Arabidopsis* ARGONAUTE1 is an RNA Slicer that selectively recruits microRNAs and short interfering RNAs. *Proc Natl Acad Sci USA* 102: 11928-33.

Baumberger N, Tsai C H, Lie M, Havecker E, Baulcombe D C (2007). The *Polerovirus* silencing suppressor P0 targets ARGONAUTE proteins for degradation. *Curr Biol* 17: 1609-14.

Beijerinck M W (1898). Ueber ein Contagium vivum fluidum als Ursache der Fleckenkrankheit der Tabaksbl tter. *Verh Kon Akad Wetensch* 5: 3-21. (English translation published in 1942: Concerning a contagium vivum fluidum as cause of the spot disease of tobacco leaves. *Phytopathol. Classics* 7: 33-52).

Benning C, Bohmert, K, Camus I, Bellini C., Bouchez D., Caboche M (1998). AGO1 defines a novel locus of *Arabidopsis* controlling leaf development. *EMBO J* 17: 170-80.

Bernstein E, Caudy A A, Hammond S M, Hannon G J (2001). Role for a bidentate ribonuclease in the initiation step of RNA interference. *Nature* 409: 363-6.

Bezier A, Lambert B, Baillieul F (2002). Study of defense-related gene expression in grapevine leaves and berries infected with *Botrytis cinerea*. *EMBO J* 108: 111-20.

Bhattacharjee S, Zamora A, Azhar M T, Sacco M A, Lambert L H, Moffett P (2009). Virus resistance induced by NB-LRR proteins involves Argonaute4-dependent translational control. *Plant J* 58: 940-51.

BIORAD (2006). Real Time PCR Applications Guide On-line Bulletin 5279 [http://www.gene-quantification.de/real-time-pcr-guide-bio-rad.pdf].

Boerjan W, Bauw G, Van Montagu M, Inze D (1994). Distinct phenotypes generated by overexpression and suppression of S-adenosyl-L-methionine synthetase reveal developmental patterns of gene silencing in tobacco. *Plant Cell* 6: 1401–1414.

Borges F, Pereira P A, Slotkin R K, Martienssen R A, Becker J D (2011). MicroRNA activity in the *Arabidopsis* male germline. *J Exp Bot* 62: 1611-20.

Bortolamiol D, Pazhouhandeh M, Marrocco K, Genschik P, Ziegler-Graff V (2007). The *Polerovirus* F box protein P0 targets ARGONAUTE1 to suppress RNA silencing. *Curr Biol* 17: 1615-21.

Bortolamiol D, Pazhouhandeh M, Ziegler-Graff V (2008). Viral suppression of RNA silencing by destabilisation of ARGONAUTE 1. *Plant Signal Behav* 3: 657-9.

Boyko V P, Karasev A V (1992). *Tombusvirus* genome may encode the 6th small protein near its 3' terminus. *Virus Genes* 6: 143-8.

Brodersen P, Sakvarelidze-Achard L, Bruun-Rasmussen M, Dunoyer P, Yoshiharu Y. Yamamoto Y, Sieburth L, Voinnet O (2008). Widespread translational inhibition by plant miRNAs and siRNAs. *Science* 320: 1185-90.

Burch-Smith T M, Anderson J C, Martin G B, Dinesh-Kumar S P (2004). Applications and advantages of virus-induced gene silencing for gene function studies in plants. *Plant Journal* 39: 734-46.

Bustin S A (2002). Quantification of mRNA using real-time reverse transcription PCR (RT-PCR): trends and problems. *J Mol Endocrinol* 29: 23-39

Bustin S A, Benes V, Garson J A, Hellemans J, Huggett J, Kubista M, Mueller R, Nolan T, Pfaffl M W,11 Gregory L. Shipley, G L, Vandesompele J, Wittwer C T (2009). The MIQE guidelines: minimum information for publication of quantitative real-time PCR experiments. *Clin Chem* 55: 611-22.

Carmell M A, Xuan Z, Zhang M Q, Hannon G J (2002). The ARGONAUTE family: tentacles that reach into RNAi, developmental control, stem cell maintenance, and tumorigenesis. *Genes Dev* 16: 2733-42.

Cartolano M, Castillo R, Efremova N, Kuckenberg M, Zethof J, Gerats T, Schwarz-Sommer Z, Vandenbussche M (2007). A conserved microRNA module exerts homeotic control over *Petunia hybrida* and *Antirrhinum majus* floral organ identity. *Nat Genet* 39: 901-5.

Ch.Embnet.Org (2012). BOXSHADE 3.21: Pretty Printing and Shading of Multiple-Alignment files. In. http://www.ch.embnet.org/software/BOX_form.html.

Chen H M, Chen L T, Patel K, Li Y H, Baulcombe D C, Wu S H (2010). 22-nucleotide RNAs trigger secondary siRNA biogenesis in plants. *Proc Natl Acad Sci U S A* 107: 15269-74.

Chen X (2003). A MicroRNA as a translational repressor of APETALA2 in Arabidopsis flower development. *Science* 303: 2022-5.

Chiu M H, Chen I H, Baulcombe D C, Tsai C H (2010). The silencing suppressor P25 of *Potato virus X* interacts with ARGONAUTE1 and mediates its degradation through the proteasome pathway. *Mol Plant Pathol* 11: 641-9.

Ciomperlik J J (2008). Anti-viral RNAi and its suppression in plants. M.S Thesis, Texas A&M University.

Cohen Y, Gisel, A., Zambryski, P. C (2000). Cell-to-cell and systemic movement of recombinant green fluorescent protein-tagged *Turnip crinkle viruses*. *Virology* 273: 258-66.

Combier J P, Frugier F, De Billy F,Boualem A, El-Yahyaoui F, Moreau S, Vernié T, Ott T, Gamas T, Crespi M, Niebel A (2006). MtHAP2-1 is a key transcriptional regulator of symbiotic nodule development regulated by microRNA169 in *Medicago truncatula*. *Genes Dev* 20: 3084-8.

CSIRO (2007). HairpinRNAi vectors for plants. In. CSIRO Plant Industry Visual Resource. http://www.pi.csiro.au/RNAi/vectors.htm

Csorba T, Bovi A, Dalmay T, Burgyan J (2007). The p122 subunit of *Tobacco mosaic virus* replicase is a potent silencing suppressor and compromises both small interfering RNA- and microRNA-mediated pathways. *J Virol* 81: 11768-80.

Cuperus J T, Carbonell A, Fahlgren N, Garcia-Ruiz H, Burke R T, Takeda A, Sullivan C M, Gilbert S D, Montgomery T A, Carrington J C (2010). Unique functionality of 22-nt miRNAs in triggering RDR6-dependent siRNA biogenesis from target transcripts in Arabidopsis. *Nat Struct Mol Biol* 17: 997-1003.

Dereeper A, Guignon V, Blanc G, Audic S, Buffet S, Chevenet F, Dufayard J F, Guindon S, Lefort V, Lescot M, Claverie J M, Gascuel O (2008). Phylogeny.fr: robust phylogenetic analysis for the non-specialist. *Nuc Acids Res* 36: W465-9.

Desvoyes B, Faure-Rabasse S, Chen M H, Park J W, Scholthof H B (2002). A novel plant homeodomain protein interacts in a functionally relevant manner with a virus movement protein. *Plant Physiol* 129: 1521-32.

Ding S W, Voinnet O (2007). Antiviral immunity directed by small RNAs. *Cell* 130: 413-26.

Diviney S, Tuplin A, Struthers M, Armstrong V, Elliott RM, Simmonds P, Evans D J (2008). A *Hepatitis C virus* cis-acting replication element forms a long-range RNA-RNA interaction with upstream RNA sequences in NS5B. *J Virol* 82: 9008-22.

Djuranovic S, Zinchenko M K, Hur J K Nahvi A, Brunelle J L, Rogers E J, Green R (2010). Allosteric regulation of ARGONAUTE proteins by miRNAs. *Nat Struct Mol Biol* 17: 144-50.

Dong J, Kim S T, Lord E M (2005). *Plantacyanin* plays a role in reproduction in *Arabidopsis*. *Plant Physiol* 138: 778-89.

Drinnenberg I A, Weinberg D E, Xie K T, Mower J P, Wolfe K H, Fink G R, Bartel D P (2009). RNAi in budding yeast. *Science* 326: 544-50.

Ekengren S K, Liu Y, Schiff M, Dinesh-Kumar S P, Martin G B (2003). Two MAPK cascades, NPR1, and TGA transcription factors play a role in *Pto-mediated* disease resistance in tomato. *Plant J* 36: 905-17.

Eleftherianos I, Won S, Chtarbanova S, Squiban B, Ocorr K, Bodmer R, Beutler B, Hoffmann J A, Imler J L (2011). ATP-sensitive potassium channel (K(ATP))-dependent regulation of cardiotropic viral infections. *Proc Natl Acad Sci USA* 108: 12024-9.

Ender C, Meister G (2010). ARGONAUTE proteins at a glance. *J of Cell Sci* 123: 1819-23.

ExPASy ViralZone (2008) *Potexvirus*. Swiss Institute of Bioinformatics. http://viralzone.expasy.org/all_by_species/272.html

Faehnle C R, Joshua-Tor L (2010). ARGONAUTE MID domain takes centre stage. *EMBO Rep* 11: 564-5.

Fagard M, Boutet S, Morel J B, Bellini C, Vaucheret H (2000). AGO1, QDE-2, and RDE-1 are related proteins required for post-transcriptional gene silencing in plants, quelling in fungi, and RNA interference in animals. *Proc Natl Acad Sci U S A* 97: 11650-4.

Fahlgren N, Montgomery T A, Howell M D Allen E, Dvorak S K, Alexander A L, Carrington J C (2006). Regulation of AUXIN RESPONSE FACTOR3 by TAS3 ta-siRNA affects developmental timing and patterning in *Arabidopsis*. *Curr Biol* 16: 939-44.

Fang Y, Spector D L (2007). Identification of nuclear dicing bodies containing proteins for microRNA biogenesis in living *Arabidopsis* plants. *Curr Biol* 17: 818-23.

Fire A, Xu S Q, Montgomery M K, Kostas S A, Driver S E, Mello C C (1998). Potent and specific genetic interference by double-stranded RNA in *Caenorhabditis elegans*. *Nature* 391: 806-11.

Fujita M, Horiuchi Y, Ueda Y, Mizuta Y, Kubo T, Yano K, Yamaki S, Tsuda K, Nagata T, Niihama M, Kato H, Kikuchi S, Hamada K, Mochizuki T, Ishimizu T, Iwai H, Tsutsumi N, Kurata N (2010). Rice expression atlas in reproductive development. *Plant and Cell Physiol* 51: 2060-81.

Garcia D, Collier S A, Byrne M E, Martienssen R A (2006). Specification of leaf polarity in Arabidopsis via the trans-acting siRNA pathway. *Curr Biol* 16: 933-8.

Gerard G F, Fox D K, Nathan M, Dalessio J M (1997). Reverse transcriptase - The use of cloned *Moloney murine leukemia virus* reverse transcriptase to synthesize DNA from RNA. *Mol Biotechnol* 8: 61-77.

Gomez G, Pallas V (2001). Identification of an in vitro ribonucleoprotein complex between a viroid RNA and a phloem protein from cucumber plants. *Mol. Plant-Microbe Interact.* 14: 910-913.

Goodin M M, Zaitlin D, Naidu R A, Lommel S A (2008). *Nicotiana benthamiana*: Its history and future as a model for plant-pathogen interactions. *Mol Plant-Microbe Interact* 21: 1015-26.

Hamilton A J, Baulcombe D C (1999). A species of small antisense RNA in posttranscriptional gene silencing in plants. *Science* 286: 950-2.

Hammond S M (2005). Dicing and slicing: the core machinery of the RNA interference pathway. *FEBS Lett* 579: 5822-9.

Hammond S M, Bernstein E, Beach D, Hannon G J (2000). An RNA-directed nuclease mediates post-transcriptional gene silencing in *Drosophila* cells. *Nature* 404: 293-296.

Harvey J J W, Lewsey M G, Patel K, Westwood J, Heimstadt S, Carr J P, Baulcombe D C (2011). An antiviral defense role of AGO2 in plants. *PLoS One* 6: e14639

Havecker E R, Wallbridge L M, Hardcastle T J, Bush M S, Kelly K A, Dunn R M, Schwach F, Doonan J H, Baulcombe D C (2010). The *Arabidopsis* RNA-directed DNA methylation ARGONAUTES functionally diverge based on their expression and interaction with target loci. *Plant Cell* **22:** 321-34.

He X, Anderson J C, Del Pozo O, Gu Y Q, Tang X, Martin G B (2004). Silencing of subfamily I of protein phosphatase 2A catalytic subunits results in activation of plant defense responses and localized cell death. *Plant J* 38: 563-77.

Hearne P Q, Knorr D A, Hillman B I, Morris T J (1990). The complete genome structure and synthesis of infectious RNA from clones of *Tomato bushy stunt virus*. *Virology* 177: 141-51.

Helliwell C, Waterhouse P (2003). Constructs and methods for high-throughput gene silencing in plants. *Methods* 30: 289-95.

Hii G, Pennington R, Hartson S, Taylor C D, Lartey R, Williams A, Lewis D, Melcher U (2002). Isolate-specific synergy in disease symptoms between *Cauliflower mosaic virus* and *Turnip vein-clearing viruses*. *Arch Virol* 147: 1371-84.

Hock J, Meister G (2008) The ARGONAUTE protein family. *Genome Biol.* 9: 210-218

Hu B, Pillai-Nair N, Hemenway C (2007). Long-distance RNA-RNA interactions between terminal elements and the same subset of internal elements on the *Potato virus X* genome mediate minus- and plus-strand RNA synthesis. *RNA* 13: 267-80.

Hunter C, Sun H, Poethig R S (2003). The *Arabidopsis* heterochronic gene ZIPPY is an ARGONAUTE family member. *Curr Biol* 13: 1734-9.

Hutvagner G, Simard M J (2008). ARGONAUTE proteins: key players in RNA silencing. *Nat. Rev. Mol. Cell Biol.* 9:22-32.

IDT Integrated DNA Technologies (2012). PrimerQuest. In. http://www.idtdna.com/Scitools/Applications/Primerquest/

EBI European Bioinformatics Institute (2012). MUSCLE - Multiple Sequence Alignment. In. http://www.ebi.ac.uk/Tools/msa/muscle/

García-Marcos A, Pacheco R, Martiáñez J, González-Jara P, Díaz-Ruíz J R, Tenllado F (2009). Transcriptional changes and oxidative stress associated with the synergistic interaction between *Potato virus X* and *Potato virus Y* and their relationship with symptom expression. *Mol. Plant Microbe Interact*. 22: 1431–1444.

INVITROGEN (2012). Gateway BP Clonase enzyme mix. In. http://products.invitrogen.com/ivgn/product/11789013#citationsList

Irvine D V, Zaratiegui M, Tolia N H, Goto D B, Chitwood D H, Vaughn M W, Joshua-Tor L, Martienssen R A (2006). ARGONAUTE slicing is required for heterochromatic silencing and spreading. *Science* 313: 1134-7.

Itoh J, Nonomura K, Ikeda K, Yamaki S, Inukai Y, Yamagishi H, Kitano H, Nagato Y (2005). Rice plant development: from zygote to spikelet. *Plant Cell Physiol* 46: 23-47.

Jones L, Keining T, Eamens A, Vaistij F E (2006). Virus-induced gene silencing of *ARGONAUTE* genes in *Nicotiana benthamiana* demonstrates that extensive systemic silencing requires ARGONAUTE1-LIKE and ARGONAUTE4-LIKE genes. *Plant Physiol.* 141: 598-606.

Jorgensen R, Atkinson R, Forster R, Lucas W (1998). An RNA-based information superhighway in plants. *Science* 279: 1486-1487.

Kataoka Y, Takeichi M, Uemura T (2001). Developmental roles and molecular characterization of a *Drosophila* homologue of *Arabidopsis* ARGONAUTE1, the founder of a novel gene superfamily. *Genes Cells* 6: 313-25.

Katiyar-Agarwal S, Gao S, Vivian-Smith A, Jin H (2007). A novel class of bacteria-induced small RNAs in *Arabidopsis*. *Genes Dev* 21: 3123-34.

Kim K W, Eamens A, Waterhouse P (2011). RNA processing activities of the *Arabidopsis* ARGONAUTE protein family. In: Grabowski P, ed. *RNA Processing.* University of Pittsburg, USA: InTech Web.org, 248.

Kim J K, Gabel H W, Kamath R S, Tewari M, Pasquinelli A, Rual J F, Kennedy S, Dybbs M, Bertin N, Kaplan J M, Vidal M, Ruvkun G (2005). Functional genomic analysis of RNA interference in *C. elegans*. *Science* 308: 1164-7.

Kotewicz M L, D'alessio J M, Driftmier K M, Blodgett K P, Gerard G F (1985). Cloning and overexpression of *Moloney murine leukemia virus* reverse transcriptase in *Escherichia coli*. *Gene* 35: 249-58.

Kotewicz M L, Sampson C M, D'alessio J M, Gerard G F (1988). Isolation of cloned *Moloney murine leukemia virus* reverse transcriptase lacking ribonuclease H activity. *Nuc Acids Res*16: 265-77.

Kuhn C, Franceschi V R, Schulz A, Lemoine R, Frommer W B. (1997). Macromolecular trafficking indicated by localization and turnover of sucrose transporters in enucleate sieve elements. *Science* 275: 1298-1300.

Langer K, Ache P, Geiger D, Stinzing A, Arend M, Wind C, Regan S, Fromm J, Hedrich R (2002). Poplar potassium transporters capable of controlling K(+) homeostasis and K(+)-dependent xylogenesis. *Plant J* 32: 997-1009.

Li C F, Pontes O, El-Shami M, Henderson IR, Bernatavichute Y V, Chan S W, Lagrange T, Pikaard C S, Jacobsen S E (2006). An ARGONAUTE4-containing nuclear processing center colocalized with Cajal bodies in *Arabidopsis thaliana*. *Cell* 126: 93-106.

Lindbo J A (2007). TRBO: a high-efficiency *Tobacco mosaic virus* RNA-based overexpression vector. *Plant Physiol* 145: 1232-40.

Lippman Z, Martienssen R (2004). The role of RNA interference in heterochromatic silencing. *Nature* 431: 364-70.

Liu J D, Carmell M A, Rivas F V Liu J, Marsden C G, Thomson J M, Song J J, Hammond S M, Joshua-Tor L, Hannon G J (2004). ARGONAUTE2 is the catalytic engine of mammalian RNAi. *Science* 305: 1437-41.

Liu Q, Yao X, Pi L, Wang H, Cui X, Huang H (2009). The ARGONAUTE10 gene modulates shoot apical meristem maintenance and establishment of leaf polarity by repressing miR165/166 in *Arabidopsis*. *Plant J* 58: 27-40.

Liu Y, Schiff M, Dinesh-Kumar S P (2002). Virus-induced gene silencing in tomato. *Plant J* 31: 777-86.

Liu Y, Schiff M, Dinesh-Kumar S P (2004). Involvement of MEK1 MAPKK, NTF6 MAPK, WRKY/MYB transcription factors, COI1 and CTR1 in N-mediated resistance to Tobacco mosaic virus. *Plant J* 38: 800-9.

Liu Y, Schiff M, Marathe R, Dinesh-Kumar S P (2002). Tobacco Rar1, EDS1 and NPR1/NIM1 like genes are required for N-mediated resistance to *Tobacco mosaic virus*. *Plant J* 30: 415-29.

Liu Z, Kearney C M (2010a). An efficient *Foxtail mosaic virus* vector system with reduced environmental risk. *BMC Biotechnol* 10: 88.

Liu Z, Kearney C M (2010b). A *Tobamovirus* expression vector for agroinfection of legumes and *Nicotiana*. *J Biotechnol* 147: 151-9.

Lobbes D, Rallapalli G, Schmidt D D, Martin C, Clarke J (2006). SERRATE: a new player on the plant microRNA scene. *EMBO Rep* **7**: 1052-8.

Loebenstein G Carr J P (2006).Springer. XXIV: 532 p.

Lucas W J, Bouche-Pillon S, Jackson D P, Nguyen L, Baker L, Ding B, Hake S. (1995). Selective trafficking of KNOTTED1 homeodomain protein and its mRNA through plasmodesmata. *Science* 270:1980-1983.

Lynn K, Fernandez A, Aida M, Sedbrook J, Tasaka M, Masson P, Barton K (1999). The PINHEAD/ZWILLE gene acts pleiotropically in *Arabidopsis* development and has overlapping functions with the ARGONAUTE1 gene. *Development* 126: 469–81.

Maldonado E, Hampsey M, Reinberg D (1999). Repression: targeting the heart of the matter. *Cell* 99: 455-8.

Mallory A C, Hinze A, Tucker M R, Bouché N, Gasciolli V, Elmayan T, Lauressergues D, Jauvion V, Vaucheret H, Laux T (2009). Redundant and specific roles of the ARGONAUTE proteins AGO1 and ZLL in development and small RNA-directed gene silencing. *PLoS Genet* 5: e1000646.

Mallory A, Vaucheret H (2010). Form, function, and regulation of ARGONAUTE proteins. *Plant Cell* 22: 3879-89

Manavella P A, Weigel D, Wu, L (2011). ARGONAUTE10 as a miRNA locker. *Cell* 145: 173-4.

Marchler-Bauer A, Lu S, Anderson J B, Chitsaz F, Derbyshire M K, DeWeese-Scott C, Fong J H, Geer L Y, Geer R C, Gonzales N R, Gwadz M, Hurwitz D I, Jackson J D, Ke Z, Lanczycki C J, Lu F, Marchler G H, Mullokandov M, Omelchenko M V, Robertson C L, Song J S, Thanki N, Yamashita R A, Zhang D, Zhang N, Zheng C, Bryant S H (2011). CDD: A Conserved Domain Database for the functional annotation of proteins. *Nuc Acids Res* 39: D225-9.

Maunoury N, Vaucheret H (2011). AGO1 and AGO2 Act redundantly in miR408-mediated *plantacyanin* regulation. *PLoS One* 6: e28729.

Meyer W J, Schreiber S, Guo Y, Volkmann T, Welte M A, Muller H (2006). Overlapping functions of ARGONAUTE proteins in patterning and morphogenesis of *Drosophila* embryos. *PLoS Genet* 2: 1224-39.

Mlotshwa S, Voinnet O, Mette M F, Matzke M, Vaucheret H, Ding S W, Pruss G, Vance V B (2002). RNA silencing and the mobile silencing signal. *Plant Cell* 14: 289-301.

Mi S, Cai T, Hu Y, Chen Y, Hodges E, Ni F, Wu L, Li S, Zhou H, Long C, Chen S, Hannon G J, Qi Y (2008). Sorting of small RNAs into *Arabidopsis* ARGONAUTE complexes is directed by the 5' terminal nucleotide. *Cell* 133: 116-27.

Miller W A, White K A (2006). Long-distance RNA-RNA interactions in plant virus gene expression and replication. *Annu Rev Phytopathol* 44: 447-67.

Montgomery T A, Howell M D, Cuperus J T, Li D, Hansen J E, Alexander A L, Chapman E J, Fahlgren N, Allen E, Carrington J C (2008). Specificity of ARGONAUTE7-miR390 interaction and dual functionality in TAS3 trans-acting siRNA formation. *Cell* 133: 128-41.

Morel J B, Godon C, Mourrain P, Béclin C, Boutet S, Feuerbach F, Proux F, Vaucheret H (2002). Fertile hypomorphic ARGONAUTE (*ago1*) mutants impaired in post-transcriptional gene silencing and virus resistance. *Plant Cell* 14: 629-39.

Moussian B, Schoof H, Haecker A, Jurgens G, Laux T (1998). Role of the ZWILLE gene in the regulation of central shoot meristem cell fate during *Arabidopsis* embryogenesis. *EMBO J* 17: 1799-809.

Napoli C, Lemieux C, Jorgensen R (1990). Introduction of a chimeric chalcone synthase gene into petunia results in reversible co-suppression of homologous genes in trans. *Plant Cell* 2: 279-89.

Boyce Thompson Insititute For Plant Research News (2012). Release of a draft genome sequence for *Nicotiana benthamiana*. In. http://bti.cornell.edu/index.php?page=NewsDetails&id=128 Boyce Thompson Institute for Plant Research at Cornell University.

National Library of Medicine (2012). Align Sequences Nucleotide BLAST. In. National Center for Biotechnology Information.

Nonomura K I, Morohoshi A, Nakano M, Eiguchi M, Miyao A, Hirochika H, Kurata N (2007). A germ cell-specific gene of the ARGONAUTE family is

essential for the progression of premeiotic mitosis and meiosis during sporogenesis in rice. *Plant Cell* 19: 2583-94.

Okamura K, Ishizuka A, Siomi H, Siomi M C (2004). Distinct roles for ARGONAUTE proteins in small RNA-directed RNA cleavage pathways. *Genes Dev* 18: 1655-66.

Olmedo-Monfil V, Duran-Figueroa N, Arteaga-Vazquez M, Demesa-Arévalo E, Autran D, Grimanelli D, Slotkin R K, Martienssen R A, Vielle-Calzada J P (2010). Control of female gamete formation by a small RNA pathway in *Arabidopsis*. *Nature* 464: 628-32.

Omarov R, Sparks K, Smith L, Zindovic J, Scholthof H B (2006). Biological relevance of a stable biochemical interaction between the *Tombusvirus*-encoded P19 and short interfering RNAs. *J Virol* 80: 3000-8.

Omarov R, Ciomperlik J, Scholthof H B (2007) RNAi-associated ssRNA-specific ribonucleases in Tombusvirus P19 mutant-infected plants and evidence for a discrete siRNA-containing effector complex. *Proc Natl Acad Sci USA* 104: 1714 – 1719

Orzaez D, Mirabel S, Wieland W H, Granell A (2006). Agroinjection of tomato fruits. A tool for rapid functional analysis of transgenes directly in fruit. *Plant Physiol* 140: 3-11.

Palauqui J C, Balzergue S (1999). Activation of systemic acquired silencing by localised introduction of DNA. *Curr Biol* 9: 59-66.

Palauqui J C, Elmayan T, Dorlhac de Borne F, Crete P, Charles C, Vaucheret H (1996). Frequencies, timing, and spatial patterns of cosuppression of *nitrate reductase* and *nitrite reductase* in transgenic tobacco plants. *Plant Physiol* 112: 1447–1456.

Palauqui J C, Elmayan T, Pollien J M, Vaucheret H (1997). Systemic acquired silencing: Transgene-specific post-transcriptional silencing is transmitted by grafting from silenced stocks to non-silenced scions. *EMBO J* 16: 4738-45.

Pantaleo V, Szittya G, Burgyan J (2007). Molecular bases of viral RNA targeting by viral small interfering RNA-programmed RISC. *J Virol* 81: 3797-806.

Papenbrock J, Mock H P, Tanaka R, Kruse E, Grimm B (2000). Role of *Magnesium Chelatase* activity in the early steps of the tetrapyrrole biosynthetic pathway. *Plant Physiol* 122: 1161-9.

Peragine A, Yoshikawa M, Wu G, Albrecht H L, Poethig R S (2004). SGS3 and SGS2/SDE1/RDR6 are required for juvenile development and the production of trans-acting siRNAs in *Arabidopsis*. *Genes Dev* 18: 2368-79.

Perez-Novo C A, Claeys C, Speleman F, Van Cauwenberge P, Bachert C, Vandesompele J (2005). Impact of RNA quality on reference gene expression stability. *Biotechniques* 39: 52-56.

Pfaffl M W, Horgan G W, Dempfle L (2002). Relative expression software tool (REST) for group-wise comparison and statistical analysis of relative expression results in real-time PCR. *Nuc Acids Res* 30: e36.

Pflieger S, Blanchet S, Camborde L, Drugeon G, Rousseau A, Noizet M, Planchais S, Jupin I (2008). Efficient virus-induced gene silencing in *Arabidopsis* using a 'one-step' TYMV-derived vector. *Plant J* 56: 678-90.

Pohl D, Wege C (2007). Synergistic pathogenicity of a phloem-limited *Begomovirus* and *Tobamoviruses*, despite negative interference. *J Gen Virol* 88: 1034-40.

Pontes O, Li CF, Costa Nunes P, Haag J, Ream T, Vitins A, Jacobsen S E, Pikaard C S (2006). The *Arabidopsis* chromatin-modifying nuclear siRNA pathway involves a nucleolar RNA processing center. *Cell* 126: 79-92.

Powers J G, Sit T L, Qu F, Morris T J, Kim K H, Lommel S A (2008) A versatile assay for the identification of RNA silencing suppressors based on complementation of viral movement. *Mol. Plant Microbe Interact* 21:879-890

QIAGEN (2007). Critical factors for succesfull Real Time PCR Electronic Resource Number 1063770. In. www.qiagen.com

Qu F, Morris T J (2002). Efficient infection of *Nicotiana benthamiana* by *Tomato bushy stunt virus* is facilitated by the coat protein and maintained by P19 through suppression of gene silencing. *MPMI* 15: 193-202.

Qu F, Ren, T, Morris T J (2003). The coat protein of *Turnip crinkle virus* suppresses posttranscriptional gene silencing at an early initiation step. *J Virol* 77: 511-22.

Qu F, Ye X, Morris T J (2008). *Arabidopsis* DRB4, AGO1, AGO7, and RDR6 participate in a DCL4-initiated antiviral RNA silencing pathway negatively regulated by DCL1. *Proc Natl Acad Sci USA* 105: 14732-7.

Raghavan V (1988). Anther and pollen development in rice (*Oryza-Sativa*). *Am J Bot* 75: 183-96.

Rajagopalan R, Vaucheret H, Trejo J, Bartel D P (2006). A diverse and evolutionarily fluid set of microRNAs in *Arabidopsis thaliana*. *Genes Dev* 20: 3407-25.

Ratcliff F, Martin-Hernandez A M, Baulcombe D C (2001). *Tobacco rattle virus* as a vector for analysis of gene function by silencing. *Plant Journal* 25: 237-45.

Renteria-Canett I, Xoconostle-Cazares B, Ruiz-Medrano R, Rivera-Bustamante R F (2011). *Geminivirus* mixed infection on pepper plants: synergistic interaction between PHYVV and PepGMV. *Virol J* 8: 104.

Rivas F V, Tolia N H, Song J J, Aragon J P, Liu J, Hannon GJ, Joshua-Tor L (2005). Purified ARGONAUTE2 and an siRNA form recombinant human RISC. *Nat Struct Mol Biol* 12: 340-9.

Robertson N L, French RC (2004). *Foxtail mosaic virus*. Viruses of *Poaceae*. In. *Viruses of Poaceae.* ARS Publication Request.

Rochow W F, Ross F (1954). Phytopath. 44: 504.

Rochow W F, Ross F (1955). Virus multiplication in plants doubly infected by *Potato viruses X* and *Y*. Virology 1: 10-27.

Romano N, Macino G (1992). Quelling: transient inactivation of gene expression in *Neurospora crassa* by transformation with homologous sequences. *Mol Microbiol* 6: 3343-53.

Ruiz-Medrano R, Xoconostle-Cazares B, Lucas W J. (1999). Phloem long-distance transport of *CmNACP* mRNA: Implications for supracellular regulation in plants. *Development* 126: 4405-4419.

Schmid M, Davison T S, Henz S R, Pape U J, Demar M, Vingron M, Schölkopf B, Weigel D, Lohmann JU (2005). A gene expression map of *Arabidopsis thaliana* development. *Nat Genet* 37: 501-6.

Scholthof H B (1999). Rapid delivery of foreign genes into plants by direct rub-inoculation with intact plasmid DNA of a *Tomato bushy stunt virus* gene vector. *J Virol* 73: 7823-9.

Scholthof H B (2006). The *Tombusvirus*-encoded P19: from irrelevance to elegance. *Nat Rev Microbiol* 4: 405-11.

Scholthof H B, Alvarado V Y, Vega-Arreguin J C, Ciomperlik J, Odokonyero D, Brosseau C, Jaubert M, Zamora A, Moffett P (2011). Identification of an ARGONAUTE for antiviral RNA silencing in *Nicotiana benthamiana*. *Plant Physiol.* 156: 1548-55.

Scholthof H B, Desvoyes B, Kuecker J, Whitehead E (1999). Biological activity of two *Tombusvirus* proteins translated from nested genes is influenced by dosage control via context-dependent leaky scanning. *Mol. Plant Microbe In.* 12: 670-9.

Scholthof H B, Jackson A O (1997). The enigma of pX: A host-dependent cis-acting element with variable effects on tombusvirus RNA accumulation. *Virology* 237: 56-65.

Scholthof H B, Scholthof K-B G, Kikkert M, Jackson A O (1995). *Tomato bushy stunt virus* spread is regulated by two nested genes that function in cell-to-cell movement and host-dependent systemic invasion. *Virology* 213: 425-38.

Scholthof K B (2004). *Tobacco mosaic virus*: a model system for plant biology. *Annu. Rev. Phytopathol.* 42: 13-34.

Scholthof K B, Scholthof H B, Jackson A O (1995). The *Tomato bushy stunt virus* replicase proteins are coordinately expressed and membrane associated. *Virology* 208: 365-9.

Schott G, Mari-Ordonez A, Himber C, Alioua A, Voinnet O, Dunoyer P (2012). Differential effects of viral silencing suppressors on siRNA and miRNA loading support the existence of two distinct cellular pools of ARGONAUTE1. *EMBO J* 31: 2553 - 2565.

Scofield S R, Nelson S (2009). Resources for virus-induced gene silencing in the grasses. *Plant Physiol* 149: 152-7.

Serrano P, Pulido M R, Saiz M, Martinez-Salas E (2006). The 3' end of the foot-and-mouth disease virus genome establishes two distinct long-range RNA-RNA interactions with the 5' end region. *J Gen Virol* 87: 3013-22.

Sharp P A (2001). RNA interference. *Genes Dev* 15: 485-90.

Sigova A, Rhind N, Zamore P D (2004). A single ARGONAUTE protein mediates both transcriptional and posttranscriptional silencing in *Schizosaccharomyces pombe*. *Genes Dev* 18: 2359-67.

Silhavy D, Burgyan J (2004). Effects and side-effects of viral RNA silencing suppressors on short RNAs. *Trends Plant Sci.* 9: 76-83.

Silver S, Quan S, Deom C M (1996). Completion of the nucleotide sequence of *Sunn-hemp mosaic virus*: A *Tobamovirus* pathogenic to legumes. *Virus Genes* 13: 83-5.

Smith N A, Singh S P, Wang M B, Stoutjesdijk P A, Green A G, Waterhouse P M (2000). Total silencing by intron-spliced hairpin RNAs. *Nature* 407: 319-20.

Song B H, Yun S I, Choi Y J, Kim J M, Lee C H, Lee Y M (2008). A complex RNA motif defined by three discontinuous 5-nucleotide-long strands is essential for *Flavivirus* RNA replication. *RNA* 14: 1791-813.

Song J J, Joshua-Tor L (2006). ARGONAUTE and RNA--getting into the groove. *Curr Opin Struct Biol* 16: 5-11.

Song L, Han M H, Lesicka J, Fedoroff N (2007). *Arabidopsis* primary microRNA processing proteins HYL1 and DCL1 define a nuclear body distinct from the Cajal body. *Proc Natl Acad Sci U S A* 104: 5437-42.

Syller J (2012). Facilitative and antagonistic interactions between plant viruses in mixed infections. *Mol Plant Pathol* 13: 204-16.

Takeda A, Iwasaki S, Watanabe T, Utsumi M, Watanabe Y (2008). The mechanism selecting the guide strand from small RNA duplexes is different among argonaute proteins. *Plant Cell Physiol* 49: 493-500.

Tang G L, Reinhart B J, Bartel D P, Zamore P D (2003). A biochemical framework for RNA silencing in plants. *Genes Dev* 17: 49-63.

Tang W, Luo XY, Sanmuels V (2001). Gene silencing: Double-stranded RNA mediated mRNA degradation and gene inactivation. *Cell Res* 11: 181-6.

Taylor S, Wakem M, Dijkman G, Alsarraj M, Nguyen M (2010). A practical approach to RT-qPCR-Publishing data that conform to the MIQE guidelines. *Methods* 50: S1-5.

Teo C H, Pui H P, Othman R Y, Harikrishna J A (2011). Comparative analysis of ARGONAUTE gene sequences in bananas (*Musa sp*.) shows conserved species-specific AGO-7 PIWI domains. *Genet Resour Crop Evol* 58: 713-25.

Thangavelu M, Belostotsky D, Bevan M W, Flavell R B, Rogers H J, Lonsdale D M (1993). Partial Characterization of the *Nicotiana tabacum Actin* gene family - Evidence for pollen-specific expression of one of the gene family members. *Mol Gen Genet* 240: 290-5.

Thomas C, Meyer D, Wolff M, Himber C, Alioua M, Steinmetz A (2003). Molecular characterization and spatial expression of the sunflower ABP1 gene. *Plant Mol Biol* 52: 1025-36.

Thomas C L, Leh V, Lederer C, Maule A J (2003). *Turnip crinkle virus* coat protein mediates suppression of RNA silencing in *Nicotiana benthamiana*. *Virology* 306: 33-41.

Unver T, Budak H (2009). Virus-induced gene silencing, a post transcriptional gene silencing method. *Int J Plant Genomics* 2009: Article ID 198680, 8 pages. doi:10.1155/2009/198680

Vance V, Vaucheret H (2001). RNA silencing in plants--defense and counterdefense. *Science* 292: 2277-80.

Vandesompele J, De Preter K, Pattyn F, Poppe B, Van Roy N, De Paepe A, Speleman F (2002). Accurate normalization of real-time quantitative RT-PCR data by geometric averaging of multiple internal control genes. *Genome Biol* 3: RESEARCH0034

Vargason J M, Szittya G, Burgyan J, Tanaka-Hall T M (2003). Size selective recognition of siRNA by an RNA silencing suppressor. *Cell* 115: 799-811.

Vaucheret H (2005). RNA polymerase IV and transcriptional silencing. *Nat Genet* 37: 659-60.

Vaucheret H (2006). Post-transcriptional small RNA pathways in plants: mechanisms and regulations. *Genes Dev* 20: 759-71.

Vaucheret H (2008). Plant ARGONAUTES. *Trends Plant Sci* 13: 350-8.

Vaucheret H, Mallory A C, Bartel D P (2006). AGO1 homeostasis entails coexpression of MIR168 and AGO1 and preferential stabilization of miR168 by AGO1. *Mol Cell* 22: 129-36.

Volpe T A, Kidner C, Hall I M, Teng G, Grewal S I, Martienssen R A (2002). Regulation of heterochromatic silencing and histone H3 lysine-9 methylation by RNAi. *Science* 297: 1833-7.

Voinnet O, Baulcombe D C (1997). Systemic signalling in gene silencing. *Nature* 389**:** 553.

Voinnet O, Vain P, Angell S, Baulcombe D C (1998). Systemic spread of sequence-specific transgene RNA degradation in plants is initiated by localized introduction of ectopic promoterless DNA. *Cell* 95: 177-187.

Wang H, Zhang X, Liu J, *et al* (2011). Deep sequencing of small RNAs specifically associated with *Arabidopsis* AGO1 and AGO4 uncovers new AGO functions. *Plant J* 67: 292-304.

Wang X B, Jovel J, Udomporn P, Wang Y, Wu Q, Li W X, Gasciolli V, Vaucheret H, Ding S W (2011). The 21-Nucleotide, but not 22-nucleotide, viral secondary small interfering RNAs direct potent antiviral defense by two cooperative ARGONAUTES in *Arabidopsis thaliana*. *Plant Cell* 23: 1625-38.

Wassenegger M, Heimes S, Riedel L, Sanger H L (1994). RNA-directed de novo methylation of genomic sequences in plants. *Cell* 76: 567-76.

Waterhouse P M, Wang M B, Lough T (2001). Gene silencing as an adaptive defence against viruses. *Nature* 411: 834-42.

Wesley S V, Helliwell C A, Smith N A, Wang M B, Rouse D T, Liu Q, Gooding P S, Singh S P, Abbott D, Stoutjesdijk P A, Robinson S P, Gleave A P, Green A G, Waterhouse P M (2001). Construct design for efficient, effective and high-throughput gene silencing in plants. *Plant J* 27: 581-90.

Williams R W, Rubin G M (2002). ARGONAUTE1 is required for efficient RNA interference in *Drosophila* embryos. *Proc Natl Acad Sci U S A* 99: 6889-94.

Wingard S A (1928). Hosts and symptoms of ringspot, a virus disease of plants. *J. Agric. Res.* 37: 127-53.

Wu B, Pogany J, Na H, Nicholson B L, Nagy P D, White K A (2009). A discontinuous RNA platform mediates RNA virus replication: building an integrated model for RNA-based regulation of viral processes. *PLoS Pathog* 5: e1000323.

Wu C J, Jia L L, Goggin F (2011). The reliability of virus-induced gene silencing experiments using *Tobacco rattle virus* in tomato is influenced by the size of the vector control. *Mol Plant Pathol* 12: 299-305.

Wu L, Zhang Q, Zhou H, Ni F, Wu X, Qi Y (2009). Rice MicroRNA effector complexes and targets. *Plant Cell* 21: 3421-35.

Xie Z, Johansen L K, Gustafson A M, Kasschau K D, Lellis A D, Zilberman D, Jacobsen S E, Carrington J C (2004). Genetic and functional diversification of small RNA pathways in plants. *PLoS Biol* 2: E104.

Xie Z X, Kasschau K D, Carrington J C (2003). Negative feedback regulation of Dicer-Like1 in *Arabidopsis* by microRNA-guided mRNA degradation. *Curr Biol* 13: 784-9.

Yamamura Y, Scholthof H B (2005). *Tomato bushy stunt virus*: a resilient model system to study virus-plant interactions. *Mol Plant Pathol* 6: 491-502.

Yang D, Lu H, Erickson J W (2000). Evidence that processed small dsRNAs may mediate sequence-specific mRNA degradation during RNAi in *Drosophila* embryos. *Curr Biol* 10: 1191-1200.

Ye K, Malinina L, Patel D (2003). Recognition of small interfering RNA by a viral suppressor of RNA silencing. *Nature* 426: 874-8.

Yigit E, Batista P J, Bei Y, Pang K M, Chen C C, Tolia N H, Joshua-Tor L, Mitani S, Simard M J, Mello C C (2006). Analysis of the *C. elegans* ARGONAUTE family reveals that distinct ARGONAUTES act sequentially during RNAi. *Cell* 127: 747-57.

Yoshikawa M, Peragine A, Park M Y, Poethig R S (2005). A pathway for the biogenesis of trans-acting siRNAs in *Arabidopsis*. *Genes Dev* 19: 2164-75.

Zhang X, Yuan Y R, Pei Y, *et al* (2006). *Cucumber mosaic virus*-encoded 2b suppressor inhibits *Arabidopsis* ARGONAUTE1 cleavage activity to counter plant defense. *Genes Dev* 20: 3255-68.

Zhang X, Zhao H, Gao S, Wang W C, Katiyar-Agarwal S, Huang H D, Raikhe N, Jin H (2011). *Arabidopsis* ARGONAUTE 2 regulates innate immunity via miRNA393(*)-mediated silencing of a Golgi-localized SNARE gene, MEMB12. *Mol Cell* 42: 356-66.

Zheng D H, Ezzeddine N, Chen C Y A, Zhu W M, He X W, Shyu A B (2008). Deadenylation is prerequisite for P-body formation and mRNA decay in mammalian cells. *J Cell Biol* 182: 89-101.

Zheng X, Zhu J, Kapoor A, Zhu J K (2007). Role of *Arabidopsis* AGO6 in siRNA accumulation, DNA methylation and transcriptional gene silencing. *EMBO J* 26: 1691-701.

Zhiyong Y, Bin Y, Xuemei C (2006). HEN1 recognizes 21-24 nt small RNA duplexes and deposits a methyl group onto the 2′ OH of the 3′ terminal nucleotide. *Nuc Acids Res* 34: 667-75.

Zhu H, Hu F, Wang R, Zhou X, Sze SH, Liou LW, Barefoot A, Zhang X (2011). *Arabidopsis* ARGONAUTE10 specifically sequesters miR166/165 to regulate shoot apical meristem development. *Cell* 145: 242-56.

Zhu Y, Green L, Woo Y M, Owens R, Ding B (2001). Cellular basis of *Potato spindle tuber viroid* systemic movement. *Virology* 279: 69-77.

Zilberman D, Cao X, Jacobsen S E (2003). ARGONAUTE4 control of locus-specific siRNA accumulation and DNA and histone methylation. *Science* 299: 716-9.

Zilberman D, Cao X, Johansen L K, Xie Z, Carrington J C, Jacobsen S E (2004). Role of *Arabidopsis* ARGONAUTE4 in RNA-directed DNA methylation triggered by inverted repeats. *Curr Biol* 14: 1214-20.

APPENDIX

Appendix Figure A.1. All currently known *N. benthamiana AGO* sequences. The shaded regions demarcate sequences inserted into the TRV vector

>*N. benthamiana AGO1*

ATGGTGCGGAAGAAGAGGACTGATGTTCCTGGTGGTGCTGAGAGTTTGAGTCCCAT
GAAACTGGAGGGGCACGAGGTGGTGCCCAACGCCCATCACAGCAGCAGCAACATCA
GCATCAGCAAGGCGGAGGAAGAGGCTGGGCACCTCAGCATGGAGGACATGGTGGC
CGTGGTGGTGGGGGAGCTCCACGTGGTGGAATGGCCCCTCAACAATCCTATGGTGG
ACCTCCTGAATACTACCAACAGGGCAGGGGAACTCAACAGTATCAACGAGGTGGAG
GACAACCCCAGCGCCGTGGTGGCATGGGGGGCCGTGGGGCACGGCCACCAGTACCC
GAGCTGCACCAAGCAACCCAGACTCCACATCAGCCTGTACCATATGGAAGACCATC
AGAAACATACTCAGAGGCTGGTTCCTCGTCTCAGCCACCTGAACCAACGACACAGC
AAGTGACTCAGCAATTCCAGCAACTTGTTGTGCAGCCAGAAGCAGCTGCAACCCAA
GCAATACAACCAGCATCGAGCAAGTCGATGAGGTTTCCACTCCGGCCAGGAAAGGG
TAGTACTGGTATTAGATGCATAGTTAAGGCCAATCACTTCTTTGCCGAGTTACCTGA
CAAAGATCTGCACCAGTATGATGTTTCAATTACTCCTGAGGTCGCCTCTCGGGGTGT
CAACCGGGCCGTCATGGAGCAGCTGGTGAAGCTTTATAGAGAATCCCATCTTGGGA
AGAGGCTTCCAGCCTATGACGGAAGAAAAAGTCTATACACAGCAGGGCCCCTCCCT
TTTGTTCAAAAGGATTTTAAAATCACTCTAATTGATGATGATGATGGACCTGGTGGT
GCTAGGAGGGAAAGAGAGTTTAAAGTTGTGATCAAGCTGGCGGCTCGTGCTGATCT
TCATCACTTGGGGATGTTCTTACAAGGGAGACAGGCTGATGCACCGCAAGAAGCAC
TTCAGGTGCTGGATATTGTGCTACGTGAGTTGCCAACATCTAGGTATTGTCCTGTGG
GCCGCTCTTTCTATTCCCCTCATTTAGGACGAAGACAACCACTGGGTGAAGGTTTAG
AGAGCTGGCGTGGCTTCTATCAAAGTATTCGTCCTACACAGATGGGATTATCCCTGA
ATATTGATATGTCTTCCACGGCTTTCATTGAGCCACTGCCGATTATTGACTTCGTGAG
CCAGCTTCTGAATCGGGATATCTCTTCTAGACCACTGTCTGATGCTGACCGCGTTAA
GATAAAGAAGGCACTGAGAGGTGTAAAGGTGGGGGTCACTCATCGTGGAAATATGC
GGAGGAAGTATCGCATTTCTGGCTTGACGTCTCAAGCAACAAGAGAGTTGACTTTTC
CTGTCGATGAAAGGGGTACGATGAAAGCTGTTGTGGAATATTTTCGGGAAACCTATG
GTTTTGTCATTCGGCATACCCAGTGGCCTTGTCTTCAAGTTGGAAATACGCAGAGGC
CAAATTACTTGCCAATGGAAGTATGTAAGATTGTAGAGGGACAGAGATACTCAAAG
CGCTTGAATGAGAGGCAGATAACAGCACTTCTAAAAGTGACCTGCCAACGTCCTCA
AGAGAGAGAACGTGATATTCTTCAGACTGTTCATCACAATGCTTATGCTGATGACCC
ATATGCGAAGGAGTTTGGTATTAAGATCAGTGAGGAGCTTGCTCAAGTTGAGGCTCG
CGTTTTGCCTGCACCTTGGCTTAAATACCATGATACAGGTCGAGAGAAAGACTGTCT
GCCACAAGTGGGCCAGTGGAATATGATGAATAAGAAAATGGTTAATGGAGGAACAG
TGAACAACTGGATCTGTGTAAACTTTTCTCGCAATGTGCAAGACACAGTTGCACGTG
GATTTTGTTCCGAGCTTGCACAAATGTGCATGATATCCGGAATGAACTTCAATCCCA
ATCCTGTTCTACCACCAGTGAGTGCTCGCCCTGATCAAGTTGAGAGAGTCTTGAAAA
CTCGATTTCACGATGCTATGACAAAGTTGCAGCCAAATGGGAGAGAGCTAGATCTTT
TGATTGTGATATTACCAGACAATAACGGCTCTCTTTATGGTGATCTAAAACGGATTT
GTGAAACTGAACTTGGAATTGTCTCACAATGCTGCTTGACAAAACATGTATTTAAGA
TGAGCAAGCAGTATTTAGCTAATGTATCCCTGAAGATAAATGTGAAGGTTGGAGGA
AGAAATACTGTGCTGGTTGATGCGCTCTCTAGACGAATTCCCCTTGTCAGCGACCGC
CCAACTATCATTTTTGGTGCAGATGTCACCCATCCCCACCCTGGGGAGGATTCTAGC
CCGTCAATTGCTGCGGTGGTTGCTTCTCAAGATTGGCCTGAAATTACAAAGTTGCTG

GTTTGGTTTCTGCTCAAGCGCATAGGCAAGAGCTTATACAAGATCTGTACAAGACTT
GGCAAGATCCAGTTAGAGGACCTGTGACTGGTGGCATGATAAAGGAATTACTTATTT
CCTTCCGTCGAGCAACTGGACAGAAGCCGCAGAGAATTATATTCTACAGAGATGGT
GTTAGTGAAGGACAATTTTACCAAGTTCTTCTTTTTGAACTTGATGCAATCCGCAAG
GCATGTGCATCTTTAGAACCCAACTATCAGCCCCCGGTTACGTTTGTTGTGGTCCAG
AAACGGCATCATACTAGGTTGTTTGCCAATAACCACCACGACAGAAATGCAGTTGAT
CGGAGTGGGAACATTTTGCCTGGTACCGTTGTAGATTCAAAGATATGCCACCCTACG
AATTTGATTTCTATCTCTGTAGCCATGCCGGCATACAGGGTACTAGCCGCCCAGCTC
ATTATCATGTTCTGTGGGATGAGAACAATTTTACTGCTGACGCCCTGCAGTCTTTGAC
TAACAATCTTTGCTATACATATGCTAGGTGTACTCGTTCTGTCTCCATTGTTCCACCA
GCATATTATGCACATTTGGCAGCTTTCCGTGCTCGGTTTTACATGGAGCCAGAGACA
TCTGATAATGGATCAGTCACAAGCGCAGCTGCTTCAAACAAGGAGGTTTAGGAGCT
ATGGGAAGGAGCACGCGAGCACCAGGTGCTGGTGCTGCTGTAAGGCCCCTTCCTGC
TCTCAAGGAGAATGTTAGAGGGTTATGTTTTATTGT

>N. benthamiana AGO2
ATGGGTTCATTCAACCAGCAACCAATTCAGCCACCACAGCAATGGGGTAACCAGCC
AAGAGCATCTGGTCCGGGTCAGTATCAGGCTCGTGGAGCTCCGTATAATCAGCCGG
GTCTGCAGCATCCAGTTGGACGAAGTCCGGGTCGTGGTGGTGCATGGGTCAGCCGTG
GAGGTGGCGGTACTGCTTGGGCCCGGCCACCACCGCAGCAGCCACAGCAACATGGT
AGTGGCAGCAGTGGTACTGCTTGGGCCCGGCCACCGCAGCAGCAACTTGTTAGTGG
CGGCAGTGGTACTGCTTGGGTCAGGCCACCGTCGCAGCAGCCACCACAACATGGTG
GTGGAAACCAGCAGCAGCGGGATGTGCAACCCAATAGCTCAGAAGCATCAACTGTT
CGCCAGTGGGGTCCACCTTCAGGCTCTAGTCCTCCTCCTCCTCAGTCTTCTGATCCTG
TTCAAGTTGATCTGAAGTCGCTGAGTATTACAGAAAAAGAGAGTACATCATCTCCTC
CGGAAAGTAACAACGGAAAGCTTGTACCTATTGCACGACCTGATACGGGAAAAGTT
GCTGTCAAGTCAATTAGACTGCTTGCTAATCATTTTCCTGTTAGATTTAATCCTCAGT
CTACCATTATGCATTATGATGTGGATATCAAGCAAATCATGACTGATGAGACCCGGG
CTGTGAAGAAGTCAATAAACAAGTCTGATCTTCGTATGATAGGAGATAAGCTGTTTG
CTGATAATCCTGGTCAATTTCCAATAGACAAAACTGCATATGATGGTGAGAAGAAC
ATTTTCAGTGCTGTCCAACTTCCTACTGGGCGATTCACTGTGAACTGCTCAGATGGG
GATGAGGGTAGGGGACGCTCGTATGTCTTTACCATCAAGTTTGTTGCTGAACTGAAA
CTTTGCAAGTTGAAAGAATATTTGAGTGGAAGCCTCTCATACATACCTCGTGATGTA
CTACAAGGAATGGATTTGGTTATGAAAGAAAATCCTTCTAGGTTAAGGATAATTGCA
GGTCGTAGCTTCTACTCAAATGAGCACTTGGCTGAACATGACTTTGGGTTTGGAGTT
GCTGCATATAGAGGTTTTCAGCAAAGCcTAAAGCCTACATCTGGAGGGCTTGCCTTG
TGCCTAGATTACTCAGTCTTGGCATTCCGCAAAGCAGTGCCGTGCTAGATTTCCTGA
GGGAATATATTGGAGAGTTTAATGAAAATAATTTTACTCGTAGAAGAGATGCAGAG
GATGCATTGGTTGGTTTGAAAGTCAAAGTAACTCATCGTCGTAGCAGTCAGAAATAT
GTTGTTAAGAAGCTGACTGATGAGATGACTCGCGACCTTCATTTTATCCTTGAAGAT
CCAGAAGGCAAAGATCCTCCTAAGAAAGTTTTTCTTGTTGACTACTTCAGGGAAAAA
TATCAGGTGGAGATTAGGTACCAAAATTTACCTTCATTAGATCTTGGAAAAGGTAAT
AAGAAAAACTATGTCCCAATGGAATTCTGTGTCTTGATCGAGGGACAGCGGTTTCCT
AAGGAGCATTTAGATAAGGATTCAGCCTTGTTTATGAAAAAAATATCACTAGTTCCA
CCACGAGAGAGAAGGGAGGCAATATGTGAAATGGTACGGGCTGAAGATGGGCCAT
GCGGGGCTGTCACCCGTAATTTTGAAATTAGAGTTGATCGGAACATGACCTGTGTTT
CGGGTCGTATCCTTCCTACCCCTGATTTGAAGCTAGGTGGTCTAAGTCGAGTTCCCCT

GGATAATAAATGCCAGTGGAACCTTGTTGGAAAATCTGTGGTGGAAGGCAAGGCGC
TTCAGCGATGGGCTCTGATTGATTTTAGCTCCCAGGAACGCAACCCCAACTTTAGGC
TAAGAACTGATGAATTTGTCTTTAGATTGAAAGAGCGGTGCAAAAAGTTAGGGATC
AACATGGAAGAACCTGTCATAACACATTTCACTGGCATGTATGAGCTCTCTGCAGTT
GAAAAGGTTGAAGATCTCCTCAGAGGTGTGGTTCGTGCAGCTGACGAGAAAATCAA
GGACAGACTACAAATGATAGTTTGTGTTATGGCAGCAAAGCACAATGGATACAAAT
ATCTTAAATGGGTCTCTGAAATAAAAATTGGTGTTGTAACGCAATGTTGCTTGTCAT
CTCTAGCCAACAAGGGACAAGATCAATATCTTGCAAACCTTTGTATTAAGATTAACG
CAAAATTGGGAGGTAGCAATATGGAACTTACGGGAAGGCTCCCTAATTTTGGAGGT
GAAGATAATGTGATGTTCATTGGAGCTGATGTTAATCATCCTGCTGCAAGGAATGTG
ACATCTCCATCTATAACAGCTGTTGTTGCCACTGTCAACTGGCCAGCCGCTAATAGA
TATGCGGCTAGAGTTTGTCCTCAGGACCACAGGACTGAGAAGATACTAAATTTTGGG
AGCATGTGTGCAGACCTACTGAATGCTTACACTCTACTCAACTCGGTTAAACCAAAC
AGAATTGTTGTTTTCCGTGATGGTGTGAGTGAGGGCCAATTTGATATGGTACTTAAT
GAAGAGCTGGTTGATTTGATGAAGGCTATATACGATGATCACTATCGACCAGCAATC
ACTCTTGTTGTGGCTCAGAAAAGACACCATACACGACTATTTCCTGATGGTGGCCCT
GGCAATGTACCTCCGGGTACTGTTGTGGACACAGTAATTGTTCATCCATCTGATTTTG
ACTTCTATCTTTGCAGCCATTTTGGAGGATTGGGAACTAGCAAGCCTACTCACTATC
ATGTTTTGTGGGATGAGAATGGCTTCAATTCTGACCGCTTACAGAAGCTTATATACA
ACATGTGCTTCACCTTCGCGCGGTGCACAAAACCTGTTTCACTTGTTCCACCAGTTTA
CTATGCTGACCTTGTTGCCTACCGGGGACGGATGTTCCAAGAGGTGCTTATGGAGAT
GCAGTCTCCTGCATCTTCAACTGCATCCTTCACAACTTCATCGTCATCTTCTTCAACT
ACCTCATTTGAACAAGGATTCTTTAAATTGCACCATGAGCTGCAGAACATAATGTTC
TTTGTCTGAGGATCCTGA

>N. benthamiana AGO4
ATGGCTGAAGAAGACAATGGTGGAGTAACAGAGGCTCTGCCTCCTCCTCCCCCTATT
CCACCTGATTTCTCTCCAGCAATAGCGGAACCAGAGCCGGTGAAGAAAAAGGTTTT
ACGTGTTCCCATGTCTAGGCGTGGCCTTGGAAGCAAGGGACAAAAGATTCCAATCCT
TACCAATCACTTTAAAGTGAACGTGTCTAATGTTGATGGACACTTCTTTCATTACAGC
GTCGCCCTATTTTATGAGGATGGTCGACCTGTCGAGGGGAAAGGAATTGGCAGAAA
AGTTCTTGATAGAGTGCATGAAACATATGATACAGAATTGGCAGGGAAGGATTTTG
CATACGATGGGGAGAAAAGCTTGTTCACCATTGGTTCACTACCTAGAAATAAATTAG
AGTTCACAGTTGTCCTAGAGGACGTCATATCTAATCGGAACAATGGGAACAATGGC
AGCTCTAGCCCTGGCAAACATGGAAGTCCAAATGAAAATGATAGGAAAAGATTAAG
GCGGCCGTACCAATCAAAATCTTATAAGGTGGAGATTAGCTTTGCTGCCAAGATTCC
GATGCAGGCAATTGCGAATGCTTTGCGAGGTCAAGAGTCTGTGAACTCTCAAGAAG
CATTGAGAGTTTTGGAAATAATTTTAAGGCAACATGCAGCCAAACAGGGGTGTCTTC
TTGTTCGACAGTCCTTTTTCCATAATGACCCAAAGAATTTTGCGGAAGTTGGAGGTG
GTGTTCTTGGCTGTCGAGGGTTCCATTCAAGTTTTCGAACCACTCAGTCTGGATTGTC
TTTGGACATTGATGTGTCTACCACGATGATAATTCAGCCTGGACCTGTTGTTGACTTT
TTGATTGCGAACCAAAATGCAAAAGATCCCTTTTCACTTGATTGGGCGAAGGCAAAA
CGTACCTTGAAGAATCTAAGGGTGAAGACTGCTCCCGCTAACCAAGAGTTCAAAAT
AACTGGATTGAGTGAAAAATCGTGTCGCGAGCAGACGTTTACTCTAAAGCAGAGG

AGCAAAAATGAGGATGGTGAAGCGCAAACATCGGAAGTGACAGTTTATGATTACTT
TGTTAATCATCGTAACATAGACTTGCGCTATTCCGCTGATTTACCGTGCATCAATGTT
GGAAAGCCCAAGCGTTCCACCTATTTCCCTGTCGAGCTCTGCTCGTTGGTCTCATTGC
AAAGGTACACAAAAGCCTTGCTCACCTTTCAGAGGTCCTCCTTGGTGGAGAAGTCTA
GGCAAAAGCCTCAAGAGAGAATGCAAATTTTGAGCAATGCTCTAAAAATCAACAAT
TATGATGCTGAGCCTCTGCTTCGTGCTAGCGGCGTCTCAATCAGTAGCAACTTTACC
CAGGTTGAAGGGCGTGTTCTGCCTGCCCCTAAGTTGAAGGCAGGAAATGGAGATGA
CCTTTTCTCACGAAATGGCAGGTGGAATTTTAATAATAAGAGATTCTTTGATCCGCA
AAGGTAGAGCGTTGGGCTGTTGTCAACTTTTCTGTACGCTGTGACATACGTGGCCTT
GTCAGAGATTTGACAAGAATTGGAGAGATGAAAGGAATTAGTGTGGAAGCTCCATT
TGAAGTGTTTGAAGAGTCTCCACAGCTTAGAAGAGCTCCACCTCTTGTCAGAGTTGA
AAAGATGTTTGAAGAGATCCAGTCAAAACTTCCCGGTGCCCCGAAATTTCTTCTTTG
CCTTCTTCCTGAGAGGAAAAATTGTGACATATATGGACCGTGGAAGCGGAAAAATC
TGGCTGATTATGGTATAGTAACCCAATGCTTGGCTCCTGGAAGGGTCAACGATCAGT
ATCTTACAAACCTTCTCCTTAAGATCAACGCGAAGCTTGGTGGTTTAAATTCTGTGTT
AGCTATTGAGCATTCACCTTCCATTCCCATGGTATCTAAGGTTCCCACCATGATTCTT
GGAATGGACGTATCACATGGCTCTCCTGGCCAGTCTGATGTTCCATCAATTGCTGCA
GTTGTAAGTTCAAGGCAGTGGCCTTCAATATCTCGTTATAGAGCTTCTGTGCGCACT
CAATCTCCTAAAGTGGAGATGATTGATAACTTATTTAAAAAAGTTTCAGACACTG
AGGATGATGGGATTATGAGGGAACTTTTGCTAGATTTTTATGTGGGTTCCGGGAAAA
GGAAGCCTGAGCATATTGTAATATTCAGGGATGGTGTCAGTGAATCTCAATTTAATC
AAGTTCTAAACATTGAATTGGACCAGCTCATTGAGGCCTGCAAATTTCTTGATGAGA
AGTGGTCACCGAAGTTTGTGATCATTGTTGCTCAGAAAAATCATCATACAAAGTTTT
TCCAGGCTGGATCTCCTGATAATGTTCCTCCAGGGACAATCATAGACAACAAAGTTT
GTCATCCAAGGAACTATGACTTCTACCTGTGTGCCCATGCAGGCATGATTGGTACCA
CTCGACCTACACATTACCATGTGTTGTTGGATGAAGTTGGTTTTTCACCTGATGATCT
TCAAGACCTTGTTCATAATCTGTCCTATGTATATCAAAGAAGCACTACTGCTATATCC
ATTGTGGCTCCGGTAAGTTATGCCCATTTGGCCGCCACACAAGTTGGACAATGGATG
AAGTTCGAGGACGCATCAGAGACATCGTCAAGCCATGGTGGTCTGACAAGTGCTGG
TCCAGTTACTGTTCCTCAGTTGCCTCGACTTCAGGAAAATGTTTCTAGTTCCATGTTC
TTCTGT

>N. benthamiana AGO5

GTGAGTCATCACGGCATCAGACGCTACAGGATCTCCGGGTTGTCCGCTCAACCAGTG
AAGGAAATAATGTTTTCCGTTGACGGCACTGGAATGAAGACATCAGTTGTTGACTAC
TTCCGGCAGAAGTACAACATTGTACTTAGGTTTCCAATGTTGCCTGCGATTCAGGCG
GGCAGCGATGCAAAGCCCGTGTATCTGCCTATGGAGATTTGCCAAATCGTTCCAGGC
CAAAGATACACAAAAATGTTGAATGGAAGGCAGGTCACAGAGATGCTAAAGGCAA
CTTGTCAGAGACCTGCTGATAGAGAGAAAAGCATTGAAAAGATTGTGAGTTCTAAC
AACTATGTTGCTGACGAAATGGTGAAAGAATTTGGTATTGAAGTTCGAAGTGAACTC
ACCACCATTGATGCACGGGTTCTTCAGCCTCCAATGCTAAAGTATCATGAATCTGGT
CAAGAATCACGAGTGGATCCTAGGATTGGTCAATGGAACATGATAAATAAGAAAAT
GGTCAATGGTGGCAAGGTAGACACTTGGACTTGTGTCAGCTTCTCACGGGTTGATCC
ATCACCGTTCTGCAAGGCACTGATTGAAATGTGCTGTAGTAAAGGGATGGTGTTCAA
TCCTCAGCCTTTGGTGCCCATTCGCTCAGCTCATGCTGGGCAGATTGAGAAGACTCT
GGTTGATATCCATACAGCGTCTACTCAAAAGCTAGCAACTATGGAGCATCAATTGAA
ACATCTTCAGCTGTTAATTGTTATTCTTCCGGAAGTTTCTGGATATTATGGGAGGATT

AAGCGAGTATGTGAAACAGATTTGGGAATTGTGTCCCAATGCTGTCAGCCTAAGAAT
TTATCTAGACCCAACAAACAGTATCTTGAAAACCTTGCTCTAAAGATAAATGTCAAG
GTGGGTGGAAGAAACTCTGTCCTGGAGCAGGCAGTTCATAGAAGAATACCTTTCCTC
ACTGATATCCCCACAATTGTCTTTGGTGCTGATGTGACACATCCACAACCAGGAGAA
GATTCTAGTCCATCTATAGCTGCTGTAGTCGCTTCAATGGATTGGCCTGAAGTGAGT
CAATATAGGTGTCTTGTTTCTGCACAACCCCACAGGAAAGAGATCATTGAGGACTTG
TATCAAAAGCACGTAGATGCTAAAAAAGGGATTGTTCATGGCGGAATGATAAGGGA
GTTACTGATTGCGTTTCGAAGATCTACAGGGATTAAGCCTGGTAGAATTATCTTTTAT
AGAGATGGAGTGAGCGAAGGTCAATTCAATCAGGTTTTATTGGAAGAAATGGACGC
AATCCGCAAGGCATGCACATCCTTGGAAGAAGGTTATCTGCCACGAGTTACCTTTGT
GGTAGTGCAGAAGAGACACCATACACGTCTGTTCCCTGTTAATCATAACGATCGTAA
TATGACGGACAAGAGTGGAAACATTCTGCCAGGTACTGTTGTTGATACCAAGATTTG
CCACCCTATGGAGTTTGATTTT

>N. benthamiana AGO6

CCAGAATGTAAAGGAGCCTCGTTATATTGATTGGGCAAGAGCAAAAAGAATGCTGA
AGAATCTGAGAGTTAAAGCTAAGCACAGCAACAAGGAATTCAAAATCATCGGTCTG
AGTGAGAGACCTTGCAATCAACAGTTATTTTCTATGAAAGTGAAAAATGGTGATGGC
CTAGATAATGGAGGAGATACCATAGAGATAACTGTTTATGAGTACTTCACTAAACAC
CGTAACATAGAACTTTCAAACTCTGCTTATATGCCATGCCTGGATGTCGGAAAACCG
AAACGACCAAACTATCTGCCACTGGAGCTGTGTTATTTGGTCTCCCTTCAAAGATAC
ACAAAAGTGTTATCATCAGTGCAGCGGGCATCTTTAGTTGAAAAATCAAGGCAGAA
GCCTCGAGAACGAATTAAAGTTATAACAGATGCTGTGAGGGATTACAGCTATGATG
ACGATCCCCTGCTTGCCACTTGTGGAGTCTCAATAGAAAAGCAGCTCATTCAAATTA
ACGGCAGGGTCCTTGAGGCTCCAAAGTTGAAAGTTGGTAATGGCGAAGAGGTCGTT
CCCCGCAACGGCCGATGGAATTTTAATAACAAGCATCTTTTGACCCCTTCACGAATT
GAACGCTGGGCAGTGGTCAACTTCTCTGCCCGTTGTGATACAAGTCACCTTTCGAGG
GAGCTTATTAGTTGTGGAAGGACCAAAGGCATTCATTTTGAACGCCCACATACACTC
ATTGAGGAAGATCCCCAGAATAGGCGAGCTGGGCCTGAATTCGAGTAAAAAAGATG
TTCGAAGAAATAATAGCTAGACTTCCTGGCCCTCCTGACTTTCTTCTCTGTGTCTTGC
CAGAACGAAAAAACTCAGAAATATATGGACCTTGGAAGAAAAAAAGCTTGACTGAC
TTGGGAATTGTTACTCAATGTATCTCTCCGTTAAAGATCAATGATCAATATCTAACG
AATGTGCTTCTCAAAATTAATGCAAAGCTTGGAAGGACCAATTCATTGTTGGCTAT
GGAACATGCATCTTATCTGCCGCATATTCAGGAAACTCCAACAATGATTCTGGGCAT
GGATGTCTCTCATGGATCTCCTGGTCAATCAGATATTCCATCAATTGCTGCGGTTGTG
GGATCCTTATATTGGCCATTAATATCCAAGTACAGGGCAGTTGTCCGTAATCAATCT
CCAAAGTTAGAAATTATAGAATCCTTATACAAGCCTTTACCAAATGGAGACAATGA
AAGAATCATGGGAGAAATTCTTCTGGACTTCTATATGACATGTAACGGCCAT

>N. benthamiana AGO7

ATTACGGCCGGGATGTCAAAGGTGTGAGCAATTGGGAATTTTCCTTAACAAGAATAC
AGTACTTAACCCCCAGTTTGAACCCATGCATTTGCTCAACAATGTAAAACACCTAGA
AACCAAACTCAAGAAGCTGCATGGAGCTTCATTTAGCAATCTCCAACTTGTTATTTG
CGTGATGGAGAAAAAACACAAAGGATACGCGACTTGAAAAGAATCGCCGAGACAA
ACATCGGGGTTGTAACCCAATGTTGTTTGTACCCAAACCTTGGCAAACATAGCTCAC
AGTTTTTGGCAAATTTGGCTCTCAAGATCAATGCCAAAGTTGGGGGATGCACAGTTG

CATTGTACAGTTCATTGCCTTCTCAAATACCACGGCTCTTCAAGCACGATGGTCCGG
TTATTTTTATGGGTGCGGACGTGACTCATCCACACCCACTTGATGATTCTAGCCCCTC
GGTTGCTGCTGTAGTTGGTAATGTGAATTGGCCAGCAGCCAACAAGTATGTCTCCAG
AATGAGGTCCCAAACACATAGGCAGGAGATCATTCAAGATCTCAGCACAATGATCG
GGGAAATTCTTGATGATTTCTACGAGGAGCTTCTAAAACTCCCCGAGCGAATAATCT
TCTTCAGGGATGGAGTAAGTGAAACTCAGTTCTTGAAAGTACTTAAAGAAGAGCTA
CAAGCAATTCGTGCAGCATGTTCGAGATTTCCAGGTTACAAACCTCCCATTACTTTC
GTGGTCGTTCAGAAAAGGCATCATACTCGGCTATTTCCATGTGAACTTGATCCGTCG
TCAACTAGAAACCAGTTCTTTAATGAAAACATCGCACCAGGTACAGTTGTTGATAGT
GTGATCACACATCCAAGAGAATTTGACTTCTATCTGTGCAGTCA

>N. benthamiana AGOX

ACAGTGCATTTGCTACTTACTCTTTTTCTCTCTCGTTACGTCGATAGCAATGTCGGAA
CGTGGACGCGGACGTCGAGGCGGTGGTGGTCGAACACCGTCGTCTTCATCCGGTGGT
CGTGGCACCGGAGGGCCGTCTTCATTCGGTGGTCGGGGCGCCGGAGGGCCGTCTTCT
TCCGGTGGTCGTGGTCGTGGAACATTTAGTAGTGGAGGTTTGCCGTCTTTCAATGCT
CCACCGGCGTCTCAACCTCAACGACCGGCGATCACGGTTTCATCGGTGTCTCGCGAG
GTAGAGCAGAAGCTTTCGCTTCAGCCTTCATCATCACAACGTCCTGTTGTGGCCCAG
CCTGTGCAACAATCGGCACCGGCGACTGGTGTAAAACCGCTACAGCCGCCGCCGCC
GTCCTCGAAAAGCATTCAGGTTCCTAATAGACCGGGATACGGAACTGTTGGACGGA
AGTGCCTTATAAGAGCAAATCATTTTCTCGTTCATGTTGCTGATCGGGATCTGCATCA
CTATGATGTTACAATCTCTCCAGAGGTTCTGTCAAAGAAAGTATGCAGAGAGATTAT
GAGCCAGCTAGTTAATGACTATAAACAGTCACACATGGGTGGTCGGAATTTAGCAT
ATGATGGCGGGAAGAGTGTTTACACTGCTGGGCCTCTCCCATTCTCCTCCAAGGACT
TCATTATCAAGCTAGATGGTAATAGTGGTGGAGCAAAGAGGGAAAGAGAGTTTAAG
TCTCTATCAAGTTTGCTGCCAAAGCTGATCTTCATCACTGAACAGTCTGCATGTAGC
ATCGATGCCCCGCAGAA

Appendix Figure A.2. MUSCLE and BOXSHADE alignment output of all known *AGO* sequences

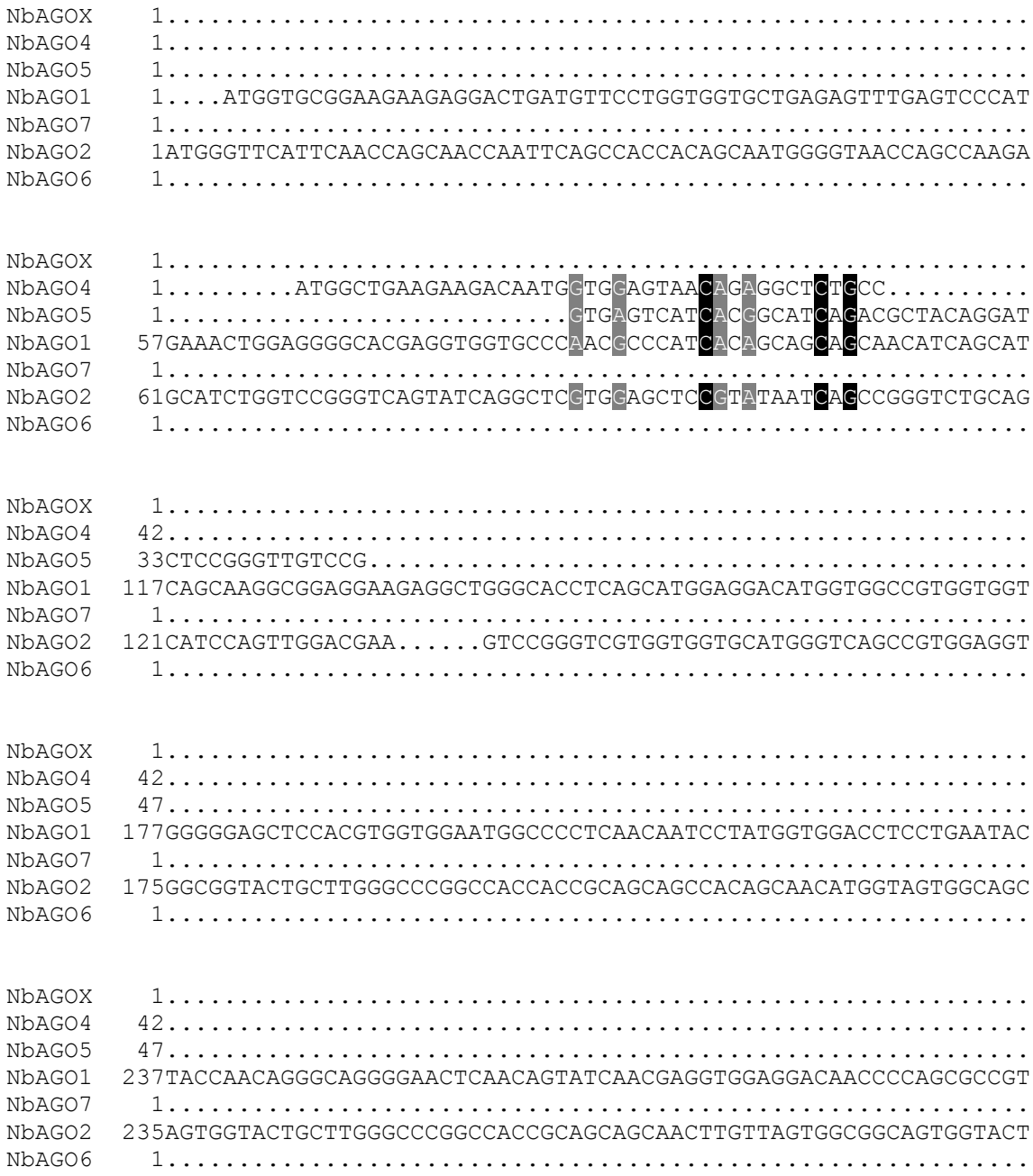

```
NbAGOX    1.....................................................
NbAGO4   42.....................................................
NbAGO5   47.....................................................
NbAGO1  297GGTGGCATGGGGGGCCGTGGGGCACGGCCACCAGTACCCGAGCTGCACCAAGCAACCCAG
NbAGO7    1.....................................................
NbAGO2  295GCTTGGGTCAGGCCACCGTCGCAGCAGCCACCACAACATGGTGGTGGAAACCAGCAGCAG
NbAGO6    1.....................................................

NbAGOX    1.....................................................
NbAGO4   42.....................................................
NbAGO5   47.....................................................
NbAGO1  357ACTCCACATCAGCCTGTACCATATGGAAGACCATCAGAAACATACTCAGAGGCTGGTTCC
NbAGO7    1.....................................................
NbAGO2  355CGGGATGTGCAACCCAATAGCTCAGAAGCATCAACTGTTCGCCAGTGGGGTCCACCTTCA
NbAGO6    1.....................................................

NbAGOX    1.....................................................
NbAGO4   42........TCCTCCTCCCCCTATTCCACCTGATTTCTCTC.................
NbAGO5   47.....................................................
NbAGO1  417TCGTCTCAGCCACCTGAACCAACGACACAGCAAGTGACTCAGCAATTCCAGCAACTTGTT
NbAGO7    1.....................................................
NbAGO2  415GGCTCTAGTCCTCCTCCTCCTCAGTCTTCTGATCCTGTTCAAGTTGATCTGAAGTCGCTG
NbAGO6    1.....................................................

NbAGOX    1.....................................................
NbAGO4   74.............CAGCAATAGCGGAACCAGAGCCGGTGAAGAAAAAGGTTTTACGTGTT
NbAGO5   47.....................................................
NbAGO1  477GTGCAGCCAGAAGCAGCTGCAACCCAAGCAATACAACCAGCATCGAGCAAGTCGATGAGG
NbAGO7    1.....................................................
NbAGO2  475AGTATTACAGAAAAAGAGAGTACATCATCTCCTCCGGAAAGTAACAACGGAAAGCTTGTA
NbAGO6    1.....................................................

NbAGOX    1.....................................................
NbAGO4  121CCCATGTCTAGGCGTGGCCTTGGAAGCAAGGGACAAAAGATTCCAATCCTTACCAATCAC
NbAGO5   47.....................................................
NbAGO1  537TTTCCACTCCGGCCAGGAAAGGGTAGTACTGGTATTAGATGCATAGTTAAGGCCAATCAC
NbAGO7    1.....................................................
NbAGO2  535CCTATTGCACGACCTGATACGGGAAAAGTTGCTGTCAAGTCAATTAGACTGCTTGCTAAT
NbAGO6    1.....................................................

NbAGOX    1.....................................................
NbAGO4  181TTTAAAGTGAACGTGTCTAATGTTGATGGACACTTCTTTCATTACAGCGTCGCCCT..AT
NbAGO5   47.....................................................
NbAGO1  597TTCTTTGCCGAGTTACCTGACAAAGATCTGCACCAGTATGATGTTTCAATTACTCCTGAG
NbAGO7    1.....................................................
NbAGO2  595CATTTTCCTGTTAGATTTAATCCTCAGTCTACCATTATGCATTATGATGTGGATATCAAG
NbAGO6    1.....................................................
```

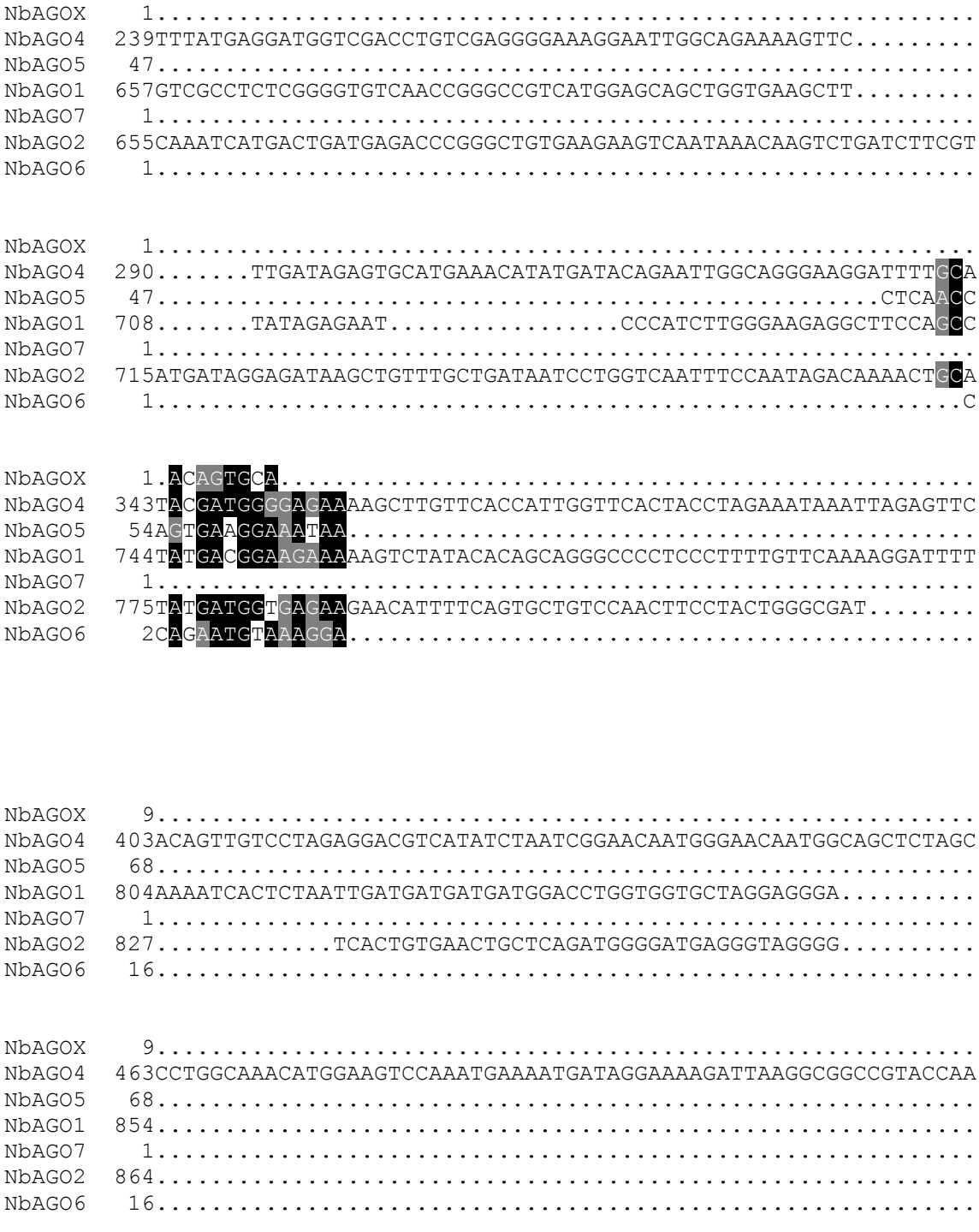
NbAGOX 1
NbAGO4 239TTTATGAGGATGGTCGACCTGTCGAGGGGAAAGGAATTGGCAGAAAAGTTC
NbAGO5 47
NbAGO1 657GTCGCCTCTCGGGGTGTCAACCGGGCCGTCATGGAGCAGCTGGTGAAGCTT
NbAGO7 1
NbAGO2 655CAAATCATGACTGATGAGACCCGGGCTGTGAAGAAGTCAATAAACAAGTCTGATCTTCGT
NbAGO6 1
NbAGOX 1
NbAGO4 290.....TTGATAGAGTGCATGAAACATATGATACAGAATTGGCAGGGAAGGATTTTGCA
NbAGO5 47.....CTCAACC
NbAGO1 708.....TATAGAGAAT.....CCCATCTTGGGAAGAGGCTTCCAGCC
NbAGO7 1
NbAGO2 715ATGATAGGAGATAAGCTGTTTGCTGATAATCCTGGTCAATTTCCAATAGACAAAACTGCA
NbAGO6 1.....C
NbAGOX 1.ACAGTGCA
NbAGO4 343TACGATGGGGAGAAAAGCTTGTTCACCATTGGTTCACTACCTAGAAATAAATTAGAGTTC
NbAGO5 54AGTGAAGGAAATAA
NbAGO1 744TATGACGGAAGAAAAAGTCTATACACAGCAGGGCCCCTCCCTTTTGTTCAAAAGGATTTT
NbAGO7 1
NbAGO2 775TATGATGGTGAGAAGAACATTTTCAGTGCTGTCCAACTTCCTACTGGGCGAT
NbAGO6 2CAGAATGTAAAGGA
NbAGOX 9
NbAGO4 403ACAGTTGTCCTAGAGGACGTCATATCTAATCGGAACAATGGGAACAATGGCAGCTCTAGC
NbAGO5 68
NbAGO1 804AAAATCACTCTAATTGATGATGATGATGGACCTGGTGGTGCTAGGAGGGA
NbAGO7 1
NbAGO2 827.....TCACTGTGAACTGCTCAGATGGGGATGAGGGTAGGGG
NbAGO6 16
NbAGOX 9
NbAGO4 463CCTGGCAAACATGGAAGTCCAAATGAAAATGATAGGAAAAGATTAAGGCGGCCGTACCAA
NbAGO5 68
NbAGO1 854
NbAGO7 1
NbAGO2 864
NbAGO6 16

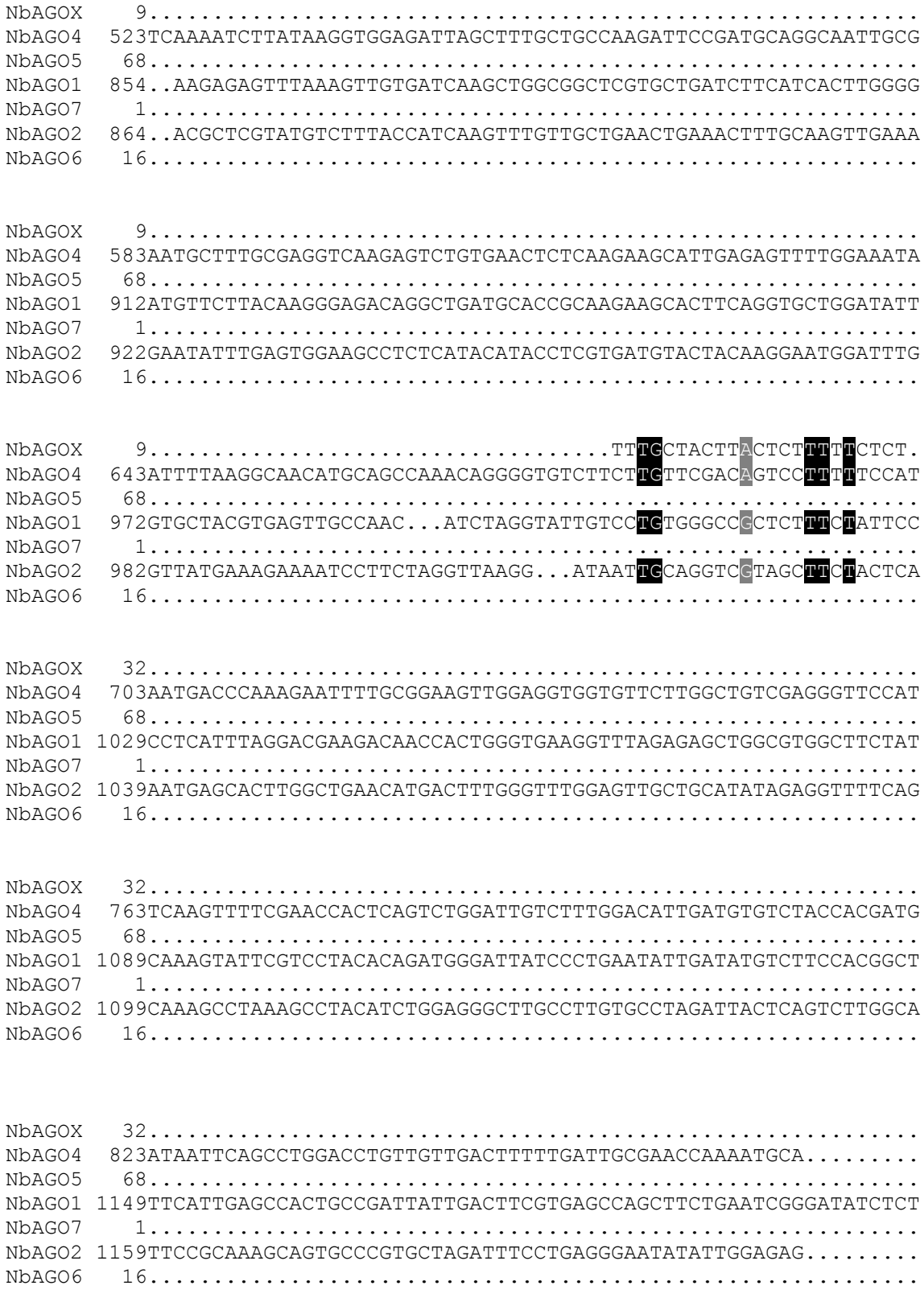
NbAGOX 9
NbAGO4 523TCAAAATCTTATAAGGTGGAGATTAGCTTTGCTGCCAAGATTCCGATGCAGGCAATTGCG
NbAGO5 68
NbAGO1 854..AAGAGAGTTTAAAGTTGTGATCAAGCTGGCGGCTCGTGCTGATCTTCATCACTTGGGG
NbAGO7 1
NbAGO2 864..ACGCTCGTATGTCTTTACCATCAAGTTTGTTGCTGAACTGAAACTTTGCAAGTTGAAA
NbAGO6 16
NbAGOX 9
NbAGO4 583AATGCTTTGCGAGGTCAAGAGTCTGTGAACTCTCAAGAAGCATTGAGAGTTTTGGAAATA
NbAGO5 68
NbAGO1 912ATGTTCTTACAAGGGAGACAGGCTGATGCACCGCAAGAAGCACTTCAGGTGCTGGATATT
NbAGO7 1
NbAGO2 922GAATATTTGAGTGGAAGCCTCTCATACATACCTCGTGATGTACTACAAGGAATGGATTTG
NbAGO6 16
NbAGOX 9.....TTTGCTACTTACTCTTTTTCTCT.
NbAGO4 643ATTTTAAGGCAACATGCAGCCAAACAGGGGTGTCTTCTTGTTCGACAGTCCTTTTTCCAT
NbAGO5 68
NbAGO1 972GTGCTACGTGAGTTGCCAAC...ATCTAGGTATTGTCCTGTGGGCCGCTCTTTCTATTCC
NbAGO7 1
NbAGO2 982GTTATGAAAGAAAATCCTTCTAGGTTAAGG...ATAATTGCAGGTCGTAGCTTCTACTCA
NbAGO6 16
NbAGOX 32
NbAGO4 703AATGACCCAAAGAATTTTGCGGAAGTTGGAGGTGGTGTTCTTGGCTGTCGAGGGTTCCAT
NbAGO5 68
NbAGO1 1029CCTCATTTAGGACGAAGACAACCACTGGGTGAAGGTTTAGAGAGCTGGCGTGGCTTCTAT
NbAGO7 1
NbAGO2 1039AATGAGCACTTGGCTGAACATGACTTTGGGTTTGGAGTTGCTGCATATAGAGGTTTTCAG
NbAGO6 16
NbAGOX 32
NbAGO4 763TCAAGTTTTCGAACCACTCAGTCTGGATTGTCTTTGGACATTGATGTGTCTACCACGATG
NbAGO5 68
NbAGO1 1089CAAAGTATTCGTCCTACACAGATGGGATTATCCCTGAATATTGATATGTCTTCCACGGCT
NbAGO7 1
NbAGO2 1099CAAAGCCTAAAGCCTACATCTGGAGGGCTTGCCTTGTGCCTAGATTACTCAGTCTTGGCA
NbAGO6 16
NbAGOX 32
NbAGO4 823ATAATTCAGCCTGGACCTGTTGTTGACTTTTTGATTGCGAACCAAAATGCA.....
NbAGO5 68
NbAGO1 1149TTCATTGAGCCACTGCCGATTATTGACTTCGTGAGCCAGCTTCTGAATCGGGATATCTCT
NbAGO7 1
NbAGO2 1159TTCCGCAAAGCAGTGCCCGTGCTAGATTTCCTGAGGGAATATATTGGAGAG.....
NbAGO6 16

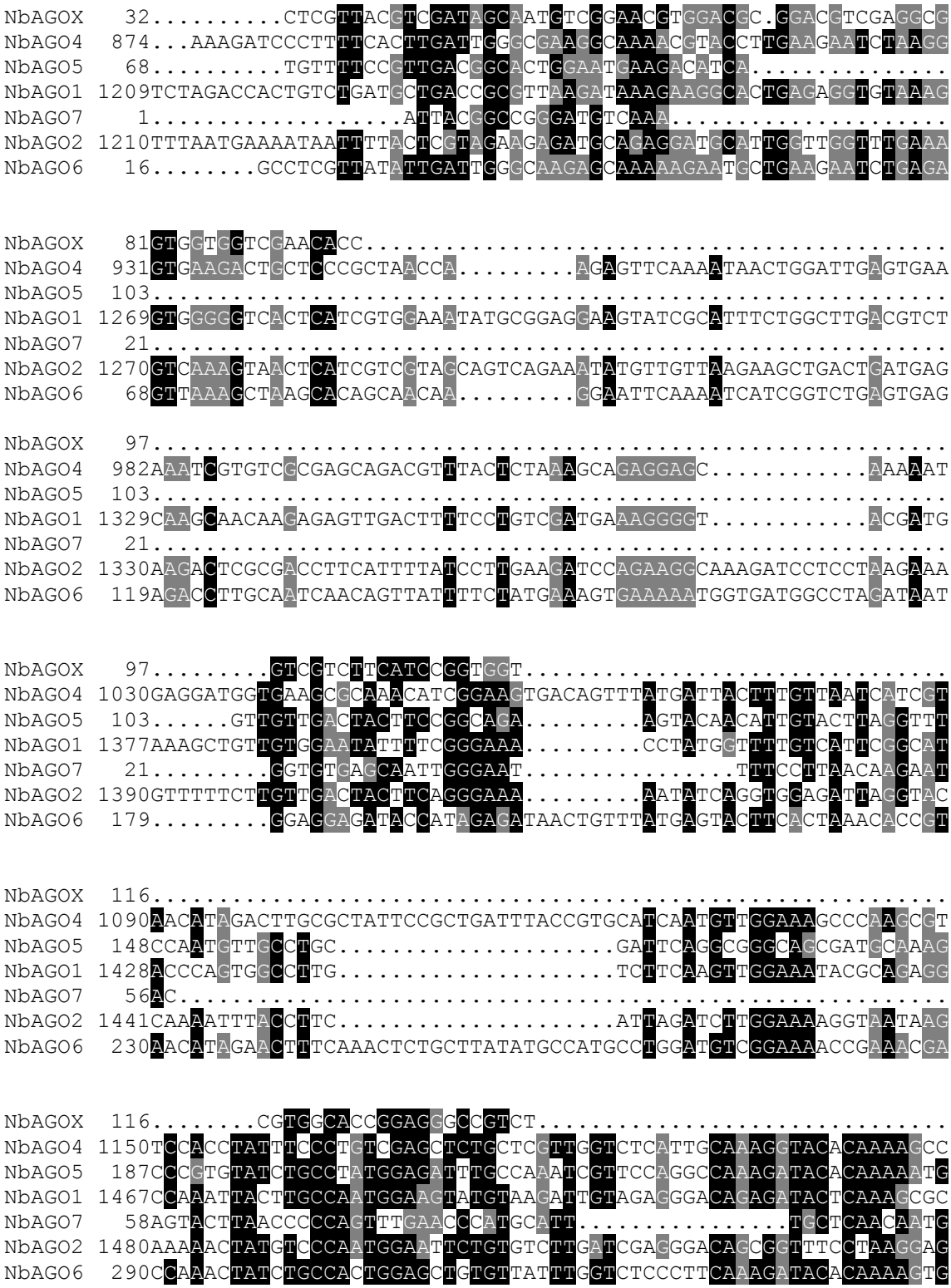
NbAGOX 32.....CTCGTTACGTCGATAGCAATGTCGGAACGTGGACGC.GGACGTCGAGGCG
NbAGO4 874...AAAGATCCCTTTTCACTTGATTGGGCGAAGGCAAAACGTACCTTGAAGAATCTAAGG
NbAGO5 68.....TGTTTTCCGTTGACGGCACTGGAATGAAGACATCA.....
NbAGO1 1209TCTAGACCACTGTCTGATGCTGACCGCGTTAAGATAAAGAAGGCACTGAGAGGTGTAAAG
NbAGO7 1.....ATTACGGCCGGGATGTCAAA.....
NbAGO2 1210TTTAATGAAAATAATTTTACTCGTAGAAGAGATGCAGAGGATGCATTGGTTGGTTTGAAA
NbAGO6 16.....GCCTCGTTATATTGATTGGGCAAGAGCAAAAAGAATGCTGAAGAATCTGAGA
NbAGOX 81GTGGTGGTCGAACACC.....
NbAGO4 931GTGAAGACTGCTCCCGCTAACCA.....AGAGTTCAAAATAACTGGATTGAGTGAA
NbAGO5 103.....
NbAGO1 1269GTGGGGGTCACTCATCGTGGAAATATGCGGAGGAAGTATCGCATTTCTGGCTTGACGTCT
NbAGO7 21.....
NbAGO2 1270GTCAAAGTAACTCATCGTCGTAGCAGTCAGAAATATGTTGTTAAGAAGCTGACTGATGAG
NbAGO6 68GTTAAAGCTAAGCACAGCAACAA.....CGAATTCAAAATCATCGGTCTGAGTGAG
NbAGOX 97.....
NbAGO4 982AAATCGTGTCGCGAGCAGACGTTTACTCTAAGCAGAGGAGC.....AAAAAT
NbAGO5 103.....
NbAGO1 1329CAAGCAACAAGAGAGTTGACTTTTCCTGTCGATGAAGGGGT.....ACGATG
NbAGO7 21.....
NbAGO2 1330AAGACTCGCGACCTTCATTTTATCCTTGAAGATCCAGAAGGCAAAGATCCTCCTAAGAAA
NbAGO6 119AGACCTTGCAATCAACAGTTATTTTCTATGAAAGTGAAAAATGGTGATGGCCTACATAAT
NbAGOX 97.....GTCGTCTTCATCCGGTGGT.....
NbAGO4 1030GAGGATGGTGAAGCGCAAACATCGGAAGTGACAGTTTATGATTACTTTGTTAATCATCGT
NbAGO5 103.....GTTGTTGACTACTTCCGGCAGA.....AGTACAACATTGTACTTAGGTTT
NbAGO1 1377AAAGCTGTTGTGGAATATTTTCGGGAAA.....CCTATGGTTTTGTCATTCGGCAT
NbAGO7 21.....GGTGTGAGCAATTGGGAAT.....TTTCCTTAACAAGAAT
NbAGO2 1390GTTTTTCTTGTTGACTACTTCAGGGAAA.....AATATCAGGTGGAGATTAGGTAC
NbAGO6 179.....GGAGGAGATACCATAGAGATAACTGTTTATGAGTACTTCACTAAACACCGT
NbAGOX 116.....
NbAGO4 1090AACATAGACTTGCGCTATTCCGCTGATTTACCGTGCATCAATGTTGGAAAGCCCAAGCGT
NbAGO5 148CCAATGTTGCCTGC.....GATTCAGGCGGGCAGCGATGCAAAG
NbAGO1 1428ACCCAGTGGCCTTG.....TCTTCAAGTTGGAAATACGCAGAGG
NbAGO7 56AC.....
NbAGO2 1441CAAAATTTACCTTC.....ATTAGATCTTGGAAAAGGTAATAAG
NbAGO6 230AACATAGAACTTTCAAACTCTGCTTATATGCCATGCCTGGATGTCGGAAAACCGAAACGA
NbAGOX 116.....CGTGGCACCGGAGGGCCGTCT.....
NbAGO4 1150TCCACCTATTTCCCTGTCGAGCTCTGCTCGTTGGTCTCATTGCAAAGGTACACAAAAGCC
NbAGO5 187CCCGTGTATCTGCCTATGGAGATTTGCCAAATCGTTCCAGGCCAAAGATACACAAAAATG
NbAGO1 1467CCAAATTACTTGCCAATGGAAGTATGTAAGATTGTAGAGGGACAGAGATACTCAAAGCGC
NbAGO7 58AGTACTTAACCCCAGTTTGAACCCATGCATT.....TGCTCAACAATG
NbAGO2 1480AAAAACTATGTCCCAATGGAATTCTGTGTCTTGATCGAGGGACAGCGGTTTCCTAAGGAG
NbAGO6 290CCAAACTATCTGCCACTGGAGCTGTGTTATTTGGTCTCCCTTCAAAGATACACAAAAGTG

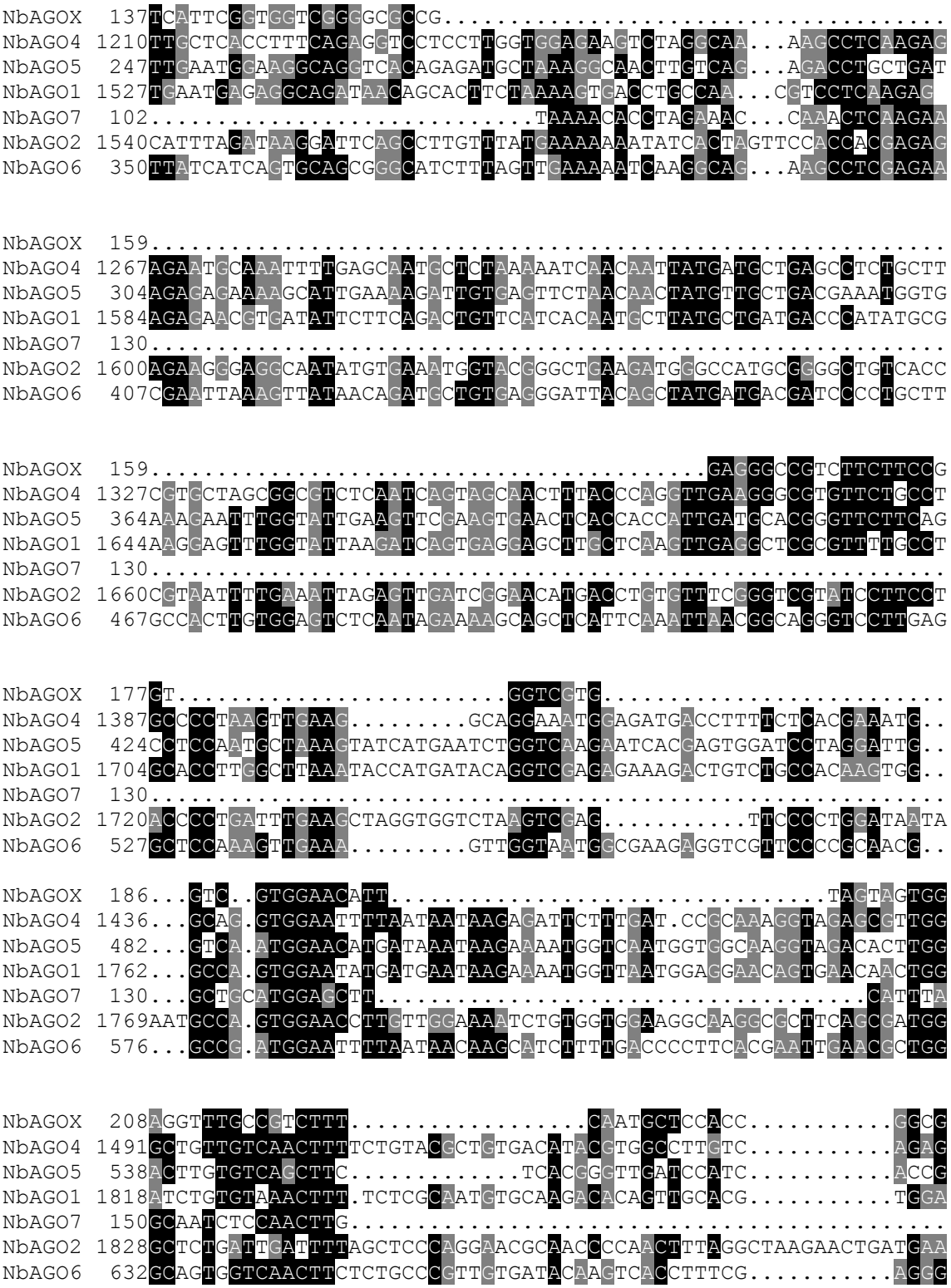
NbAGOX 137TCATTCGGTGGTCGGGGCGCCG
NbAGO4 1210TTGCTCACCTTTCAGAGGTCCTCCTTGGTGGAGAAGTCTAGGCAA...AAGCCTCAAGAG
NbAGO5 247TTGAATGGAAGGCAGGTCACAGAGATGCTAAAGCCAACTTGTCAG...AGACCTGCTGAT
NbAGO1 1527TGAATGAGAGGCAGATAACAGCACTTCTAAAACTGACCTGCCAA...CGTCCTCAAGAG
NbAGO7 102.....TAAAACACCTAGAAAC...CAAACTCAAGAA
NbAGO2 1540CATTTAGATAAGGATTCAGCCTTGTTTATGAAAAAAATATCACTAGTTCCACCACGAGAG
NbAGO6 350TTATCATCAGTGCAGCGGGCATCTTTAGTTGAAAAATCAAGGCAG...AAGCCTCGAGAA
NbAGOX 159
NbAGO4 1267AGAATGCAAATTTTGAGCAATGCTCTAAAAATCAACAATTATGATGCTGAGCCTCTGCTT
NbAGO5 304AGAGACAAAAGCATTGAAAAGATTGTGAGTTCTAACAACTATGTTGCTGACGAAATGGTG
NbAGO1 1584AGAGAACGTGATATTCTTCAGACTGTTCATCACAATGCTTATGCTGATGACCCATATGCG
NbAGO7 130
NbAGO2 1600AGAAGGAGGCAATATGTGAAATGGTACGGGCTGAAGATGGGCCATGCGGGGCTGTCACC
NbAGO6 407CGAATTAAAGTTATAACACGATGCTGTGAGGGATTACAGCTATGATGACGATCCCCTGCTT
NbAGOX 159.....GAGGGCCGTCTTCTTCCG
NbAGO4 1327CGTGCTAGCGGCGTCTCAATCAGTAGCAACTTTACCCAGGTTGAAGGGCGTGTTCTGCCT
NbAGO5 364AAAGAATTTGGTATTGAAGTTCGAAGTGAACTCACCACCATTGATGCACGGGTTCTTCAG
NbAGO1 1644AAGGAGTTTGGTATTAAGATCAGTGAGGAGCTTGCTCAAGTTGAGGCTCGCGTTTTGCCT
NbAGO7 130
NbAGO2 1660CGTAATTTTGAAATTAGAGTTGATCCGAAACATGACCTGTGTTTCGGGTCGTATCCTTCCT
NbAGO6 467GCCACTTGTGGAGTCTCAATAGAAAAGCAGCTCATTCAAATTAACGGCAGGGTCCTTGAG
NbAGOX 177GT.....GGTCGTG.....
NbAGO4 1387GCCCCTAAGTTGAAG.....GCAGGAAATGGAGATGACCTTTTCTCACGAAATG..
NbAGO5 424CCTCCAATGCTAAAGTATCATGAATCTGGTCAAGAATCACGAGTGGATCCTAGGATTG..
NbAGO1 1704GCACCTTGGCTTAAATACCATGATACAGGTCGAGAGAAAGACTGTCTGCCACAAGTGG..
NbAGO7 130
NbAGO2 1720ACCCCTGATTTGAAGCTAGGTGGTCTAAGTCCAG.....TTCCCCTGGATAATA
NbAGO6 527GCTCCAAAGTTGAAA.....GTTGGTAATGGCGAAGAGGTCGTTCCCCGCAACG..
NbAGOX 186...GTC..GTGGAACATT.....TACTAGTGG
NbAGO4 1436...GCAG.GTGGAATTTTAATAATAAGAGATTCTTTGAT.CCGCAAAGGTAGAGCGTTGG
NbAGO5 482...GTCA.ATGGAACATGATAAATAAGAAAATGGTCAATGGTGGCAAGGTAGACACTTGG
NbAGO1 1762...GCCA.GTGGAATATGATGAATAAGAAAATGGTTAATGGAGGAACAGTGAACAACTGG
NbAGO7 130...GCTGCATGGAGCTT.....CATTTA
NbAGO2 1769AATGCCA.GTGGAACCTTGTTGGAAAATCTGTGGTGGAAGGCAAGGCGCTTCAGCGATGG
NbAGO6 576...GCCG.ATGGAATTTTAATAACAAGCATCTTTTGACCCCTTCACGAATTGAACGCTGG
NbAGOX 208AGGTTTGCCGTCTTT.....CAATGCTCCACC.....GGCG
NbAGO4 1491GCTGTTGTCAACTTTTCTGTACGCTGTGACATACGTGGCCTTGTC.....AGAG
NbAGO5 538ACTTGTGTCAGCTTC.....TCACGGTTGATCCATC.....ACCG
NbAGO1 1818ATCTGTGTAAACTTT.TCTCGCAATGTGCAAGACACAGTTGCACG.....TGGA
NbAGO7 150GCAATCTCCAACTTG
NbAGO2 1828GCTCTGATTGATTTTAGCTCCCAGGAACGCAACCCCAACTTTAGGCTAAGAACTGATGAA
NbAGO6 632GCAGTGGTCAACTTCTCTGCCCGTTGTGATACAAGTCACCTTTCG.....AGGG

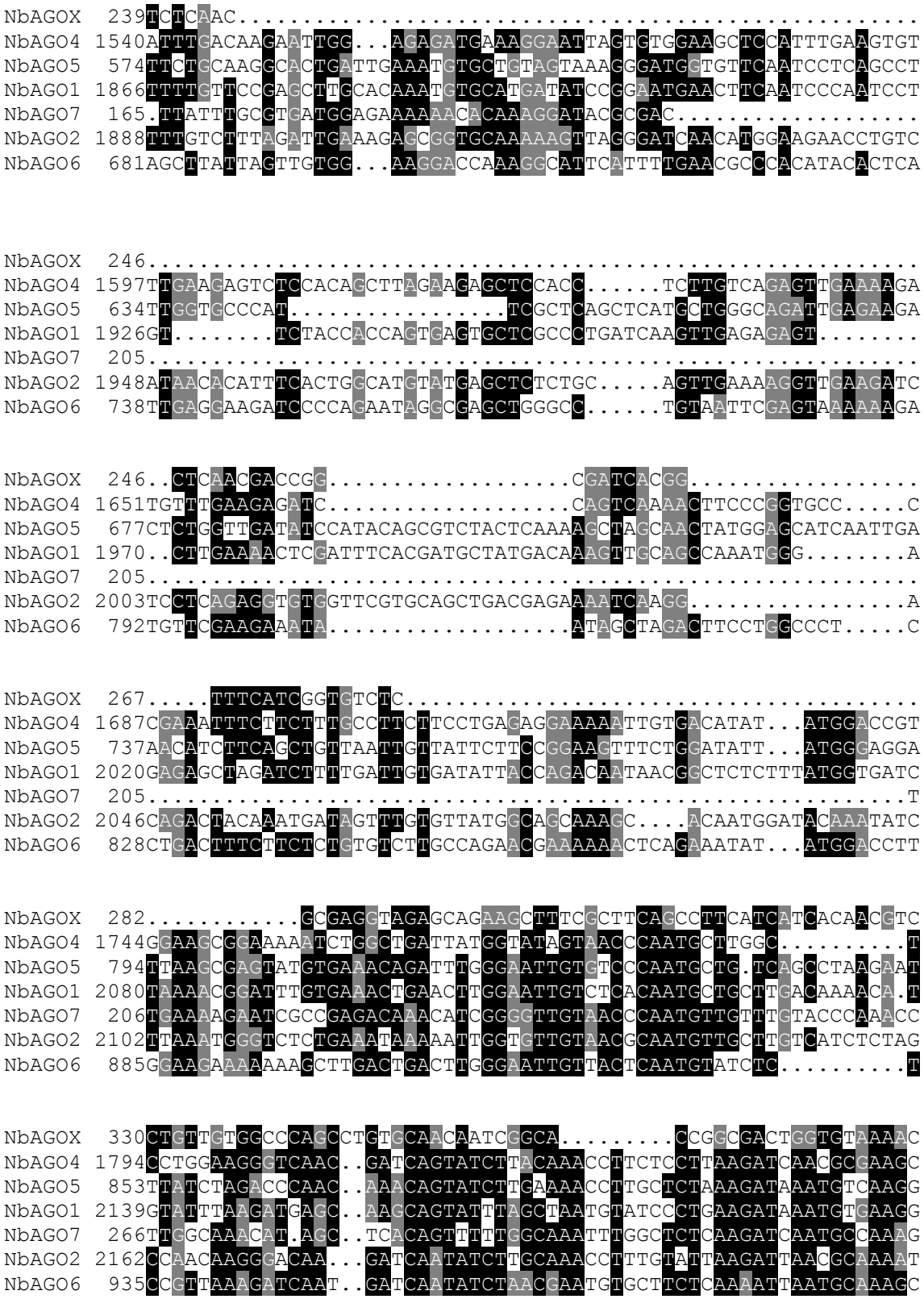
NbAGOX 239TCTCAAC
NbAGO4 1540ATTTCACAAGAATTGG...AGAGATGAAAGGAATTAGTGTGGAAGCTCCATTTGAAGTGT
NbAGO5 574TTCTCCAAGGCACTGATTGAAATGTGCTGTAGTAAAGGGATGGTGTTCAATCCTCAGCCT
NbAGO1 1866TTTTGTTCCGACCTTGCACAAATGTGCATGATATCCGGAATGAACTTCAATCCCAATCCT
NbAGO7 165.TTATTTGCGTCATGGAGAAAAACACAAAGGATACGCGAC
NbAGO2 1888TTTGTCTTTAGATTGAAAGAGCGGTGCAAAAAGTTAGGGATCAACATGGAAGAACCTGTC
NbAGO6 681AGCTTATTAGTTGTGG...AAGGACCAAAGGCATTCATTTTGAACGCCCACATACACTCA
NbAGOX 246
NbAGO4 1597TTGAAGAGTCTCCACAGCTTAGAAGAGCTCCACC......TCTTGTCAGAGTTGAAAAGA
NbAGO5 634TTGGTGCCCAT.....TCGCTCAGCTCATGCTGGGCAGATTGAGAAGA
NbAGO1 1926GT.....TCTACCACCAGTGAGTGCTCGCCCTGATCAAGTTGAGAGAGT.....
NbAGO7 205
NbAGO2 1948ATAACACATTTCACTGGCATGTATGAGCTCTCTGC.....AGTTGAAAAGGTTGAAGATC
NbAGO6 738TTGAGGAAGATCCCCAGAATAGGCGAGCTGGGCC.....TGTAATTCGAGTAAAAAAGA
NbAGOX 246..CTCAACGACCGG.....CGATCACGG.....
NbAGO4 1651TGTTTGAAGAGATC.....CAGTCAAAACTTCCCGGTGCC.....C
NbAGO5 677CTCTGGTTGATATCCATACAGCGTCTACTCAAAAGCTAGCAACTATGGAGCATCAATTGA
NbAGO1 1970..CTTGAAAACTCGATTTCACGATGCTATGACAAAGTTGCAGCCAAATGGG.....A
NbAGO7 205
NbAGO2 2003TCCTCAGAGGTGTGGTTCGTGCAGCTGACGAGAAAATCAAGG.....A
NbAGO6 792TGTTCGAAGAATA.....ATAGCTAGACTTCCTGGCCCT.....C
NbAGOX 267.....TTTCATCGGTGTCTC
NbAGO4 1687CGAAATTTCTTCTTTGCCTTCTTCCTGAGAGGAAAAATTGTGACATAT...ATGGACCGT
NbAGO5 737AACATCTTCAGCTGTTAATTGTTATTCTTCCGGAAGTTTCTGGATATT...ATGGGAGGA
NbAGO1 2020GAGAGCTAGATCTTTTGATTGTGATATTACCAGACAATAACGGCTCTCTTTATGGTGATC
NbAGO7 205.....T
NbAGO2 2046CAGACTACAAATGATAGTTTGTGTTATGGCAGCAAAGC....ACAATGGATACAAATATC
NbAGO6 828CTGACTTTCTTCTCTGTGTCTTGCCAGAACGAAAAAACTCAGAAATAT...ATGGACCTT
NbAGOX 282.....GCGAGGTAGAGCAGAAGCTTTCGCTTCAGCCTTCATCATCACAACGTC
NbAGO4 1744GGAACCGGAAAAATCTGGCTGATTATGGTATAGTAACCCAATGCTTGGC.....T
NbAGO5 794TTAAGCGAGTATGTGAAACAGATTTGGGAATTGTGTCCCAATGCTG.TCAGCCTAAGAAT
NbAGO1 2080TAAAACGGATTTGTGAAACTGAACTTGGAATTGTCTCACAATGCTGCTTGACAAAACA.T
NbAGO7 206TGAAAAGAATCGCCGAGACAAACATCGGGGTTGTAACCCAATGTTGTTTGTACCCAAACC
NbAGO2 2102TTAAATGGGTCTCTGAAATAAAAATTGGTGTTGTAACGCAATGTTGCTTGTCATCTCTAG
NbAGO6 885GGAACAAAAAAAGCTTGACTGACTTGGGAATTGTTACTCAATGTATCTC.....T
NbAGOX 330CTGTTGTGGCCCAGCCTGTGCAACAATCGGCA.....CCGGCGACTGGTGTAAAAC
NbAGO4 1794CCTGGAAGGGTCAAC..GATCAGTATCTTACAAACCTTCTCCTTAAGATCAACGCGAAGC
NbAGO5 853TTATCTAGACCCAAC..AAACAGTATCTTGAAAACCTTGCTCTAAAGATAAATGTCAAGG
NbAGO1 2139GTATTTAAGATGAGC..AAGCAGTATTTAGCTAATGTATCCCTGAAGATAAATGTGAAGG
NbAGO7 266TTGGCAAACAT.AGC..TCACAGTTTTTGGCAAATTTGGCTCTCAAGATCAATGCCAAAG
NbAGO2 2162CCAACAAGGGACAA...GATCAATATCTTGCAAACCTTTGTATTAAGATTAACGCAAAAT
NbAGO6 935CCGTTAAAGATCAAT..GATCAATATCTAACGAATGTGCTTCTCAAAATTAATGCAAAGC


NbAGOX 381C.GCTACAGCCCCCGCCGCCGTCCTCGAAAAGCATTCAGGTT.....CCTAA
NbAGO4 1852TTGGTGGTTTAAATTCTGTGTTAGCTATTGAGGCATTCACCTTCCATTCC.....CATGG
NbAGO5 911TGGGTGGAAGAAACTCTGTCCTGGAGCAGGCAGTTCATACAAGAATACC.....TTTCC
NbAGO1 2197TTGGAGGAAGAAATACTGTGCTGGTTGATGCGCTCTCTACACGAATTCC.....CCTTG
NbAGO7 323TTGGGGGATGCACAGTTGCATTGTACAGTTCATTGCCTTCTCAAATACCACGGCTCTTCA
NbAGO2 2219TGGGAGGTAGCAATATGGAACTTACGGGAAGGCTCCCTAA.....TTTTG
NbAGO6 993TTGGAAGGACCAATTCATTGTTGGCTATGGAACATGCATCTTATCTGCC.....GCATA
NbAGOX 427TAGACCGGGATACGGAACTGTT.....GGACGGAAGTGCCTTATA.....AGAGCAAA
NbAGO4 1906TATCTAAGGTTCCCACCATGATTCTTGGAATGGACGTATCACATGGCTCTCCTGGCCAGT
NbAGO5 965TCACTGATATCCCCACAATTGTCTTTGGTGCTGATGTGACACATCCACAACCAGGAGAAG
NbAGO1 2251TCAGCGACCGCCCAACTATCATTTTTGGTGCAGATGTCACCCATCCCCACCCTGGGGAGG
NbAGO7 383AGCACGATGGTCCGGTTATTTTTATGGGTGCGGACGTGACTCATCCACACCCACTTGATG
NbAGO2 2264GAGGTGAAGATAATGTGATGTTCATTGGAGCTGATGTTAATCATCCTGCTGCAAGGAATG
NbAGO6 1047TTCAGGAAACTCCAACAATGATTCTGGGCATGGATGTCTCTCATGGATCTCCTGGTCAAT
NbAGOX 475TCATTTTCTCGTTCAT.....GTTGCTGATCGGGATCTGC.....ATCACT
NbAGO4 1966CTGATGTTCCATCAATTGCTGCAGTTGTAAGTTCAAGGCAGTGGCCTTCAATATCTCGTT
NbAGO5 1025ATTCTAGTCCATCTATAGCTGCTGTAGTCGCTTCAATGGATTGGCCTGAAGTGAGTCAAT
NbAGO1 2311ATTCTAGCCCGTCAATTGCTGCGGTGGTTGCTTCTCAAGATTGGCCTGAAATTACAAAGT
NbAGO7 443ATTCTAGCCCCTCGGTTGCTGCTGTAGTTGGTAATGTGAATTGGCCAGCAGCCAACAAGT
NbAGO2 2324TGACATCTCCATCTATAACAGCTGTTGTTGGCACTGTCAACTGGCCAGCCGCTAATAGAT
NbAGO6 1107CAGATATTCCATCAATTGCTGCGGTTGTGGGATCCTTATATTGGCCATTAATATCCAAGT
NbAGOX 516ATGATGTTACAATCTCTCCAGAGGTTC.TGTCAAAGAAAGTATG.....
NbAGO4 2026ATAGAGCTTCTGTGCGCACTCAATCTCCTAAAGTGGAGATGATTGATAACTTATTTAAAA
NbAGO5 1085ATAGGTGTCTTGTTTCTGCACAACCCCACAGGAAAGAGATCATTGAGGACTTGTATCAAA
NbAGO1 2371.TGCTGGTTTGGTTTCTGCTCAAGCGCATAGGCAAGAGCTTATACAAGATCTGTACAAGA
NbAGO7 503ATGTCTCCAGAATGAGGTCCCAAACACATAGGCAGGAGATCATTCAAGATCT.....
NbAGO2 2384ATGCGGCTAGAGTTTGTCCTCAGGACCACAGGACTGAGAAGATACTAAATTT.....
NbAGO6 1167ACAGGGCAGTTGTCCGTAATCAATCTCCAAAGTTAGAAATTATAGAATCCTTATACAAGC
NbAGOX 559.....CAGAGAGATTATGAGCCAGCTAGTTAATG
NbAGO4 2086AAGTTTCAGACACTGAGGA.....TGATGGGATTATGAGGGAACTTTTGCTAG
NbAGO5 1145AGCACGTAGATGCTAAAAAAGGGATTGTTCATGGCGGAATGATAAGGGAGTTACTGATTG
NbAGO1 2430CTTGGCAAGATCCAGTTAGAGGACCTGTGACTGGTGGCATGATAAAGGAATTACTTATTT
NbAGO7 555.....CAGCACAATGATCGGGGAAATTCTTGATG
NbAGO2 2436.....TGGGAGCATGTGTGCAGACCTACTGAATG
NbAGO6 1227CTTTACCAAATGGAGACAA.....TGAAAGAATCATGGGAGAAATTCTTCTGG
NbAGOX 588ACTATAAACAGTCACACATGGG.....TGGTCGGAATTTAGCATATGATGGCGGGA
NbAGO4 2134ATTTTTATGTGGGTTCCGGGAAAAGGAAGCCTGAGCATATTGTAATATTCAGGGATGGTG
NbAGO5 1205CGTTT...CGAAGATCTACAGGGATTAAGCCTGGTAGAATTATCTTTTATAGAGATGGAG
NbAGO1 2490CCTTCCGTCGAGCAACT...GGACAGAAGCGGCAGAGAATTATATTCTACAGAGATGGTG
NbAGO7 584ATTTCTA.CGAGGAGCTTCTAAAACTC..CCCGAGCGAATAATCTTCTTCAGGGATGGAG
NbAGO2 2465CTTACACTCTACTCAACTCGG...TTAAACCAAACAGAATTGTTGTTTTCCGTGATGGTG
NbAGO6 1275ACTTCTA.....


NbAGOX 639AGAGTGTTTACACTGCTGGGCCTCTCCCATTCTCCTCCAAGGACT.....
NbAGO4 2194TCAGTG.....AATCTCAATTTAATCAAGTTCTAAACATTGAATTGGACCAGCTCATTGA
NbAGO5 1262TGAGCG.....AAGGTCAATTCAATCAGGTTTTATTGGAAGAAATGGACGCAATCCGCAA
NbAGO1 2547TTAGTG.....AAGGACAATTTTACCAAGTTCTTCTTTTTGAACTTGATGCAATCCGCAA
NbAGO7 641TAAGTG.....AAACTCAGTTCTTGAAAGTACTTAAAGAAGAGCTACAAGCAATTCGTGC
NbAGO2 2522TGAGTG.....AGGGCCAATTTGATATGGTACTTAATGAAGAGCTGGTTGATTTGATGAA
NbAGO6 1282.....
NbAGOX 684.....TCATTATCAAGCTA.GATGGTAATAGTGGTGGAGCAAAG
NbAGO4 2249GGCCTGCAAATTTCTTGATGAGAAGTGGTCACCGAAGTTTGTGATCATTGTTGCTCAGAA
NbAGO5 1317GGCATGCACATCCTTGGAAGAAGGTTATCTGCCACGAGTTACCTTTGTGGTAGTGCAGAA
NbAGO1 2602GGCATGTGCATCTTTAGAACCCAACTATCAGCCCCCGGTTACGTTTGTTGTGGTCCAGAA
NbAGO7 696AGCATGTTCGAGATT...TCCAGGTTACAAACCTCCCATTACTTTCGTGGTCGTTCAGAA
NbAGO2 2577GGCT.....ATATACGATGATCACTATCGACCAGCAATCACTCTTGTTGTGGCTCAGAA
NbAGO6 1282.....
NbAGOX 722AGGCAA.....AGAGAGTTT.....
NbAGO4 2309AAATCATCATACAAAGTTTTTCCAGGCTGGATCT.....
NbAGO5 1377GAGACACCATACACGTCTGTTCCCTGTTAATCATAACGATCGTAATATGACGGACAAG..
NbAGO1 2662ACGGCATCATACTAGGTTGTTTGCCAATAACCACCACGACAGAAATGCAGTTGATCGG..
NbAGO7 753AAGGCATCATACTCGGCTATTTCCATGTGAACTTGATCCGTCGTCAACTAGAAACCAGTT
NbAGO2 2631AAGACACCATACACGACTATTTCCTCATGGTGGC.....
NbAGO6 1282.....
NbAGOX 737.....AAGTCTCTATCAAGT....TTGCTGCCAAAGCTGATCTTCATCACTGAAC
NbAGO4 2343....CCTGATAATGTTCCTCCAGGGACAATCATAGACAACAAAGTTTGTCATCCAAGGAA
NbAGO5 1435....AGTGGAAACATTCTGCCAGGTACTGTTGTTGATACCAAGATTTGCCACCCTATGGA
NbAGO1 2720....AGTGGGAACATTTTGCCTGGTACCGTTGTAGATTCAAAGATATGCCACCCTACGAA
NbAGO7 813CTTTAATGAAAACATCGCACCAGGTACAGTTGTTGATAGTGTGATCACACATCCAAGAGA
NbAGO2 2665....CCTGGCAATGTACCTCCGGGTACTGTTGTGGACACAGTAATTGTTCATCCATCTGA
NbAGO6 1282.....
NbAGOX 783AGTCTGCATGTAGCATCGATGCCCCGCAGAA.....
NbAGO4 2399CTATGACTTCTACCTGTGTGCCCATGCAGGCATGATTGGTACCACTCGACCTACACATTA
NbAGO5 1491GTTTGATTTT.....
NbAGO1 2776.TTTGATTTCTATCTCTGTAGCCATGCCGGCATACAGGGTACTAGCCGCCCAGCTCATTA
NbAGO7 873ATTTGACTTCTATCTGTGCAGTCA.....
NbAGO2 2721TTTTGACTTCTATCTTTGCAGCCATTTTGGAGGATTGGGAACTAGCAAGCCTACTCACTA
NbAGO6 1282.TATGACATGTAAC.....GGCCAT.....
NbAGOX .....
NbAGO4 2459CCATGTGTTGTTGGATGAAGTTGGTTTTTCACCTGATGATCTTCAAGACCTTGTTCATAA
NbAGO5 .....
NbAGO1 2835TCATGTTCTGTGGGATGAGAACAATTTTACTGCTGACGCCCTGCAGTCTTTGACTAACAA
NbAGO7 .....
NbAGO2 2781TCATGTTTTGTGGGATGAGAATGGCTTCAATTCTGACCGCTTACAGAAGCTTATATACAA
NbAGO6 .....

```
NbAGOX     ............................................................
NbAGO4 2519TCTGTCCTATGTATATCAAAGAAGCACTACTGCTATATCCATTGTGGCTCCGGTAAGTTA
NbAGO5     ............................................................
NbAGO1 2895TCTTTGCTATACATATGCTAGGTGTACTCGTTCTGTCTCCATTGTTCCACCAGCATATTA
NbAGO7     ............................................................
NbAGO2 2841CATGTGCTTCACCTTCGCGCGGTGCACAAAACCTGTTTCACTTGTTCCACCAGTTTACTA
NbAGO6     ............................................................


NbAGOX     ............................................................
NbAGO4 2579TGCCCATTTGGCCGCCACACAAGTTGGACAAT..................GGATGAAGTT
NbAGO5     ............................................................
NbAGO1 2955TGCACATTTGGCAGCTTTCCGTGCTCGGTTTT..................ACATGGAGCC
NbAGO7     ............................................................
NbAGO2 2901TGCTGACCTTGTTGCCTACCGGGGACGGATGTTCCAAGAGGTGCTTATGGAGATGCAGTC
NbAGO6     ............................................................


NbAGOX     ............................................................
NbAGO4 2621CGAGGACGCATCAGAGACATCGTC.....................................
NbAGO5     ............................................................
NbAGO1 2997AGAGACATCTGATAATGGATCAGTCACAAGCGCAGCTGCTTCAAACAAGGAGGTTTAGGA
NbAGO7     ............................................................
NbAGO2 2961TCCTGCATCTTCAACTGCATCCTTCACAACTTCATCGTCATCTTCTTCAACTACCTCATT
NbAGO6     ............................................................


NbAGOX     ............................................................
NbAGO4 2645........AAGCCATGGTGGTCTGACAAGTGCTGGTCCAGTTACTGTTCCTCAGTTGCCT
NbAGO5     ............................................................
NbAGO1 3057GCTATGGGAAGGAGCACGCGAGCACCAGGTGCTGGTGCTGCTGTAAGGCCCC....TTCC
NbAGO7     ............................................................
NbAGO2 3021TGAACAAGGATTCTTTAAATTGCACCATGAGCTGCAGAACATAATGTTCTTTGTCTGAGG
NbAGO6     ............................................................


NbAGOX      ....................................
NbAGO4 2697 CGACTTCAGGAAAATGTTTCTAGTTCCATGTTCTTCTGT
NbAGO5      ....................................
NbAGO1 3113 TGCTCTCAAGGAGAATGTTAGAGGGTTATGTTTTATTGT
NbAGO7      ....................................
NbAGO2 3081 ATCCTGA.............................
NbAGO6      ....................................
```

Appendix Figure A.3 Original and averaged C_t values used in the calculation of qRT PCR individual primer efficiencies

	Template Concentration	ORIGINAL CT VALUES																							
		qrt ACTIN			NbAGO1			NbAGO2			NbAGO4			NbAGO5			NbAGO6			NbAGO7			NbAGOX		
	1	23.2	22.9	22.8	21.3	21.2	21.2	24.3	24.6	24.6	22.9	23	22.8	25.8	25.8	25.7	27.6	27.5	27.6	22.1	22.2	22.2	21.8	22.1	21.9
	0.5	24	23.8	23.5	22.2	22	21.9	25.4	25.1	25.3	23.7	23.7	23.6	26.4	26.6	26.7	28.1	28.1	28.1	22.6	22.8	22.8	22.6	22.7	22.7
	0.25	24.6	24.7	24.7	22.7	22.6	22.6	26.2	26.2	26.5	24.3	24.4	24.6	27.6	27.5	27.5	29.3	29.2	29.4	24.3	24.3	24.3	24	23.9	23.4
	0.125	25.9	25.9	25.8	24.1	23.9	24	27.5	27	27.1	25.2	25.1	25.2	28.3	28.1	28.1	30.3	30.1	30.2	24.8	24.8	24.9	24.7	25	24.4
	0.065	26.5	26.8	26.6	24.5	24.6	24.4	26.8	26.9	31.4	25.3	25.6	25.6	29.4	29.2	29	31	31.1	31	25.6	25.7	25.8	25.5	25.6	27.2

	Log base 10 (concentration	CT AVERAGES							
		qrt ACTIN	NbAGO1	NbAGO2	NbAGO4	NbAGO5	NbAGO6	NbAGO7	NbAGOX
1	0.0000	23.0	21.2	24.5	22.9	25.8	27.6	22.2	22.0
0.5	-0.3010	23.8	22.0	25.3	23.7	26.6	28.1	22.7	22.7
0.25	-0.6021	24.7	22.6	26.3	24.4	27.5	29.3	24.3	23.8
0.125	-0.9031	25.9	24.0	27.2	25.2	28.2	30.2	24.8	24.7
0.0625	-1.1871	26.6	24.5	28.4	25.5	29.2	31.0	25.7	26.1

Appendix Figure A.4. C_t values obtained from qRT PCR in the determination of the distribution of specific *AGOs* in 3 and 8 week old *N. benthamiana* tissues

ORGINAL CT VALUES

	3WK LEAF			3WK STEM			3WK ROOT			8WK LEAF			8WK STEM			8WK ROOT		
ACTIN	17.8	17.4	17.3	18.3	18.3	18.2	18	17.8	17.9	20.6	20.6	20.7	18.5	18	18	18.9	18.9	18.8
	25.4	25	25.7	23.7	23.3	23.3	24.1	24.7	24.8	24.4	24.4	24.5	22.2	22.4	22.2	23	22.9	22.9
AGO1	29	29	28.8	25.8	25.8	25.6	25	25.1	25.4	26.8	26.8	27	23.9	23.8	23.5	23.8	23.8	23.9
AGO2	21.1	21.2	21.1	20.3	20.4	20.3	20.9	21.1	21.1	23.4	23.6	23.6	21.3	21	21	22.1	22.1	22.1
AGO4	29.1	29.6	29.5	25.1	24.9	25	23.7	23.6	23.6	30.2	29.6	30	23.6	23.7	23.6	24.1	24	23.9
AGO5	32.6	33.1	33.4	28.7	29.6	28.8	29.1	29	29	31.4	31.6	31.5	28.2	28.3	28.3	28.9	29	28.9
AGO6	33.3	33.9	33.8	28.1	27.9	27.9	29.6	29.4	29.4	31.5	31.2	31.9	27.4	27.2	27.4	28.4	28.2	28.3
AGO7	33.2	33.2	33.1	28.2	27.8	28	27.2	27.2	27.2	32.6	32.4	32.4	26.2	26.1	25.8	25.7	25.7	25.9
AGOX																		

Appendix Figure A.5. Identification number and combinations of TRV-AGO constructs used to silence multiple *NbAGO* genes using the TRV VIGS system

ID#	7 Knockouts Combinations						
1	NbAGO-1	NbAGO-2	NbAGO-4	NbAGO-5	NbAGO-6	NbAGO-7	NbAGO-X

ID#	6 Knockout Combinations						
2		NbAGO-2	NbAGO-4	NbAGO-5	NbAGO-6	NbAGO-7	NbAGO-X
3	NbAGO-1		NbAGO-4	NbAGO-5	NbAGO-6	NbAGO-7	NbAGO-X
4	NbAGO-1	NbAGO-2		NbAGO-5	NbAGO-6	NbAGO-7	NbAGO-X
5	NbAGO-1	NbAGO-2	NbAGO-4		NbAGO-6	NbAGO-7	NbAGO-X
6	NbAGO-1	NbAGO-2	NbAGO-4	NbAGO-5		NbAGO-7	NbAGO-X
7	NbAGO-1	NbAGO-2	NbAGO-4	NbAGO-5	NbAGO-6	NbAGO-7	NbAGO-X
8	NbAGO-1	NbAGO-2	NbAGO-4	NbAGO-5	NbAGO-6		NbAGO-X
9	NbAGO-1	NbAGO-2	NbAGO-4	NbAGO-5	NbAGO-6	NbAGO-7	

ID#	5 Knockout Combinations						
10			NbAGO-4	NbAGO-5	NbAGO-6	NbAGO-7	NbAGO-X
11		NbAGO-2		NbAGO-5	NbAGO-6	NbAGO-7	NbAGO-X
12		NbAGO-2	NbAGO-4		NbAGO-6	NbAGO-7	NbAGO-X
13		NbAGO-2	NbAGO-4	NbAGO-5		NbAGO-7	NbAGO-X
14		NbAGO-2	NbAGO-4	NbAGO-5	NbAGO-6		NbAGO-X
15		NbAGO-2	NbAGO-4	NbAGO-5	NbAGO-6	NbAGO-7	
16	NbAGO-1			NbAGO-5	NbAGO-6	NbAGO-7	NbAGO-X
17	NbAGO-1		NbAGO-4		NbAGO-6	NbAGO-7	NbAGO-X
18	NbAGO-1		NbAGO-4	NbAGO-5		NbAGO-7	NbAGO-X
19	NbAGO-1		NbAGO-4	NbAGO-5	NbAGO-6		NbAGO-X
20	NbAGO-1		NbAGO-4	NbAGO-5	NbAGO-6	NbAGO-7	
21	NbAGO-1	NbAGO-2			NbAGO-6	NbAGO-7	NbAGO-X
22	NbAGO-1	NbAGO-2		NbAGO-5		NbAGO-7	NbAGO-X
23	NbAGO-1	NbAGO-2		NbAGO-5	NbAGO-6		NbAGO-X
24	NbAGO-1	NbAGO-2		NbAGO-5	NbAGO-6	NbAGO-7	
25	NbAGO-1	NbAGO-2	NbAGO-4			NbAGO-7	NbAGO-X
26	NbAGO-1	NbAGO-2	NbAGO-4		NbAGO-6		NbAGO-X
27	NbAGO-1	NbAGO-2	NbAGO-4		NbAGO-6	NbAGO-7	
28	NbAGO-1	NbAGO-2	NbAGO-4	NbAGO-5			NbAGO-X
29	NbAGO-1	NbAGO-2	NbAGO-4	NbAGO-5		NbAGO-7	
30	NbAGO-1	NbAGO-2	NbAGO-4	NbAGO-5	NbAGO-6		

ID#	4 Knockout Combinations						
31				NbAGO-5	NbAGO-6	NbAGO-7	NbAGO-X
32			NbAGO-4		NbAGO-6	NbAGO-7	NbAGO-X
33			NbAGO-4	NbAGO-5		NbAGO-7	NbAGO-X
34			NbAGO-4	NbAGO-5	NbAGO-6		NbAGO-X
35			NbAGO-4	NbAGO-5	NbAGO-6	NbAGO-7	
36		NbAGO-2			NbAGO-6	NbAGO-7	NbAGO-X
37		NbAGO-2		NbAGO-5		NbAGO-7	NbAGO-X
38		NbAGO-2		NbAGO-5	NbAGO-6		NbAGO-X
39		NbAGO-2		NbAGO-5	NbAGO-6	NbAGO-7	
40		NbAGO-2	NbAGO-4			NbAGO-7	NbAGO-X
41		NbAGO-2	NbAGO-4		NbAGO-6		NbAGO-X
42		NbAGO-2	NbAGO-4		NbAGO-6	NbAGO-7	
43		NbAGO-2	NbAGO-4	NbAGO-5			NbAGO-X
44		NbAGO-2	NbAGO-4	NbAGO-5		NbAGO-7	
45		NbAGO-2	NbAGO-4	NbAGO-5	NbAGO-6		
46	NbAGO-1				NbAGO-6	NbAGO-7	NbAGO-X
47	NbAGO-1				NbAGO-6	NbAGO-7	NbAGO-X
48	NbAGO-1			NbAGO-5		NbAGO-7	NbAGO-X
49	NbAGO-1			NbAGO-5	NbAGO-6		NbAGO-X
50	NbAGO-1			NbAGO-5	NbAGO-6	NbAGO-7	
51	NbAGO-1		NbAGO-4			NbAGO-7	NbAGO-X
52	NbAGO-1		NbAGO-4		NbAGO-6		NbAGO-X
53	NbAGO-1		NbAGO-4		NbAGO-6	NbAGO-7	
54	NbAGO-1		NbAGO-4	NbAGO-5			NbAGO-X
55	NbAGO-1		NbAGO-4	NbAGO-5		NbAGO-7	
56	NbAGO-1		NbAGO-4	NbAGO-5	NbAGO-6		
57	NbAGO-1	NbAGO-2				NbAGO-7	NbAGO-X
58	NbAGO-1	NbAGO-2			NbAGO-6		NbAGO-X
59	NbAGO-1	NbAGO-2			NbAGO-6	NbAGO-7	
60	NbAGO-1	NbAGO-2		NbAGO-5			NbAGO-X
61	NbAGO-1	NbAGO-2		NbAGO-5		NbAGO-7	
62	NbAGO-1	NbAGO-2	NbAGO-4				NbAGO-X
63	NbAGO-1	NbAGO-2	NbAGO-4			NbAGO-7	
64	NbAGO-1	NbAGO-2	NbAGO-4		NbAGO-6		
65	NbAGO-1	NbAGO-2	NbAGO-4	NbAGO-5			

ID#	3 Knockout Combinations						
66	NbAGO-1	NbAGO-2	NbAGO-4				
67	NbAGO-1	NbAGO-2		NbAGO-5			
68	NbAGO-1	NbAGO-2			NbAGO-6		
69	NbAGO-1	NbAGO-2				NbAGO-7	
70	NbAGO-1	NbAGO-2					NbAGO-X
71	NbAGO-1		NbAGO-4	NbAGO-5			
72	NbAGO-1		NbAGO-4		NbAGO-6		
73	NbAGO-1		NbAGO-4			NbAGO-7	
74	NbAGO-1		NbAGO-4				NbAGO-X
75	NbAGO-1			NbAGO-5	NbAGO-6		
76	NbAGO-1			NbAGO-5		NbAGO-7	
77	NbAGO-1			NbAGO-5			NbAGO-X
78	NbAGO-1				NbAGO-6	NbAGO-7	
79	NbAGO-1					NbAGO-7	NbAGO-X
80		NbAGO-2	NbAGO-4	NbAGO-5			
81		NbAGO-2	NbAGO-4		NbAGO-6		
82		NbAGO-2	NbAGO-4			NbAGO-7	
83		NbAGO-2	NbAGO-4				NbAGO-X
84		NbAGO-2		NbAGO-5	NbAGO-6		
85		NbAGO-2		NbAGO-5		NbAGO-7	
86		NbAGO-2		NbAGO-5			NbAGO-X
87		NbAGO-2			NbAGO-6	NbAGO-7	
88		NbAGO-2			NbAGO-6		NbAGO-X
89		NbAGO-2				NbAGO-7	NbAGO-X
90			NbAGO-4	NbAGO-5	NbAGO-6		
91			NbAGO-4	NbAGO-5		NbAGO-7	
92			NbAGO-4	NbAGO-5			NbAGO-X
93			NbAGO-4		NbAGO-6	NbAGO-7	
94	NbAGO-1	NbAGO-2	NbAGO-4		NbAGO-6		NbAGO-X
95			NbAGO-4			NbAGO-7	NbAGO-X
96				NbAGO-5	NbAGO-6	NbAGO-7	
97				NbAGO-5	NbAGO-6		NbAGO-X
98					NbAGO-6	NbAGO-7	NbAGO-X

ID#	2 Knockout Combinations						
99	NbAGO-1	NbAGO-2					
100	NbAGO-1		NbAGO-4				
101	NbAGO-1			NbAGO-5			
102	NbAGO-1				NbAGO-6		
103	NbAGO-1					NbAGO-7	
104	NbAGO-1						NbAGO-X
105		NbAGO-2	NbAGO-4				
106		NbAGO-2		NbAGO-5			
107		NbAGO-2			NbAGO-6		
108		NbAGO-2				NbAGO-7	
109		NbAGO-2					NbAGO-X
110			NbAGO-4	NbAGO-5			
111			NbAGO-4		NbAGO-6		
112			NbAGO-4			NbAGO-7	
113			NbAGO-4				NbAGO-X
114				NbAGO-5	NbAGO-6		
115				NbAGO-5		NbAGO-7	
116				NbAGO-5			NbAGO-X
117					NbAGO-6	NbAGO-7	
118					NbAGO-6		NbAGO-X
119						NbAGO-7	NbAGO-X

ID#	1 Knockout Combinations
120	NbAGO-1
121	NbAGO-2
122	NbAGO-4
123	NbAGO-5
124	NbAGO-6
125	NbAGO-7
126	NbAGO-X

Appendix Figure A.6. C_t values obtained in qRT PCR analysis of *AGOs 1,2, 4, 5, 6*, and *7* silenced plants including non-silenced controls WT (virus free plant) and OO (infiltrated with TRV empty vector) using the primers designed to amplify endogenous *AGOs 1, 2, 4, 5, 6,* and *7*.

	WT (NON INOCULATED)			OO (EMPTY VECTOR)			AGO1 SILENCED			AGO2 SILENCED		
ACTIN	25.1	25.0	24.9	22.7	22.7	22.6	24.7	24.8	24.6	22.9	23.0	23.4
AGO1	28.0	28.0	27.9	24.9	24.8	24.9	29.3	29.4	29.3	26.0	25.3	25.3
AGO2	31.9	31.2	31.9	30.6	30.0	29.9	33.1	33.5	33.1	29.7	29.6	29.8
AGO4	26.6	27.0	27.0	24.8	24.7	24.8	26.7	26.8	27.3	26.0	26.7	25.9
AGO5	32.0	32.4	32.2	28.3	28.5	28.3	31.8	31.5	31.3	29.2	29.3	28.9
AGO6	32.7	32.9	32.5	30.0	29.9	29.9	34.7	33.9	34.3	30.3	30.4	30.4
AGO7	31.2	31.2	31.2	30.3	30.4	30.5	34.8	34.6	34.2	31.3	31.6	32.0
AGOX	35.8	35.7	35.9	30.5	30.6	31.1	34.6	35.5	34.2	31.8	31.8	31.9

	AGO4 SILENCED			AGO5 SILENCED			AGO6 SILENCED			AGO7 SILENCED		
ACTIN	19.56	19.54	19.37	19.94	19.89	19.88	21.65	21.65	21.66	22.66	22.70	22.74
AGO1	25.94	25.92	25.85	27.43	27.35	27.34	30.16	30.05	29.99	31.71	31.79	31.97
AGO2	24.11	24.11	24.12	24.47	23.89	23.73	36.65	36.89	37.05	34.90	33.87	33.84
AGO4	27.50	27.51	27.49	25.09	25.01	24.94	25.96	25.92	25.89	27.35	27.51	27.55
AGO5	26.37	26.42	26.52	28.12	28.21	28.37	31.12	31.12	31.13	35.68	35.89	35.98
AGO6	27.69	27.59	27.50	28.32	28.38	28.42	39.91	38.56	37.07	37.88	37.79	38.01
AGO7	29.90	29.89	29.82	30.31	30.12	30.21	31.61	31.42	31.32	35.98	35.88	36.00
AGOX	30.65	30.66	30.64	31.06	31.05	31.08	36.02	35.90	35.42	37.89	38.99	37.94

Appendix A.8.

***N. benthamiana* transformation Protocol**.

By Dr. Jintao Zhang Texas AgriLife Research, Weslaco. TX

The plasmids are electro-transformed into *Agrobacterium* strains *GV3101 or LBA4404* and cultured in 25 mL LB + 50 ng/mL kanamycin antibiotics. They were grown at 28^{o}C while vigorous shaking (250RPM) for 16 to 20 hours or until the concentration of the cultures is about 600 nm. The cultures were then each transferred into 50 mL tube and centrifuged for 5 min at 5000 rpm. The resulting pellet was resuspended in liquid MS medium to make a final concentration between 0.3 and 0.6 OD.

Young *N. benthamiana* explants leaves were cut into ~1cm X 1cm disk, and placed in a small amount of liquid MS medium as shown in Figure A.8.1. The transformed *Agrobacterium* was added onto the cut leaf pieces for about 15 min after which the excess bacteria solution was blotted off using pieces of filter paper. The leaf pieces were transferred to a co-culture medium (MS0+ 6-BA 1.0mg/L+NAA 0.1mg/L) and the petri dishes were placed in a dark incubator at 28^{o}C.

Upon visual perception of *Agrobacterium* growth in the plates (about 1-2 days), explants were transferred to a fresh **Selection Medium** (MS0 + 6-BA 1.0mg/L + NAA 0.1mg/L+ Kan 100mg/L + **Carbenicillin 300mg/L**) (Carbenicillin is suggested as Agro-killing antibiotic). When *Agrobacterium* growth was excessive, explants were rinsed three times in sterile water and filter paper was used to blot off the excess water before moving them to selection medium. The plates were placed in a 28^{o}C incubator with 16-8 hour light-dark conditions.

One week later, transfer explants to fresh **Selection Medium** plates (MS0 + 6-BA 1.0 mg/L + NAA 0.1 mg/L+ Kan 100 mg/L + Carbenicillin 200 mg/L). The explants were then transferred to fresh Selection Medium plates every 16 - 20 days (MS0 + 6-BA 1.0 mg/L + NAA 0.1 mg/L+ Kan 100 mg/L + Carbenicillin 200 mg/L) until the shoots are about 1.5 cm long.

When the shoots reached a length of about 1.5 cm, they were carefully removed from the explants callus. A clean cut was made at the base of each shoot to ensure there was no callus attached to it. The shoots were placed in **Rooting Medium** (MS0 + NAA 0.1 mg/L + Kan 100 mg/L + Carbenicillin 200 mg/L) where they were allowed to grow until proper roots developed.

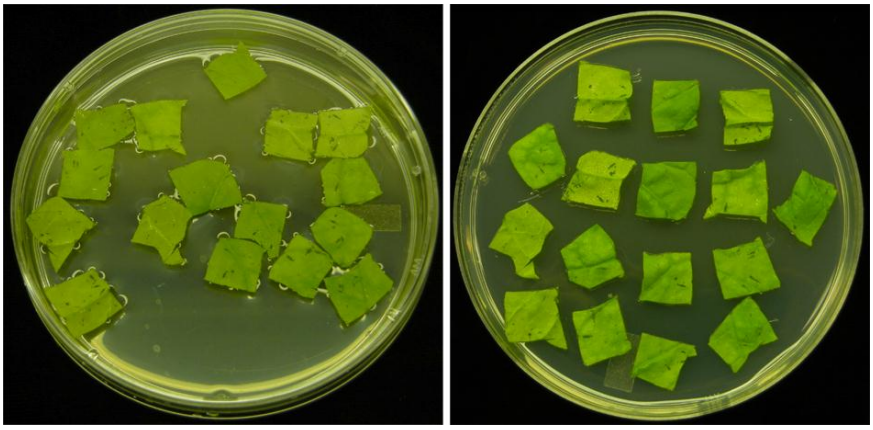

Figure A.8.1. Agroinoculation of *N. benthamiana* leaves. Left: Explants in agrobacterium solution; Right: Explants on co-culture medium.